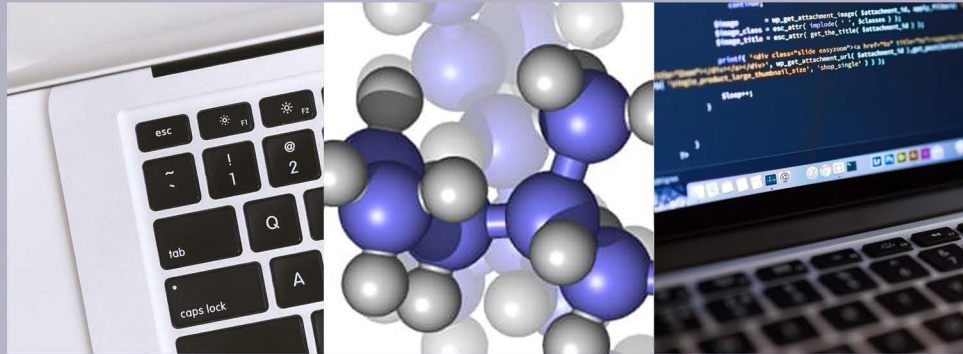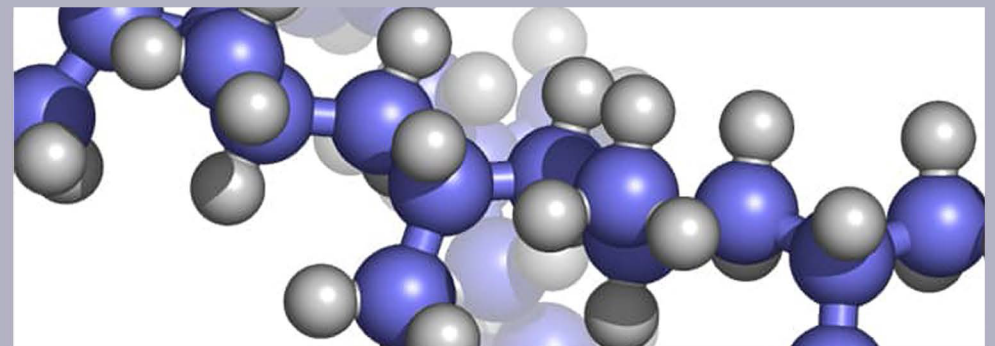**Rezanova V.G., Rezanova N.M.**

SOFTWARE FOR THE RESEARCH OF MICROFIBRILLAR COMPOSITES

The first chapter of the monograph describes the theoretical basis of obtaining microfibrills by processing melts of polymer mixtures. The experimentally confirmed mechanism of the phenomenon, necessary and sufficient conditions for its implementation, and ways of controlling this process are given.

The second section contains programs developed by the authors for mathematical modeling of the influence of various parameters (the content of components in the mixture, the ratio of viscoelastic properties of polymers, the value of interfacial tension, the angle of entry of a drop into the capillary, etc.) on the morphology of the system and for calculating the dimensional characteristics of microfibrils. Of particular interest is the created computer animation model, which adequately reflects the real processes of deformation of drops of one polymer in the mass of another under the flow of melts of mixtures in the entrance zone of the forming hole and allows to visually demonstrate the process of formation of microfibrillar morphology.

Monograph is intended for a wide range of teachers, scientists, post-graduate students, masters and students majoring in computer science and chemical technologies of specialized higher educational institutions, engineering and technical workers in the computer and chemical industries.

MINISTRY OF EDUCATION AND SCIENCE OF UKRAINE
KYIV NATIONAL UNIVERSITY OF TECHNOLOGIES AND
DESIGN

Rezanova V.G., Rezanova N.M.

SOFTWARE FOR THE RESEARCH OF MICROFIBRILLAR COMPOSITES

Recommended by the Academic Council of the Kyiv National University of
Technologies and Design (Protocol № 1 of September, 4, 2023)

Kyiv -2023

UDK 004.42:[544+001.894]

Author:

REZANOVA V. G. – Candidate of Technical Sciences, Associate Professor of the Department of Computer Science, Kyiv National University of Technologies and Design;
REZANOVA N. M. – Laureate of the State Prize of Ukraine in the field of science and technology, candidate of technical sciences, Kyiv National University of Technologies and Design.

Reviewers:

OPANASENKO V, M. - Laureate of the State Prize of Ukraine in the field of science and technology, Doctor of Technical Sciences, Professor, Leading Research Fellow of the Institute of Cybernetics of the National Academy of Sciences of Ukraine;
KRASNITSKIY S. M. - Doctor of Physics and Mathematics, Professor of the Department of Computer Science, Kyiv National University of Technologies and Design

Rezanova V.G., Rezanova N.M. Software for the research of microfibrilar composites. Monograph. – K.: ArtEk, 2023. – 269 p.

The first chapter of the monograph describes the theoretical basis of obtaining microfibrils by processing melts of polymer mixtures. The experimentally confirmed mechanism of the phenomenon, necessary and sufficient conditions for its implementation, and ways of controlling this process are given.

The second section contains programs developed by the authors for mathematical modeling of the influence of various parameters (the content of components in the mixture, the ratio of viscoelastic properties of polymers, the value of interfacial tension, the angle of entry of a drop into the capillary, etc.) on the morphology of the system and for calculating the dimensional characteristics of microfibrils. Of particular interest is the created computer animation model, which adequately reflects the real processes of deformation of drops of one polymer in the mass of another under the flow of melts of mixtures in the entrance zone of the forming hole and allows to visually demonstrate the process of formation of microfibrillar morphology.

Monograph is intended for a wide range of teachers, scientists, post-graduate students, masters and students majoring in computer science and chemical technologies of specialized higher educational institutions, engineering and technical workers in the computer and chemical industries.

INTRODUCTION

Analysis of the current state and prospects of the field of information and nanotechnology shows that active scientific research has state priorities in countries with the most developed economies. The implementation of their results changes global development trends in the direction of significantly expanding the capabilities of a wide range of economic sectors: chemistry, pharmaceuticals, pharmacology, construction, aviation, aeronautics and cosmonautics, energy, defense, transport, etc.

Polymer composite materials are widely used in many spheres of life, however, in recent years the demand for them has grown dramatically and the fields of application have expanded from household goods (fabrics, textiles, knitwear, packaging, biomedical products) to high-tech products (aerospace and military equipment). This is due to the fact that composites with two or more separate components that structurally complement each other have unique characteristics that are absent in each individual component. The properties of composites are largely determined by the nature of polymers and modifying additives (plasticizers, compatibilizers, fillers, or their combination). The priority role among them belongs to polymer nanocomposites, in which at least one of the components has dimensions from 1 to 100 nm. The use of substances in the nanostate allows you to effectively solve the problems of increasing strength, elasticity, providing non-flammability, unique tribotechnical, electrical, magnetic, optical, sorption, antimicrobial properties, etc. Layered silicates, single- and multi-layered

carbon nanotubes, nanoparticles of metals and their oxides, carbon, silicas, detonating nanodiamonds, bifunctional additives, etc. are widely used as nanofillers.

Technologies related to the creation, production, investigation of properties and use of structures and systems whose dimensions are smaller than 10^{-9} meters are classified as nanotechnologies. Their goal is to establish fundamental laws regarding nanoscale materials, to create and use structures and systems with the latest properties and functions. Until recently, the development of nanotechnology lagged behind the achievements of other breakthrough industries, but today they have become one of the most promising high technologies of the 21st century [1,2]. There are already many examples of the commercial application of these developments, while their wide industrial production is restrained by the rather high price of substances in the nanostate. Therefore, the development of accessible and inexpensive methods of obtaining nanomaterials is the most difficult and urgent task facing science and industry.

One of the priority directions for the development of nanotechnology is the modification of polymers (or their mixtures) and the creation of products with improved predetermined characteristics by introducing into their structure nano additives of different chemical nature, size and configuration, which is evidenced by a significant number of scientific articles and fundamental monographs [3-21]. Nanofillers are most widely used for reinforcement [8-12] and improvement of mechanical parameters of mixtures of secondary polymers [13-16]. When nanoscale carbon

4

derivatives are introduced, composites with increased electrical conductivity are obtained [17, 18], and carbon nanotubes provide shielding from electromagnetic waves and dissipation of electrostatic charge [3, 4, 8, 10]. Polyester textile threads filled with nanoparticles of metal oxides exhibit a wide antibacterial spectrum against pathogenic flora, photocatalytic activity, protection against UV radiation, antistatic properties, and resistance to abrasion [19,20]. Modification of fibers with nanoparticles of titanium and zinc oxides gives their products the ability to self-clean, similar to plant leaves, insect wings, etc. [21-23].

Nanofillers in melts of thermodynamically incompatible polymer mixtures play a dual role. First of all, they give composite materials unique properties inherent to substances in the nanostate. Secondly, the introduction of nano-additives into the melt of the mixture of polymers also allows you to adjust their characteristics by changing the type of structure formed by one of the polymers (dispersed phase) in the other (matrix). Thus, by processing melts of polymer mixtures, a new class of composites is obtained, in which the component of the dispersed phase *in situ* forms micro- or nanofibrils in the matrix [3-5, 12, 24-36]. Thus, the structure of the composite film (or monofilament) is a continuous phase of the dispersion medium, reinforced with thin jets of the dispersed phase. Composites with fiber diameters (10÷100) μm are called microfibrillar (MFC), and in the range smaller than 100 nm - nanofibrillar (NFC) [24]. Ultrafine fibers and new fibrous materials are obtained by extraction from MFC and NFC matrix polymer with an inert solvent [3,25-36]. At the same

time, the diameter of microfibrils is largely determined by the rheological characteristics of the components of the mixture and the degree of their compatibility at the boundary of phase separation. Improvement of microfibrillar morphology (reduction of fibril diameters and increase of their mass fraction) can be achieved by introducing into the mixture not only nanoadditives [12,27-29], but also other special substances — compatibilizers [30,31] or their compositions with nanofillers [27, 32,33]. Thus, the use of organosilicon liquids as compatibilizers allows the realization of a microfibrillar structure for ratios of components related to the phase change region [30]. The addition of carbon nanotubes [12], silica nanoparticles (NPs) [27,28] or composite additives based on it [34,35] to the melt of polypropylene/copolyamide (PP/SPA) leads to the improvement of the microstructure and allows obtaining complex threads from nanofilled PP microfibrils, which have a high specific surface, improved mechanical and hygienic indicators. The use of silver-containing additives gives fibers and filter materials based on them bactericidal properties [35,36]. The simultaneous introduction of a mixture of compatibilizer and nanoadditive into the melt is more effective than separate substances, due to the manifestation of their synergistic action [29,32,33].

Despite the large amount of experimental data on the effect of modifying additives on the micro- and macrorheological characteristics of multicomponent polymer systems and their wide use, scientifically based principles of creating materials with a given set of properties are still missing. Established regularities and mechanisms, as well as

proposed theories, often explain only individual results of experimental research. In recent years, work has been actively carried out to determine the physicochemical factors that affect rheological properties, the processes of combination and segregation of components, the formation of a microheterogeneous structure, the peculiarities of the combination of nano-, micro- and macrophases and their relationship with the characteristics of composites.

Conducting studies of polymer compositions requires a large number of multivariate experiments (even without taking into account parallel experiments). This is associated with significant costs of time and materials, since the impact of each factor is evaluated separately. Sometimes the number of experiments is artificially reduced by reducing the volume of the investigated factor space or the number of levels of parameter variation. In both cases, the degree of reliability of conclusions drawn from the results of experiments decreases.

Based on this, one of the ways that allows conducting scientific research at an accelerated pace and finding solutions as close as possible to the optimal with minimal costs is the use of mathematical methods for planning and analyzing experiments and creating software for processing the obtained results. A wide range of scientific research on the formation and improvement of the microfibrillar structure during the melt flow of a mixture of thermodynamically incompatible polymers using mathematical modeling methods was carried out at the Kyiv National University of Technology and Design. Based on the structural-continuum approach, a mathematical model has been developed that allows you to

calculate the amount of deformation of a polymer droplet of the dispersed phase depending on the change in the ratio of viscosities, the content of components, and interfacial tension [37-39]. With the help of simplex-lattice and simplex-centroid methods, plans for conducting experiments in the investigated area of the factor space for three- and four-component heterogeneous systems were developed. Mathematical models in the form of a system of regression equations were created in order to optimize the content of the ingredients and establish their relationship with the properties of the compositions. To process the results of the experiments, software was developed in the Delphi environment [40-42].

Taking into account all of the above, in order to increase the effectiveness of research into the physico-chemical regularities of processes in multicomponent polymer systems and reduce material and time costs, it is mandatory and necessary to involve methods of mathematical modeling and planning of experiments, as well as the creation of software for their processing.

CHAPTER 1
NANO-FILLED POLYMER COMPOSITES
WITH ADJUSTABLE STRUCTURE
AND PROPERTIES

1.1. Nanofillers, their classification, methods of synthesis and properties

1.1.1. Classification, features of the structure and properties of substances in the nanostate. The science of nanotechnology is based on the research, development and modification of objects that contain in their structure components with dimensions smaller than 100 nanometers in at least one dimension. The root "nano" is of Greek origin, the word nanos in translation means a dwarf, a dwarf. For a better idea of a particle of 1 nm (10-9 m), you can compare the dimensions of a globe and a soccer ball, because this is how the ball and the nanoparticle are related to each other. This branch of knowledge is relatively new. Its history spans no more than a century. Albert Einstein is considered to be the first scientist who used nanoscale measurement in his work, who in 1905 theoretically proved that the size of a sugar molecule is one nanometer. The idea of creating special devices capable of penetrating the depths of matter to the limits of the nanoworld was put forward by the outstanding American electrical engineer, inventor, physicist and philosopher Nikola Tesla, in particular, his developments formed the basis for the creation of the electron microscope.

According to their chemical structure, nanomaterials are divided into two types: inorganic and organic (hydrocarbon). Nanoparticles (NPs) based on metal, oxide/hydroxide, and

transition metals are inorganic, and those based on carbon and hydrogen are organic. Carbon derivatives (graphene, carbon nanotubes and fibers, fullerenes) are often separated into a separate class due to a wide range of applications and a large number of studies.

Substances in the nanostate have unique, fundamentally new properties. The peculiarity of small atomic aggregations is that they are intermediate between the structure and properties of individual atoms and the mass (volume) of a solid body. The specificity of the characteristics of a substance on a nanometer scale and the related new physical phenomena are caused by the fact that the sizes of the elements of the structure of nanoobjects lie in the range $(10^{-9} \div 10^{-7})$ m. They behave like chameleons: if you consider them as a molecule, then, due to their relatively large size, the structural elements show peculiar quantum behavioral features, and as materials they exhibit properties that are not characteristic of larger structures (even with a size of about 1.0 μm). Nanoobjects are characterized by a complex internal organization, the ability to pack very tightly, significant lateral (side) interactions, etc. An important feature of substances in the nanostate is a very high specific surface area (ratio of surface area to volume). By changing the size and shape of nanostructures, they can be given fundamentally new functional characteristics [3-5,43-47].

When studying nano-objects, the term "nanoparticles" is used, but until now there is no consensus on what should be considered a nano-size. Sometimes the definition of nanoparticles is associated not with their geometric size, but with the manifestation of new properties in them, different

from those of the bulk phase. It is believed that the size of NPs is equal to the correlation radius of this or that physical phenomenon (for example, the length of the free path of electrons or photons and coherence in a superconductor, the size of a magnetic domain or a nucleus of a solid phase). In this case, NPs are characterized by quantum effects, the appearance of which depends on both the nature of substances and their properties. Most researchers believe that the limit (maximum) size of nanoparticles corresponds to 100 nm, although they recognize that this value is conditional and necessary only for formal classification. There are two types of nanoparticles: clusters, or nanocrystals, and NPs themselves. The first type includes particles of an ordered structure with a size of $(1.0 \div 5.0)$ nm, containing up to 1000 atoms, and the second type includes NPs with a size of $(5 \div 100)$ nm, which consist of $(103 \div 106)$ atoms. However, the last definition is valid only for isotropic (spherical) nanoparticles, and filamentous and lamellar particles, which contain a much larger number of atoms and have one or two linear dimensions, do not fall under it, although they are typical nanoparticles in terms of their properties. The shape of the fillers can be both isodiametric (balls) and anisodiametric (fibers, nanotubes, plates). To characterize the degree of anisometry, the geometric parameter "form factor" (f) is used, which is defined as the ratio of the largest particle size to the smallest. Theoretical and experimental studies show that additives with a high value of f show a greater reinforcing (strengthening) effect [48].

The world around us is saturated with a great variety of natural nano-objects. A significant number of natural and

artificially created materials fall into the nanometer range: particles of alumina, silica, diamonds, molecules of polymers, proteins, amino acids and DNA, viruses (10÷160 nm), latexes (100÷1000 nm), nanoparticles of metals, oxides, semiconductors (1÷10 nm), etc. All of them, at least in one plane, have a size smaller than 100 nm. In reality, the limits of nanoscale are much wider - from individual atoms (0.1 nm) to their conglomerates with a size in one or two planes ≤ 1.0 μm.

Today, there are two fundamentally different approaches to processing matter in order to obtain a nanoproduct of the required structure - "top-down" and "bottom-up". The "top-down" method is based on reducing the size of physical bodies by mechanical or other processing, up to obtaining objects with nanometer parameters. The "bottom-up" idea is that the necessary structure is formed directly from "low-order" elements (atoms, molecules, structural fragments of biological cells) by placing and connecting them in a certain sequence. All the variety of artificially created nanostructures can be conventionally divided into the following types: nanoparticles, fullerenes, nanofilms, nanotubes, nanoflakes, nanofibers, nanofabrics and complex structures - biochips, nanorobots, nanomotors, etc. [2,47]. The simplest nanocomponents are nanopowders, i.e. fragments of matter crushed to a nanosized state. These nanoobjects can be used as an independent material (high-strength products can be obtained from them by sintering or pressing), as well as as fillers.

Modern nanotechnology originates from the invention of the tunneling microscope in 1981, which made it possible to

see the atomic level of the structure of matter. The modernization of the tunneling microscope in 1986 made it possible to manipulate atoms and process particles with a size of (1÷100) nm. In the coming years, the main technological innovations will be related to nanotechnology. Their development and use will make it possible to create material objects that will consist of given chemical elements and will be characterized by a set of necessary properties. Nanotechnology fundamentally changes the level of achievements in many fields of science and technology. The number of published monographs, articles and patents, as well as the amount of research funding for their development in the developed countries of the world, have grown exponentially in recent years.

Today, nanosized carbon derivatives, silicas, aluminas, nanoparticles of metals and oxides of various chemical nature, etc., are widely used to modify the properties of polymers and their mixtures. Achieving success in scientific research and practical use of additives in the nanostate largely depends on the possibilities of their synthesis methods. At the same time, one of the most important problems is the synthesis of NPs of given sizes and geometric shapes, which retain their functional activity for a long time.

1.1.2. Nanoscale carbon derivatives, their structure and properties. Today, various forms of carbon are known (fullerenes, graphene, nanodiamonds, single- and multi-layered carbon nanotubes and nanofibers), which differ in structure and properties. Fullerenes are spherical molecules consisting of 60,

70 or more carbon atoms. The most studied is fullerene C60. Its surface consists of 20 hexagons and 12 pentagons (Fig. 1.1).

Fig. 1.1. Computer model of fullerene C_{60}

Fullerene molecules can easily accept up to six electrons, forming the corresponding polyanions. They can add a significant number of reagents both with the preservation of the C_{60} composition and with its expansion, as well as form various molecular complexes. Fullerenes can "absorb" free radicals, forming new stable radicals [49].

Graphene is a film of carbon atoms with a wall thickness of one atom. It is flexible, strong and conducts electricity. Two classes of carbon nanostructures are known as morphological varieties of graphene structures: carbon nanotubes (CNTs) and carbon nanofibers. In fig. 1.2 shows some possible designs of graphene layers in nanotubes and nanofibers.
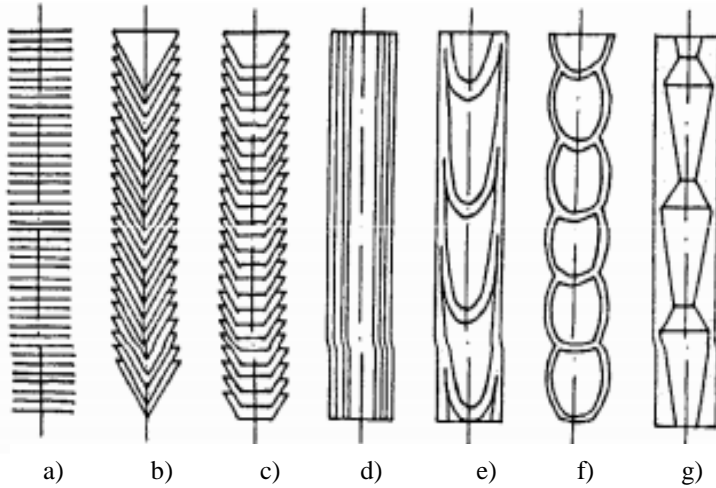
Fig. 1.2. Types of structures of graphene layers: nanofiber - a)
column of coins, b) herringbone structures; nanotube - c) a column of cups,
d) matryoshka, e) bamboo-like, f) with a spherical cross-section, g) with a
polyhedral cross-section

Carbon nanotubes were first discovered in the products
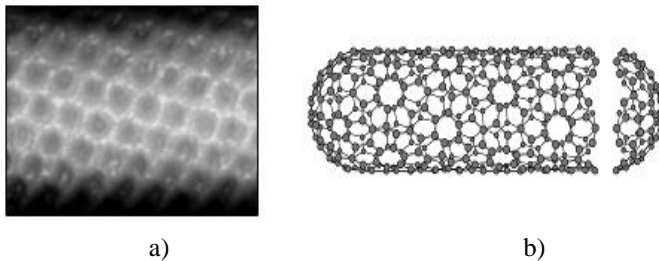of electric arc evaporation of graphite in 1991. They are hollow
fibers (Fig. 1.3).

Fig. 1.3. A photomicrograph of CNTs obtained using a scanning
tunneling microscope (a) and a schematic representation of CNTs (b)

There are two types of carbon nanotubes - single- and multi-layer, which differ in the number of rolled layers. The main element of single-layer CNTs is a graphene sheet rolled into a cylinder (graphite sheet of monatomic thickness) [8,50,51]. The diameters of single-layer CNTs are within (0.8÷5.0) nm, mostly ~ (1.0÷2.0) nm, and the length is (5÷500) μm, most often ~ (10÷50) μm. They can form sufficiently strong molecular aggregates, in which the axes of individual single-layer tubes are located parallel to each other (they are called bundles, strands, ropes or bundles). Single-layer CNTs are very prone to aggregation, which is why problems arise when processing them. Multilayer nanotubes have from 2 to 50 coaxial hollow cylinders of various diameters, formed by rolled graphene layers, which are held together by van der Waals forces. Multilayered nanotubes have a cylinder diameter of (1÷50) nm and a length of (10÷50) nm. They are much easier to process (mix with the polymer matrix) than single-layer ones. Both types come with open and closed ends, that is, cylinders of the appropriate length have so-called "caps" at the ends. The final structures that close the tubules are of different shapes, for example in the form of a half of a fullerene structure (Fig. 1.4). The simplest model of CNT is a system of coaxial cylinders (the so-called "Russian nesting doll"), placed from each other at a distance of 0.344 nm (Fig. 1.4 c), which is typical for carbon materials with a tubular structure.

a   б   в
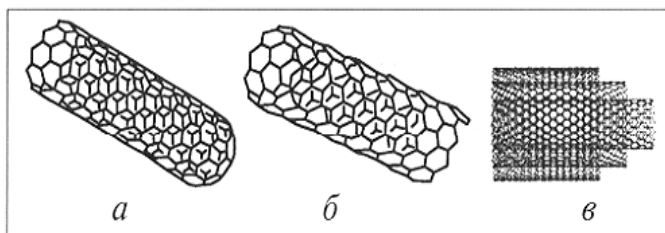
a)   b)   c)

Fig. 1.4. Schematic representation of a single-walled carbon nanotube
closed on one side (a) and open (b) and a multi-walled nanotube (c)

Complex configurations of CNTs are known, which differ in the structure of both the transverse and longitudinal sections (prismatic, scroll-like, etc.). Carbon nanotubes can have different atomic structure and properties. The walls of CNT are composed of hexagonal cycles of carbon atoms. At the same time, hexagons can form closed cycles, where C–C bonds are perpendicular to the axis of the cylinder, or various kinds of helicoidal spiral structures [8]. Carbon nanotubes are formed in the process of their synthesis, but the formation of different types of structures can be explained by the virtual folding of a graphite sheet into a cylinder. In fig. 1.5 shows examples of nanotube structures that can be obtained by rolling a graphene sheet around a vector differently oriented relative to the basic directions of the graphite plane. Provided that the vector is placed perpendicular to the C–C bonds in carbon hexagons, the formed structure is called an armchair (Fig. 1.5a). The tubes shown in fig. 1.5b and 1.5c have zigzag and chiral structures, respectively; they are formed by folding around other orientations of the vector relative to the graphene sheet. At the same time, a spiral series of carbon atoms is characteristic of tubes of a chiral structure.
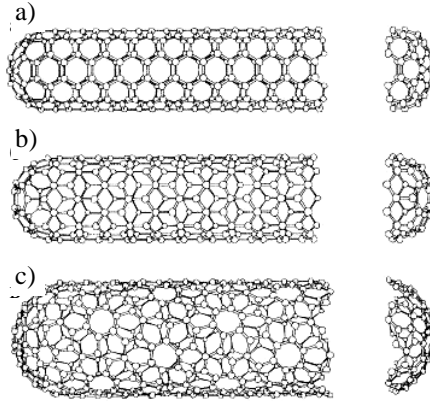
Fig. 1.5. Schematic representation of single-layer carbon
nanotubes with different structures: armchair (a), zigzag (b) and chiral (c)

Carbon nanotubes are obtained by various methods: laser evaporation in an argon medium at a temperature (T) of 1200 ^{0}C, pyrolysis of methane at T = 1100 ^{0}C, arc method, catalytic pyrolysis of benzene, pyrolysis of toluene, electrochemical synthesis, pyrolysis of poly-n-phenylene vinylene using the so-called self-assembly [8,50,51]. The diameter, length, structure of CNTs, the presence of impurities largely depend on the conditions of their synthesis - voltage, temperature, pressure, type of hydrocarbon raw material and catalyst, composition of graphite rods, etc. Thus, nanotubes with a diameter of   (10-20) nm and a length of 100 μm are obtained by laser evaporation. Single-layer CNTs are obtained by the carbon arc method using catalysts (cobalt, nickel, or iron), and multilayer nanotubes are obtained without catalysts. The electric arc method ensures the formation of single-layer nanotubes with a diameter of (1-5)

nm and a length of about 1.0 μm. Today, the most promising method for creating industrial production of nanotubes is chemical pyrolysis from the vapor phase, which consists in the decomposition of gaseous hydrocarbon with the formation of free carbon atoms. The method makes it possible to obtain CNTs practically without impurities of other forms of carbon (with a purity of more than 98%), thanks to which the stages of cleaning nanotubes (treatment with acid at elevated temperatures, annealing, etc.) can be eliminated and the cost of the product can be significantly reduced.

Carbon nanotubes have a complex of unique mechanical, thermophysical, chemical and electrical properties. The listed characteristics significantly depend on the method of their synthesis. The most interesting property of carbon nanotubes is that they can be metallic or semiconducting, depending on their diameter and structure. As a result of the synthesis, as a rule, a mixture of tubes is formed, two-thirds of which have the properties of semiconductors and one-third - metallic. The last tubes have a chair structure. In the metallic state, the electrical conductivity of CNTs is extremely high: they can pass a billion amperes per square centimeter. For example, copper wire fails (melts) at a million amps per square centimeter. One of the reasons for the high conductivity of carbon nanotubes is the minimal number of defects that cause electron scattering, which means very low resistance. Therefore, a high voltage heats up CNTs to a much lesser extent than a copper wire. This is also facilitated by the high thermal conductivity of nanotubes. It almost doubles this indicator for diamond, that is, CNTs are very good conductors

of heat: the coefficient of thermal conductivity along the axis reaches 5500 W/m·K (for comparison: in silicon - 150 W/m·K, in copper - 400 W/m·K).

An important property of materials is magnetoresistance, that is, the dependence of the electrical resistance of a substance upon application of a constant magnetic field. Carbon nanotubes exhibit a negative magnetoresistive effect at low temperatures, as the resistance decreases with an increase in the magnetic field. At the same time, the inverse value - conductivity - increases. This effect is a consequence of the fact that the magnetic field applied to the tube leads to the appearance of new energy levels of electrons associated with their spiral movement in the field. For nanotubes, these levels (so-called Landau levels) approach the highest of the filled levels (Fermi level) [8,50].

Carbon nanotubes also have record values of strength and elasticity. The tensile strength of single-layer CNTs is 45 GPa, while steel alloys break under a load of 2 GPa, i.e. CNTs are approximately 20 times stronger than steel. Multilayer nanotubes have better mechanical characteristics than steel, but they are not as high as single-layer ones. For example, a multilayer CNT with a diameter of 200 nm has a tensile strength of 7 GPa and a Young's modulus of 0.6 TPa. The elasticity of the material is characterized by the value of Young's modulus: the larger its value, the less pliable the material. Thus, the Young's modulus of steel is 0.21 TPa, which is approximately 30 thousand times greater than that of rubber. The tensile modulus of single-layer nanotubes is (1.28÷1.80) TPa, which is 10 times higher than that of steel.

The elasticity of multilayer CNTs can reach 5000 GPa. The concentric arrangement of the basic graphite planes in the nanotubes gives them extreme stiffness and high resistance to compression, meaning that it was predictable that they should be stiff and difficult to bend. However, this is not entirely true. Due to the low defectivity of the polycyclic structure in the layers, as well as the ability to deform the hexagonal carbon rings, the tubes, having high tensile strength, are capable of significant deformations during bending. A carbon nanotube is very elastic: it bends like a straw, but does not break and can straighten without damage. This is due to the fact that its wall is only one atom thick and has no structural defects. In addition, they do not break because the carbon rings of the walls have the form of almost regular hexagons, which change their structure when bent, but do not break.

Carbon nanotubes are also characterized by very high hardness and corrosion resistance, they do not dissolve either in "royal vodka" or in concentrated alkaline solutions. The large specific surface area of nanotubes ($500 \div 1500$ m^2/g) provides them with significant adsorption capacity. They effectively absorb hydrogen sulfide, sulfur dioxin, mercaptans, disulfides, dioxins, chlorine, fluorine, ammonia, etc. So, for example, their adsorption capacity for ammonia is (10-16 cm^3/g). In addition, carbon nanotubes have a significant antibacterial effect against a number of strains of microorganisms (*E. coli* and *B. Subtilis*) [52,53]. The properties of CNTs can be modified by introducing metal nanoparticles and their oxides into the middle of the tubes, and the surface can be activated with functional groups [8,50,51].

1.1.3. Nanoparticles of metals and their oxides. The unique properties of metals and their oxides in the nanostate (optical, electrical, catalytic, antimicrobial) open wide opportunities for the creation of new polymer materials. Metal nanoparticles consist of only one element. They exist as individual atoms or their clusters. For example, gold and silver particles can form different nanocluster forms: Au_8, $Au_{11}...Ag_{25}$ with characteristic electronic transitions. Ag, Au, Cu, Pd, Pt, Re, Ru, Zn, Co, Al, Cd, Pb, Fe and Ni nanoparticles have been synthesized today. In addition, metal NPs can be bimetallic (Pt – Pd, Cu – Ni), which often exist as shells or alloys. Bimetallic nanoparticles are more effective than monometallic ones. Metal nanoparticles are produced in the form of colloidal solutions or solid particles by methods of biological, hydrothermal or microwave synthesis.

Nanoparticles of metals and their oxides are divided by morphology into NPs with low and high anisotropy. Nanostructures with low anisotropy include nanospheres, nanocubes, nanopyramids, nanohelices, and those with high anisotropy include nanozigzags, nanotubes, nanostructures, and nanopillars. Images of various geometric shapes of nanoscale structures obtained by scanning and transmission electron microscopy are shown in Fig. 1.6 [2].

Silver occupies a special place among a large number of metals. Due to its developed surface, its nanoparticles have a higher antibacterial effect than in the form of Ag+ ions. At small concentrations, silver NPs are harmless to human cells, but kill most bacteria and viruses, so it is used to disinfect water, food in everyday life and fight infections.
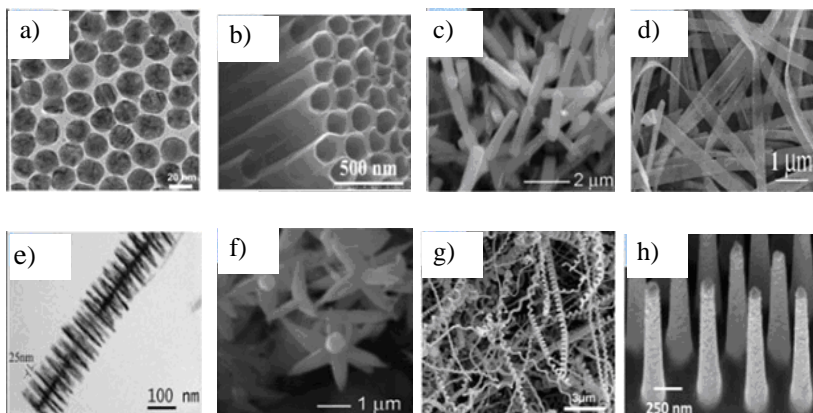
Fig. 1.6. Electron micrographs of various substances in the nanostate:
a) array of Au nanoparticles, b) TiO$_2$ nanotubes, c) ZnO nanorods,
d) Ag nanostrips, e) branched structures-SiC dendrites, f) ZnO nanoflowers,
g) C nanosnakes, h) Si nanopillars with SiO$_2$

To date, there is no information that microorganisms in the process of mutations are able to produce resistance to silver (except when it exists *a priori*).

There are many methods of synthesis of silver nanoparticles, which can be divided into traditional and non-traditional [54]. Among the traditional methods, the most famous are the citrate and borohydride methods, which are based on the recovery of silver ions from solutions of its salts. They make it possible to obtain NPs of spherical shape with diameters from 1.0 to 20.0 nm. These traditional methods of obtaining silver NPs have a significant drawback - the need to use surface-active substances and stabilizers in the synthesis process and the impossibility of completely cleaning the surface of nanoparticles from them. Meanwhile, in most fields

of application of silver NPs (microelectronics, medicine, spectroscopy, catalysis, etc.), the presence of even the smallest impurities is unacceptable. The task of obtaining chemically pure NPs of precious metals is an important problem that is partially solved by non-traditional methods. These include the method of laser ablation of massive samples of metallic silver in liquid media or microparticles in aerosols and the Swedberg electrocondensation method (direct evaporation of atomic silver in a vacuum) [55,56].

Along with silver, copper and iron in the nanostate are also used to create biologically active materials. Copper nanoparticles are synthesized in the form of chains, rings or three-dimensional lattices. Their bactericidal effect is (4÷5) times weaker than that of silver, but taken together, these metals multiply the properties of each other [54,57].

Iron in the nanostate has a significant number of indicators that distinguish this biomaterial from microscopic iron. First, they will show increased chemical reactivity; secondly, NPs have unique superparamagnetic properties, which is why they are called superparamagnetic iron nanoparticles. Since nanoiron is easily oxidized, it is usually used in the form of iron oxide NPs. The latter are widely used in medicine: for contrast enhancement in magnetic resonance imaging, magnetic-fluid hyperthermia, for drug delivery, in cell separation, tissue regeneration, detoxification of biological fluids, etc. The most common method of obtaining iron oxide NPs is synthesis using the method of co-precipitation of iron salts in an alkaline medium and by electron beam evaporation in a vacuum [58].

It is known that the bactericidal, catalytic, optical and other properties of nanoscale objects are largely determined by their size and geometric shape. Today, metals and their oxides are obtained in the form of flat (triangles, pentagons and hexagons, round plates) and three-dimensional (tetrahedra, cubes, prisms, rods, wires) nano-objects [59]. Thus, by reducing Ag+ ions with oligopeptides, spherical, triangular and hexagonal silver structures with a size of (60÷150) nm are synthesized. Thermodynamically, the most stable form of particles is the minimum surface at a given volume. If the reduction reaction of silver ions takes place under conditions of thermodynamic control, then the spheres are the main product. In the course of the synthesis, it is quite difficult to realize the conditions for the formation of NPs of non-spherical shape.

The bactericidal effect of spherical silver NPs increases as their size decreases from 25 to 3 nm. Almost complete inhibition of the growth of microorganisms is provided by Ag nanoparticles in the form of truncated triangles at their minimum content (1 μg). For silver nanorods, the growth of individual colonies was noted even at the maximum concentration of 100 μg [60]. The reason for the unequal biological effect of clusters of different shapes is obviously the different contribution of the faces to the total surface of the particles. It is known that the faces of silver crystals in polyhedra exhibit increased chemical activity [61]. Studies of the geometric shape of silver nanoparticles with a size of (1÷10) nm showed that in this range, almost 98.0% of NPs are decahedra and icosahedra, formed by tetrahedral clusters, which are connected to each other by faces. In addition, the

decrease in the size of NPs affects the increase in the specific surface area of the bactericidal sample and, as a result, its total activity.

Оксиди Metal oxides are one of the most stable natural compounds. They have polar surfaces due to the presence of anionic oxygen. With their use, semiconductors, superconductors and even insulators are obtained. There are many types of metal oxides in the nanostate, namely: Al_2O_3, TiO_2, Fe_3O_4, Fe_2O_3, ZnO, MgO, ZrO_2 and CeO_2. They are used for water purification, in cosmetology, biomedicine, energy and environmental fields. Metal oxides can be easily modified by doping, resulting in heterostructures and mixed oxides. Due to their large specific surface area, high heat resistance, and ion exchange ability, these materials are used in catalysis, supercapacitors, fuel cells, flame retardants, sensors, and pollutant removal.

The bactericidal effect of nanoparticles of oxides is higher than that of the original metals and depends on the shape, nanorelief of the surface, the average size of the particles and the nature of their diameter distribution [22,23]. When studying the antimicrobial properties of several metal oxides in relation to a number of microorganisms, it was shown that aluminum oxide exhibits the maximum antibacterial effect [23].

1.1.4. Siliceous soils. Silicas, or aerosils, are among the most common and widely known nanostructures used to modify the properties of resins, rubbers, thermoplastics, etc. Today, Aerosil ranks first in the global production of nanopowders. Various modifications of nanodisperse aerosol

are obtained by hydrolysis of silicon tetrachloride in an oxygen-hydrogen flame at 1000 ^{0}C. Therefore, this product is called fumed silica. The production method ensures the production of extremely fine-grained silicon dioxide (SiO_2). By changing the reaction conditions, it is possible to purposefully adjust the properties of aerosols. Silica is an amorphous powder with particles of colloidal size (from 4 to 40 nm), with a specific surface area from 50 to 450 m^2/g (Fig. 1.7).
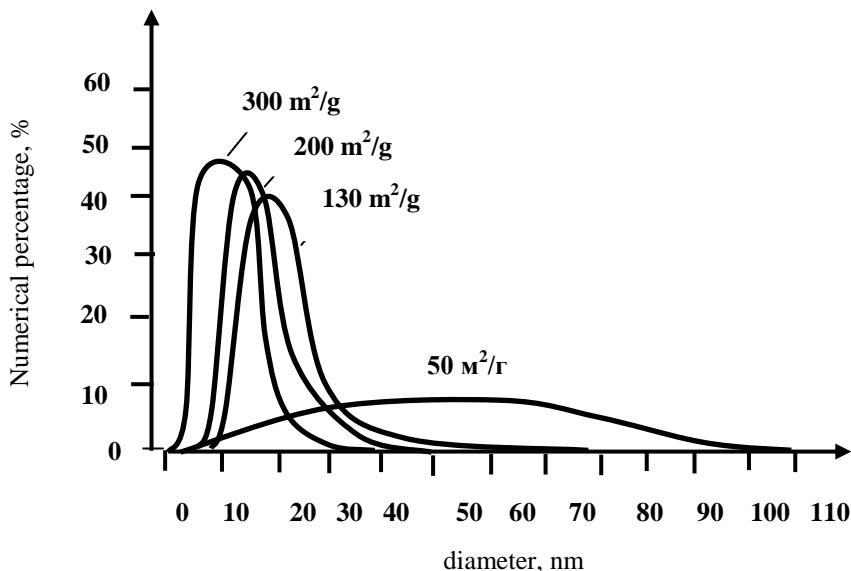

Fig. 1.7. Distribution of silica nanoparticles by diameters
for samples with different specific surface areas

Electron microscopy showed that silica nanoparticles have a spherical or almost spherical shape. Due to the high specific surface, NPs are combined into chains, which in turn

form flaky aggregates [62]. High-temperature hydrolysis produces chemically ultrapure silica with nanoparticles that are very uniform in size and shape. однорідними за величиною і формою наночастинками.

Silanol (Si-OH) and siloxane (Si-O-Si) groups are located on the outer surface of NPs. Silanol groups have a quantitative advantage, and they give silicas hydrophilic properties. Chemical modification of the surface of NPs is carried out by replacing Si-OH groups with methyl or ethyl ones, thus obtaining hydrophobic silica samples (Fig. 1.8).

Due to their high chemical purity and physiological harmlessness, silicas are approved for use in the pharmaceutical, food, cosmetic industries and in the manufacture of consumer goods. In addition, silicon plays an important role in human life. It takes part in metabolic processes, neutralizes a number of pathogenic microbes and viruses, acts as a biocatalyst capable of accelerating redox reactions in water 1000 times.

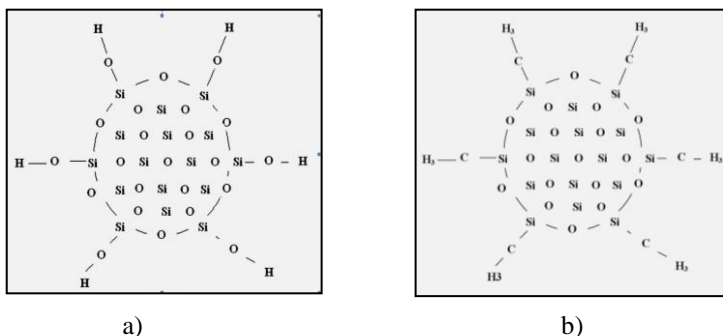a)   b)

Fig. 1.8. Schematic representation of silicas: pyrogenic (a) and methylated (b)

It
level, and absorbs radionuclides. Silicon and its compounds change the structure of water and give it healing properties.

28

1.1.5. Aluminosilicates (alumina). The main elements of the structure of aluminosilicates are silicon oxide ion SiO_4^{-4} and aluminum oxide ion $Al(O/OH)_6^{3-}$. These structural units form, respectively, tetrahedral and octahedral two-dimensional networks, which are able to connect with each other through oxide ions and form layers (plates). The ratio of tetrahedra and octahedra in the layer of clay minerals is: 1:1; 2:1; 2:1:1. Natural layered aluminosilicates, which are usually used as nanofillers, have a 2:1 structure. The sizes of the alumina plates are within ~ (1000x1000x1) nm. Due to van der Waals interactions, aluminosilicate plates self-organize and form packets and crystallites, the interlayer space between which is up to 50 nm. An important characteristic of clay silicate is the cation exchange capacity (ECC), that is, the number of exchangeable cations capable of being replaced by cations of a different type (per 100 g of clay).

The outer and inner surfaces of layered silicates are hydrophilic and polar. This contributes to the wetting and penetration into the space between the layers (planes) of both low- and high-molecular compounds that have polar groups in their structure. At the same time, the polarity of the surface of silicates complicates their interaction with nonpolar and weakly polar polymers and prevents the uniform distribution of plates in the polymer matrix. The surface of the plates can be modified in various ways: by ionic exchange of clay cations for organic cations; adsorption on the surface of particles of polyvinyl alcohol, polyacrylamide, other water-soluble polymers, alkyl ketones, methyl acrylate, etc.; grafting of organosilanes to the clay surface with the formation of Si-

O-Si bonds, introduction of organic molecules capable of Van der Waals or ion-dipole interaction with the clay surface [48]. At the same time, it is the nature of the packing of the modifier molecules in the interlayer space that determines the distance between the silicate plates, the organophilicity of the clay interlayer space.

     *1.1.6. **Bifunctional nano additives.*** Bifunctional nanoadditives are substances in which nanoparticles of metals or their oxides are applied to the surface of mineral or organic sorbents. The most studied are silver composites on activated carbon, zeolites and silicas. They exhibit the antimicrobial effect of silver-containing preparations, as well as high sorption and antitoxic properties. At the same time, the rate of release of silver nanoparticles is regulated by the properties of the sorbent and provides the necessary concentration for reliable antibacterial protection. The costs of silver are minimized, which leads to a decrease in the toxicity and cost of silver-containing composites [63-66]. Bactericidal composite - nanosilver on silica particles (Ag/SiO_2) was obtained by reducing silver ions from aqueous solutions of its salts or by pyrolysis of metallic silver (Fig. 1.9). The figure shows the accumulation of silver nanoparticles on the SiO2 matrix (highlighted in a square) [63]. The diameter of silver nanoparticles in the composite was ($1\div10$) nm, and they were discretely distributed on the silica surface. The bactericidal effect of the bifunctional additive Ag/SiO_2 is about 10 times higher, compared to silver ions, which contributes to its safety for human health and the environment.
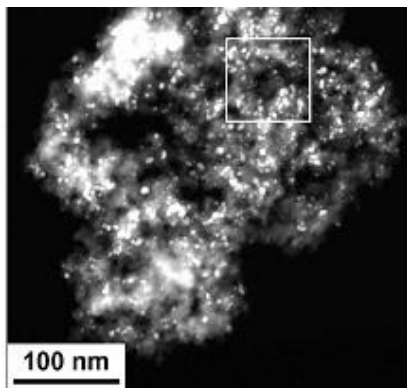
Fig. 1.9. Electron micrograph of amorphous silicon dioxide particles with metallic silver nanoparticles deposited on the surface

Bifunctional substances with high biochemical activity have also been created, which contain Ag nanoparticles on organic matrices (activated carbon, carboxyl cation exchangers) and on porous aluminum oxide [64,65,67]. The results of research on water disinfection showed that Ag/Al_2O_3 additives are most effective, reducing the total microbial count to zero, which is due to the synergistic effect of the two most effective antimicrobial nanoadditives [67].

Нанесенням Applying silver or copper nanoparticles to the TiO2 surface produces complex antimicrobial substances with high and stable bactericidal activity at low concentrations. The complex TiO_2/SiO_2 nanoadditive combines the photocatalytic activity of TiO_2 and the sorption properties of silica [66]. Such nanoadditives are both sorbents and photocatalysts and absorb a wide range of metal ions from water, destroy organic compounds, concentrate and separate radionuclides.

Bifunctional nanocomposites based on montmorillonite clays, modified with ions of silver, copper, zinc, iron, magnesium, cobalt, manganese, were obtained by the method of intercalation of metal ions in the interpacket spaces of the clay layer structure [22,48]. Individual layers (plates) and the spaces between them in the clay system are nanosized and, thanks to the highly developed active surface, they absorb metal ions. When interacting with biological environments, active metal ions are dosed and released at a constant rate from such peculiar reservoirs. Evaluation of the bactericidal properties of the created composites showed that 5.0% aqueous dispersions have high antimicrobial activity against gram-positive, gram-negative and spore-forming flora. Dispersions containing Ag, Zn and Cu ions show maximum activity.

1.2. Morphology and properties of nanofilled polymer systems

Today, only a small part of polymer products do not contain any modifying additives. Polymer technology has long followed the path of creating composite materials in which a set of necessary characteristics is achieved by a purposeful combination of components. The market of polymer nanocomposites is developing at a much higher rate than that of unmodified polymers. Its volume in 2020 should exceed the indicators achieved in 2010 by 3–5 times (Fig. 1.10).
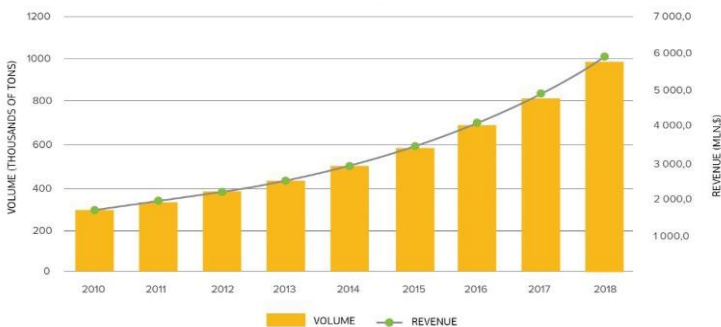
Fig. 1.10. Growth of the nanocomposite market

1.2.1. The effect of nanoadditives on the morphology of thermodynamically incompatible polymer mixtures. Mixing polymers significantly expands the possibilities of creating materials with improved physicochemical and operational properties, even compared to the synthesis of new monomers and polymers. Polymer mixtures are a special class of dispersions in which, unlike low molecular weight substances, when two components come into contact, partial interdiffusion of segments of macromolecules occurs, which leads to the formation of a transition layer. Its properties are significantly different from the characteristics of the components in the volume, and the length depends on the chemical nature of the polymers and is (2÷20) nm [68].

The properties of polymer dispersions are largely determined by the phase structure, which is determined, first of all, by the degree of thermodynamic compatibility of the components (absolutely compatible homogeneous systems, partially compatible and completely incompatible systems). Until recently, the low affinity of the components was

considered a significant drawback of such compositions, however, in many cases, it is precisely due to the multiphase nature of polymer dispersions that the materials based on them have unique characteristics. The dispersed phase of the polymer mixture is deformed and destroyed under the conditions of mixing and processing into products, which leads to the formation of particles of a fairly wide range of sizes (from submicron to tens of micrometers), while they can have a spherical, ellipsoidal, cylindrical or ribbon-like shape. The final morphology of the mixtures is the result of a dynamic balance between the phenomena of deformation and capillary instability, on the one hand, and coalescence, on the other [3,68].

To create composite materials with specified characteristics based on thermodynamically incompatible polymer mixtures, a necessary condition is the achievement of the appropriate structural organization of the components of the heterogeneous system and the determination of the ways of regulation by morphology. The potential of this approach remains largely unused, in particular due to the lack of fundamental laws and universal mechanisms for the formation of predetermined structures. The morphology of incompatible mixtures depends on many factors: the composition, relative viscosity of the components, the amount of surface tension at the boundary of phase separation, thermodynamic instability, time and speed of mixing, geometry and dimensions of the extruder screw, etc. Traditional approaches to controlling the structure of polymer dispersions consist in changing the number of ingredients and their rheological properties,

controlling the kinetics of mixing and dispersing processes, as well as using interphase modifiers that improve the affinity between polymers [3,27,68-70]. The introduction of an additional component into the mixture, which has a compatibilizing effect, helps to increase the interaction between the phases and the formation of a finer stable dispersion. The most effective compounds for compatibilization are amphipathic (translated from Greek: "one that has a feeling for both"), block copolymers and grafted polymers [69,71]. These substances have fragments of macromolecules with different degrees of affinity to the components of the mixture. One of the chains of these copolymers is partially or fully compatible with one of the polymers in the blend, and the other with the other.

Nanoadditives can also have a compatibilizing effect, which contributes to improving the dispersion of the component of the dispersed phase, increasing the stability of the dispersion, and forming the microfibrils of one polymer in the matrix of another [3,10-18,27-29]. Regulation of the morphology of polymer mixtures can be carried out due to the chemical nature, size and geometric shape of nanoparticles, their orientation, mutual location in the system (ordered, chaotic), predominant localization in one of the phases (or on the border of their separation), the possibility of the formation of spatial structures in the system , the degree of filling, the polymerophilicity of the components (the ability to wet the filler), the type of interaction between the NPs and the functional groups of the ingredients (strength of the adhesive bond), the size and properties of the interfacial layer, the effect

of nano-additives on the supramolecular structure of polymers, etc. [3-6,32-36, 72-80]. At the same time, the most studied is the change in the degree of dispersion of components in nanofilled polymer compositions. For the modification of melts of polymer mixtures, silicas are widely used [27,28,72,78-82]. So, when introducing into the mixture polypropylene /polystyrene (PP/PS) 3.0 wt. % of hydrophilic or hydrophobic silica, the average particle size of the dispersed phase (PS) decreased from 3.7 to 0.85 μm (for hydrophilic SiO_2 particles) and to 1.25 μm (for the hydrophobic additive) [72]. The authors explain this effect by the heterogeneous distribution of nanoparticles in the system due to their affinity for one or another component. With the preliminary introduction of hydrophilic SiO_2 into the PP melt, nanoparticles migrated to the PS phase, and hydrophobic silica NPs moved into the transition layer. The degree of influence of clay nanoparticles on the morphology of PP/PS mixtures also depends on their hydrophobicity – the droplet sizes decreased as the hydrophilicity of the NP additive increased [82]. With the simultaneous introduction of nanoparticles of different chemical nature (hydrophilic and hydrophobic) into the polymer mixture, the modification effect increases [83-86]. Placing in the matrix polymer NPs that have an affinity for it leads to an increase in the viscosity of the melt. At the same time, incompatible particles accumulate in the interphase zone, forming a kind of "shell", which reduces the probability of droplet coalescence and ensures the formation of a finer morphology of the mixture [86].

Along with other factors, an effective factor that

ensures the achievement of the desired characteristics of nanocomposites is the control and regulation of the localization of solid nanoadditives in polymer mixtures. The migration and location of nanoparticles in the melt depends on thermodynamic and kinetic factors. The distribution of fillers in incompatible polymer mixtures occurs in such a way that the total free energy of the system becomes minimal, i.e. uneven placement of NPs ensures a decrease in free energy, which depends on the surface tension and/or surface energy of the components. The final distribution of the modifying additive is determined by the mixing conditions (the sequence of introduction of the ingredients, the equipment used, temperature and time) and the rheological properties of the components [25,75-77]. The localization of NPs also depends on the degree of interaction between the filler and polymer macromolecules, which determines their adsorption on the surface of the additive particles [72,78,87]. Another factor that determines the preferential placement of NPs in a mixture of polymers is their geometric dimensions and shape [88].

The selective arrangement of nanoparticles at the polymer/polymer interface is one of the most effective factors in controlling the microstructure of polymer mixtures [25,72,75-79,90]. The mechanism of this process has not yet been definitively established. The influence of nano-additives on the ratio of visco-elastic properties of system components and on interphase phenomena is experimentally confirmed. Using the example of a polylactide/polyethylene (PL)/(PE) mixture, the dependence of migration and localization of silica micro- and nanoparticles on thermodynamic and kinetic

parameters was investigated [25]. When the indicated mixture of nanoparticles of unmodified microbial nanosilica is introduced into the melt, they are placed in the PL phase, while particles of silica modified with grafted succinic anhydride are concentrated in the volume of polyethylene. The authors explain the obtained result by the preferential encapsulation of particles in the phase with which they have a better affinity, i.e., minimal surface tension. To study the influence of the kinetic parameters of the migration process of silica NPs, they were pre-mixed with molten polyethylene, and then the obtained granules were made from PL. At the same time, the nanoadditives of the original and modified silicas remained localized in the PE phase. In mixtures with a lower viscosity of polyethylene, silicon dioxide particles migrate and are located in a thermodynamically favorable region. Electron microscopy showed that 35% of hydrophilic silica NPs moved from the PE phase into the PL melt, most of the filler particles (65%) remained in the polyethylene volume in the form of aggregates. Thus, selective placement at the phase separation boundary is characteristic of nanoadditives with high compatibility to one of the components, if they are previously introduced into a polymer with low affinity. Simultaneous mixing of all ingredients contributes to the uniform distribution of NPs in the mixture, and two-stage mixing promotes their preferential localization in one of the phases or on the border of their separation.

Most researchers associate the reduction of the geometric size of the particles of the dispersed phase and the formation of a finer morphology of the mixture with the

addition of a nanofiller with their influence on the degree of affinity in the transition layer and on the rheological characteristics of the components. A decrease in interfacial tension after the addition of NPs has been established in many works [27-29, 32-36]. A comparison of the degree of dispersion of particles of the dispersed phase and the value of surface tension in the original and nanofilled systems shows that there is a direct relationship between these indicators. The influence of nano-additives on the morphology of mixtures is also manifested through a change in the ratio of viscosities and elasticities of polymers, which can shift the balance in the processes of deformation, decay and coalescence. An increase in the viscosity of any of the phases counteracts the coalescence of the droplets. In addition, nanoparticles can act as a physical barrier, creating certain steric hindrances and preventing direct contact between droplets of the dispersed phase [91-93]. Lamellar clay particles show a high ability to form such barriers at the phase boundary.

Thus, nanoadditives in melts of incompatible polymer mixtures have a compatibilizing (emulsifying) effect, reduce the surface tension, increase interphase adhesion (i.e., improve affinity) and inhibit droplet coalescence due to physical shielding, which contributes to reducing the dimensional characteristics of the dispersed phase component.

1.2.2. Nanofilled polymer composites. Qualitatively new materials with enhanced adjustable characteristics are obtained due to the combination of polymer matrices with nanofillers of different chemical nature, configuration and size. The properties of nanocomposites are influenced by the

chemical nature of the polymer and additives, the volume fraction of the filler, the degree of dispersion and orientation of the particles, the uniformity of their distribution, the size and properties of the interfacial layer. In accordance with the terminology adopted by IUPAC (International Union of Theoretical and Applied Chemistry), nanocomposites include systems in which filler particles have at least one size in the nanometer range. At the same time, they can be of different shapes, for example plates, tubes, spheroids, but, at least in one dimension, their size should be from 1 to 100 nm. In zero-dimensional (OD) nanocomposites, all three dimensions of the additive have a size of approximately 1 nm (spherical silicas, NPs of metals and their oxides, detonation nanodiamonds, etc.). One-dimensional (1D) contain an additive that is nano-sized in two dimensions (nanotubes, fibers), and two-dimensional (2D) are nanometer-thick layers (layered silicates, metal chalcogenides, graphite). According to the fields of use, composites can be divided into structural and functional. For composites of the first group, the introduction of a nanofiller allows to effectively solve the problems of increasing strength, non-flammability, changing barrier characteristics, the ability of polymer materials to be processed, etc. The role of the nanofiller in functional composites is much more important, since the electrical, magnetic, optical, bactericidal, sorption and other properties of the materials are usually determined by the corresponding characteristics of the nanoadditive. At the same time, the interaction between nanoparticles and the polymer matrix at the molecular level is of great importance, which can

lead to synergism of the properties of the organic and inorganic components of the material [3,4].

The acquisition of new characteristics by composites is explained by quantitative changes in the ratio of surface and bulk atoms of individual nanoparticles, i.e., a high specific surface area. Compared to conventional materials, nano-filled composites have such fundamental characteristics as specific heat capacity, modulus of elasticity, diffusion coefficient, and magnetic properties that increase dramatically. This is due not only to a decrease in the size of structural elements, but also to the manifestation of quantum mechanical effects, the wave nature of transport processes, and the dominant role of the phase separation surface.

Nanocomposites and nanomaterials have always existed in nature in the form of systems filled with carbon black or natural clay, and have been used for many centuries. At the same time, they are new, little-studied substances for materials science. Fundamental studies of the mechanisms of creating nanocomposites and achieving the desired properties of materials of this class have been intensively conducted in recent years in almost all countries of the world, since a decrease in size below a certain critical value can lead to a change in the main physical and chemical parameters. Today, various forms of carbon, silica, alumina, nanoparticles of metals, oxides, etc. are widely used as nano additives.

Значний The significant influence of nanofillers on the properties of the original polymers and mixtures is also due to the fact that an interphase layer is formed around the nanoparticles at the filler/polymer interface, the properties of

which differ sharply from similar characteristics of the melt in the volume. The experimentally determined thickness of the transition layer ranges from (0.0004÷0.16) μm and depends on the affinity between the polymer and nanoparticles, as well as on their volume concentration [94]. Thus, it was theoretically calculated that with an additive content of 15 vol. % with nanoparticles with a diameter of 10 nm, the distance between them will be 5 nm. In this case, the entire polymer matrix in the nanocomposite can behave as a transition layer [83].

1.2.2.1. Polymer composites filled with carbon nanotubes.

By introducing carbon nanotubes into polymers and their mixtures, a sharp increase in the mechanical characteristics of the products is achieved without increasing the weight [9-11,19,20,95]. Thus, the modulus of elasticity of industrial synthetic fibers modified by CNT increases almost 3 times, and their strength is 6 times higher than steel, while they are 100 times lighter than steel [19,20]. The presence of carbon nanotube fibers in the structure provides shielding from electromagnetic waves and dispersion of electrostatic charge [3,4,8,10]. Lead into the polymer melt (5÷20) wt. % CNT with a different structure can give products electrical conductivity comparable to copper, antistatic properties, as well as chemical resistance to the action of many reagents [96,97]. Significant modifying effects in nanofilled polymer composites, in comparison with traditional filled ones, are due to the formation of a more perfect homogeneous structure. The performed theoretical calculations showed that the

homogeneous dispersion and orientation of CNTs in the volume of the melt will ensure a fourfold increase in the strength of the polymer at a content of 0.6 vol. %, and if CNTs occupy 10% of the volume of the polymer, its strength will increase 20 times. If CNTs are placed between polymer macromolecules and connected by chemical bonds, the strength of the material will approach the strength of carbon nanotubes [97].

The CNT surface is inert and hydrophobic and poorly wetted by melts of many polymers, so mechanical mixing is not always effective. To achieve a uniform dispersion of nanotubes in a polymer matrix, many methods have been developed, which can be divided into physical and chemical. Physical approaches are direct, simple and involve dispersion due to mechanical force. Preparation of compositions using polymer melt is the most acceptable for industry. As a rule, the polymer/nanoadditive mixture is prepared on planetary, disk, rotary or screw mixers. The high intrinsic viscosity of the melts provides a double advantage. First, it contributes to the increase of shear stresses, which lead to the destruction of carbon clusters; secondly, a highly viscous environment with low molecular mobility prevents the re-aggregation of nanofillers. In order to improve the dispersion of nanotubes, methods of orientation of nanoparticles have been developed due to the effect on them of ultrasound and various types of fields: external uniform electric, external magnetic, non-uniform electric and uniform electrostatic fields.

The essence of chemical modification methods is to improve the affinity between nanotubes and the polymer

matrix. To increase the compatibility of the additive with the polymer, compatibilizers, surface-active substances (surfactants) are introduced into the mixture, chemical modification of the CNT surface is carried out, for example, they are covered with a layer of polymer or silica gel, surfactant adsorption, surface oxidation reaction, etc. are carried out [8,43,50,95]. The listed methods are used both individually and in combination. Chemical modification of nanotubes helps increase the homogeneity of their distribution in the polymer matrix and ensures effective transfer of stresses from it to the filler. Thus, a composite based on polyvinyl chloride (PVC) and CNTs, on which a copolymer of styrene and maleic anhydride is grafted, is characterized by 5 times higher strength, compared to a composite filled with unmodified tubes, and 37 times greater than that of the original PVC [98] . The introduction of polypropylene additives as a compatibilizer into the co-polyamide/BNT composition leads to a decrease in the percolation threshold due to the orderly distribution of nanotubes in the heterogeneous polymer matrix [99].

1.2.2.2. Polymer composites filled with nanoparticles of metals and their oxides. Depending on the chemical nature of nanoparticles of metals and oxides, polymer composites acquire new volume and/or surface properties. Volumetric properties include thermal, electrical, light conductivity, density, and other characteristics that depend on the content, dispersion, and continuity of the particle structure in the volume of the material. Surface characteristics are sorption properties in relation to various substances (liquids, gases,

ions, dyes), catalytic activity, reflectivity, color, etc. Thus, textile polyester threads filled with Ag, Zn, Cu nanoparticles exhibit biocatalytic and bactericidal properties and effectively absorb proteins, influenza viruses, and bacteria [20]. Nanofilaments filled with particles (5÷15) nm in size were obtained by electroforming from solutions of polymers containing salts of noble metals (Au, Ag, Pt) and their subsequent reduction to the nanostate. Metal-containing nanofibers exhibit high antibacterial and catalytic properties, and their threads have a prolonged bactericidal effect and are used for the production of medical textiles [100].

Введення The introduction of nanoparticles of metal oxides (TiO_2, Al_2O_3, ZnO and MgO) into textile threads provides products from them with a broad antibacterial spectrum against pathogenic flora, photocatalytic activity, protection against UV radiation, antistatic properties, resistance to abrasion [19,20]. Polypropylene fibers filled with NPs of zinc oxide in the form of nanorods are characterized, in addition to antibacterial, antiallergic and improved mechanical properties [21]. Modification of fibers with micro- and nano-sized filaments with TiO_2 and ZnO nanoparticles gives them the ability to self-clean, similar to plant leaves, insect wings, etc. [19,23].

1.2.2.3. *Polymer-silica nanocomposites.* Pyrogenic nanosized silicas are widely used to modify almost all polymers and provide nanocomposites with increased strength, stiffness, chemical resistance, as well as high sorption and bactericidal properties [62,101-104]. The reinforcing effect of aerosols correlates with the value of their

specific surface area (Sпт): the modulus begins to increase when Sпт ≥ 50 m2/g, and the degree of reinforcement increases with the increase of the specific surface area [62]. Thus, it was established that the addition of aerosols with a specific surface from 50 to 455 g/m2 in the amount of (1÷5) wt. % causes an increase in the resistance of the epoxy polymer to destruction in concentrated nitric acid. The use of A-50 silica increases the service life of samples by 1.5 times. An increase in the specific surface causes a further increase in chemical resistance: an additive of 1 wt. % of aerosol A-300 or A-455 in epoxy polymer extends the service life of the composite up to 15 days [103]. The authors [104] showed the possibility of using mechanochemical, photochemical, and radiation-chemical effects to change the structure of thermoplastics made of polyethylene and polypropylene filled with nanodispersed silica. It has been established that the action of these aggressive factors on polymers with nano-additives provides new positive opportunities for directed modification of the structure and properties of high-molecular compounds, namely the improvement of the physical and mechanical characteristics of composite materials. Studies of the effect of A-300 aerosol content on heat resistance, chemical resistance to solvents, and mechanical parameters of ED-20 epoxy resin showed that there are optimal concentrations at which the maximum values of these characteristics are achieved [101]. Yes, with an aerosil content of 4 wt. % there is minimal swelling in the solvent, the maximum heat resistance was observed in the sample that had 5 wt. % additives, and the highest strength is achieved at

a concentration of (2÷5) wt. %. At the same time, in the interval (10÷15) wt. % of air force, the strength of the composite drops sharply. By introducing SiO_2 nanoparticles into the polypropylene melt, a nanocomposite with a 35% reduced fluidity was obtained. The presence of silica threads with a specific surface area from 75 to 342 m^2/g in the PP structure improved their mechanical characteristics: the strength increased by (1.5-2.0) times, and the initial modulus by almost 2.5 times. At the same time, the hydrophilicity of the threads increases to 1.3%, and the shrinkage decreases by a factor of 2 [105]. Composite nanofibers with diameters ranging from 119 to 405 nm were obtained by electroforming from polyvinyl alcohol/silicon dioxide mixtures [106]. Modification of polyamide fibers with nanosized SiO_2 made it possible to give them bactericidal and antiseptic properties [107]. Polyvinyl alcohol (PVA) extraction from the PP/PVA/silica composite resulted in a porous material surface-modified with silica nanoparticles with hydrophilic or hydrophobic properties [108].

  1.2.2.4. Polymer-silicate nanocomposites. The surface of natural clays (layered silicates) is hydrophilic and polar, which facilitates wetting and penetration into the space between the layers of substances that have polar groups in their structure. At the same time, due to the high hydrophilicity of the surface of silicates, melts of nonpolar and weakly polar polymers do not wet their particles well, which prevents the uniform distribution of plates in the polymer matrix. Therefore, to create polymer-silicate composites, clay must be modified beforehand. The nature of

the packing of the modifier molecules in the interlayer space determines the distance between the silicate plates, the organophilicity of the clay interlayer space and, as a result, the structure of nanocomposites when mixing silicates with polymers.

The use of clays with different values of the cation exchange capacity, the selection of organic cations for modification, the directed formation of organophilic layers and taking into account the properties of the polymer matrix make it possible to obtain composites of several types. The first type of structure is a two-phase composite with separate clay phases in the polymer. In the case when individual elongated polymer chains penetrate into the interlayer space of clays, an ordered structure of polymer and silicate layers is formed. At the same time, the clay layers are pushed apart by (2-3) nm and a second type of structure, the so-called intercalated, is formed. In composites of the third type, the clay is delaminated, disoriented and thinly dispersed in the polymer matrix with the formation of exfoliated or delaminated structures [48,109]. For the nanocomposite based on layered silicate and polyamide-6, which contained 4.7 wt. % additives, modulus of elasticity and strength exceeded the corresponding characteristics of the original polymer by 1.7 and 1.4 times [110]. The improvement of the mechanical properties was accompanied by a 1.5-fold decrease in the coefficient of thermal expansion and an increase in the softening temperature. Polyamide-based nanocomposites are used in industry for the production of special coatings, packaging films, car parts, electronic devices, etc. [48,111].

Polar water-soluble polymers, as a rule, spontaneously intercalate in the interplanar space of clay [48]. It is more difficult to obtain nanocomposites based on nonpolar or weakly polar polymers. Modification of polyolefins (PO) with nanoclays is of considerable interest, as they are widely used in industry, and their production accounts for more than half of all polymers produced in the world. The incompatibility of hydrophilic clays and hydrophobic POs is a fundamental problem that must be eliminated when developing such nanocomposites. For a better distribution of nanoclays in the polymer matrix, it is proposed to preliminarily obtain a PE/silicate superconcentrate, which is then introduced into polyethylene. The films obtained in this way have an intercalated structure and are characterized by increased strength [48]. Nanocomposites with an exfoliated structure, which are synthesized in situ on the basis of ultrahigh molecular weight polyethylene and layered aluminosilicates, also have a complex of improved mechanical indicators [112]. High-modulus fibers with modulus of elasticity (25÷28) GPa and strength (0.65÷0.70) GPa were formed by processing ultrahigh molecular weight PE filled with modified montmorillonite [113]. An effective method that allows obtaining both intercalated and exfoliated structures is the use of co-modifiers (usually functionalized low molecular weight polyolefins) [114,115]. Polymer-silicate composites are characterized by low gas permeability, improved heat and fire resistance, high ionic conductivity and low coefficient of thermal expansion. Thus, the gas permeability of polyethylene films for food packaging, which contain (2÷3) wt. %. clay,

decreases several times. When introducing (5÷7) wt. % additive changes the nature of the combustion of the PE/clay composite: the resistance to thermal action increases, the burning rate decreases, the molten polymer does not drip [109].

Thus, the properties of polymer-silicate nanocomposites depend on the distribution of the additive in the matrix and the type of structure obtained.

1.2.2.5. Nanocomposites with bifunctional additives. The most studied bifunctional additives are substances in which nanoparticles of metals or oxides are applied to a mineral or organic base of micro- and nanosize (activated carbon, zeolites, silicas, etc.), while they combine the properties of both components. Thus, a silver-containing nano-additive obtained by glucose reduction of Ag+ ions adsorbed on the surface of silica particles gives polypropylene monofilaments improved mechanical and manipulation properties [116]. The modified threads are monolithic, have a smooth surface, are uniform in diameter along the length, retain the high hydrophobicity inherent in the original polypropylene. They have an antimicrobial effect, are biologically compatible with living tissues and can be used as a surgical suture material. Polystyrene/Ag/SiO_2 nanocomposite is characterized by high antibacterial activity against a number of strains of microorganisms. Using it as an antiseptic additive made it possible to reduce the consumption of silver and, thus, reduce the toxicity and cost of products [63]. Biochemical activity is demonstrated by materials filled with bifunctional substances with Ag nanoparticles on organic matrices

50

(activated carbon, carboxyl cation exchangers) and on porous aluminum oxide. Alumina-based materials have the maximum bactericidal effect [64,65,67]. Antimicrobial complex substances synthesized by coating Ag, Cu, and Zn nanoparticles on the surface of titanium dioxide (TiO_2) or silicon particles are used to provide antibacterial properties to textile materials and polymer products [106,117]. Polyvinyl alcohol nanofibers filled with Ag/TiO_2 composite additive nanoparticles have a high specific surface area (200 m^2/g), the presence of silver provides them with bactericidal properties, and TiO_2 provides photocatalytic activity and the ability to protect against UV radiation [20]. The introduction of the bifunctional additive TiO_2/SiO_2 into polymers makes it possible to create a new generation of effective nanocomposites for the treatment of industrial effluents and waste disposal [118]. Such materials combine the photocatalytic activity of TiO_2 and the sorption properties of silica and, in terms of their characteristics, exceed ion exchange resins (at the same time, they are 5 times cheaper).

1.2.3. Composites based on nanofilled polymer mixtures. The properties of composites from nanofilled thermodynamically incompatible polymer mixtures are determined by the type of structure formed by the dispersed phase in the dispersion medium, the characteristics of the nanoadditive, and its predominant placement in the system. Targeted control of the morphology of polymer dispersions by the introduction of nanoparticles makes it possible to significantly improve the performance of products made from them, as well as their rheological properties and recyclability

[119]. An increase in the mechanical characteristics, impact strength, and elasticity of polymer mixtures takes place under the condition that they are filled with mineral nanoadditives [3-6,9,24,27,68,120], which is achieved due to the action of a number of factors. First of all, solid nanodisperse fillers affect the thermodynamic compatibility of two-phase polymer systems and their morphology, which determines the properties of composites. The size and high specific surface area of nanoparticles are also important, which ensures the formation of a large number of different types of physical connections between them and chains of macromolecules in the transition layer. The probability of simultaneous breaking of several such bonds is much lower than that of one chemical bond, so relatively weak physical forces ensure strong adhesion between macromolecules of the polymer and the filler. At the same time, the mixing sequence of the system components has a significant influence, which determines the degree of filling of the phase separation boundary with a nano-additive [120]. The best results are achieved under the condition of preferential localization of NPs in the interphase zone.

By changing the morphology of PP/elastomer mixtures by introducing conductive nanofillers, composites with improved impact strength and electrical conductivity were obtained. Their microstructure was regulated by using one-stage and two-stage processes. In the first, the elastomer and filler were mixed directly in the PP melt, and in the second, the nanoadditive was dispersed in the elastomer and then the composition was added to the matrix. Two-stage mixing made it possible to improve the phase morphology of the system,

which became a decisive factor for achieving the best indicators of electrical and mechanical properties of the composition [17].

The introduction of highly dispersed conductive fillers into incompatible polymer mixtures makes it possible to reduce the concentration of the additive needed to lower the percolation threshold, compared to individual components. Nanoparticles form continuous structures in the system, as a result, the composition becomes a conductor of electric current. The formation of a percolation-type network of carbon nanotubes under the condition of increasing their local concentration in the volume of phases or at the boundary of their separation was confirmed by electron microscopy [121]. A sharp decrease in the percolation threshold is achieved under the condition of selective localization of CNTs in the transition layer [122,123].

Polymer compositions with the morphology of continuous and interwoven structures are widely used. The additional introduction of nanoparticles into them contributes to the reduction of the geometric dimensions of the morphological elements and the improvement of mechanical and electrical properties, expands the possibilities of their purposeful control [124]. Thus, the addition of silicon dioxide nanoparticles with different polymerophilicity to the polyethylene/polyethylene oxide mixture to the components counteracts the coarsening of the composite structure. The greatest effect was achieved when using hydrophobic silica NPs [79].

Nano additives also allow modification and use of

polymer waste. Mixing secondary polyvinyl chloride (PVC) with polypropylene and a small amount of nanoparticles of surface-modified calcium carbonate makes it possible to produce a composite containing up to 30% of PVC [13]. At the same time, the nano-sized filler lowers the melting point of PP and does not affect the thermo-oxidative destruction of PVC. For mixtures based on secondary PET filled with nanoparticles of silica or alumina, a significant improvement in their mechanical characteristics has been established [14,125]. Enhancement of the modifying effect of nanoadditives in secondary polymer mixtures is achieved with the simultaneous use of nanoparticles and compatibilizers [15,16].

Nanofillers are used to regulate the morphology and properties of compositions based on biodegradable polymers. The study of the structure of thermoplastic starch/polylactide (TPK/PL) mixtures using electron microscopy showed a significant influence of the clay content on the morphology of the system and the mechanical characteristics of the composites [126,127]. When adding a polyamide (PA-11)/PL organoclay mixture to the PA-11 phase, its structure changes qualitatively, a transition from a drop-matrix to an interwoven type takes place. As a result, the heat resistance of the composition increases [128]. When filling this mixture with halluisite nanotubes, its physical and mechanical properties improve. The method of morphological analysis established a significant interaction between the two polymer phases through hydrogen bonds, the presence of migration of tubes during the mixing process and their selective localization in one of the phases. The formation of the fibrillar structure of the polyamide phase

in the presence of a nanofiller contributed to an increase in the plasticity of the composite material without a negative effect on its stiffness and strength [128].

To find the optimal balance between strength and impact toughness, nanoparticles of silicon dioxide were introduced into the mixture of PL/PE and PL/thermoplastic polyurethane [129,130]. Interphase-adsorbed silica NPs increase adhesion between components at the separation boundary. At the same time, the impact viscosity increases, and the strength and modulus of elasticity remain at a high level, which is associated with the transition from a droplet to a network structure of the composition.

On the basis of polymer nano-filled composites, materials with an adjustable porous structure are obtained by selective removal of one of the components, while nanoparticles can also be used as an effective tool for creating a mixture with the required morphology. Thus, microporous polymer membranes are obtained by the so-called template method [131-133]. The porosity of the material and the average diameter of the pores were adjusted by changing the number of particles of organomodified montmorillonite in the film [131]. Polyethylene membranes with antibacterial properties for water purification were obtained from a PE/polyethylene oxide (PEO) mixture filled with graphene oxide nanoparticles by dissolving PEO in water [132,133]. Composites of polypropylene and water-soluble polyvinyl alcohol are environmentally friendly semi-finished products for the production of porous materials [108]. Their morphology was regulated by changing the ratio of components, as well as by

introducing polar and nonpolar NPs of silicon dioxide. Increasing the PVA content to (40-50) wt. % contributes to the formation of a continuous morphology, and SiO_2 nanoparticles are localized in the system in accordance with their polymerophilicity to the components. A porous material made of PP modified on the surface of silica NPs is obtained by further extraction of PVA.

Thus, the introduction of nanoparticles into polymer composites makes it possible to purposefully control their microstructure and obtain materials with improved predetermined characteristics.

1.3. Polymer composites with microfibrillar morphology

1.3.1. The mechanism of microfibrillar structure formation in polymer mixtures. A melt mixture of two incompatible polymers is a two-phase system in which one component (disperse phase) is distributed in a certain way in another (dispersion medium). At the same time, polymer mixtures are specific colloidal systems, in which there are interphase layers, the properties and length of which depend on the degree of compatibility of the components in the melt [68]. The characteristics of the interphase layer differ from the similar indicators of the bulk phases of the components. This layer is compatible with the materials of both phases and ensures the transfer of stresses from the dispersion medium to the dispersion phase and stabilization of the structure of the polymer system. The technological and operational properties of polymer composites are largely determined by their

morphology, that is, the mutual distribution of components, the type, size and shape of structures formed by one polymer in another. The following types of structures can be formed during the melt flow of a mixture of two viscoelastic liquids: dispersion of drops, jets (cylinders), layers (films), continuous interwoven structures, etc. [3,4,27,68]. It is known that during the processing of melts of two-phase systems in the dispersion medium, stresses arise that contribute to the deformation and orientation of the droplets. With small velocity gradients, the drop takes the shape of an ellipsoid of rotation, and with large ones, it turns into a liquid cylinder. A special place among polymer systems is occupied by matrix-fibrillar composites. Under the conditions of mixing and processing of mixtures, the component of the dispersed phase forms *in situ* micro- and nanofibrils in the matrix polymer [3-5, 12, 24-27]. Composites with fibril diameters (10÷100) μm are called microfibrillar (MFC), and in the range of less than 100 nm - nanofibrillar (NFC) [24]. Bundles of micro- and nanofibrils are obtained by extraction of the matrix polymer with a solvent inert to the component of the dispersed phase. Thus, polybutylene terephthalate (PBTF) and polytetrafluoroethylene (PTFE) nanofibers were obtained by forming a jet from a melt of PBTF/PP and PTFE/PL mixtures with a composition of 20/80 wt. % on a capillary viscometer followed by thermal extraction. At the same time, polypropylene was extracted with hot xylene, and PL with chloroform. The average diameter of PBTF fibers was 600 nm, and the length was 100 μm; the diameters of polytetrafluoroethylene nanofibers ranged from 100 to 500 nm (Fig. 1.11) [25].

<center>a)   b)</center>
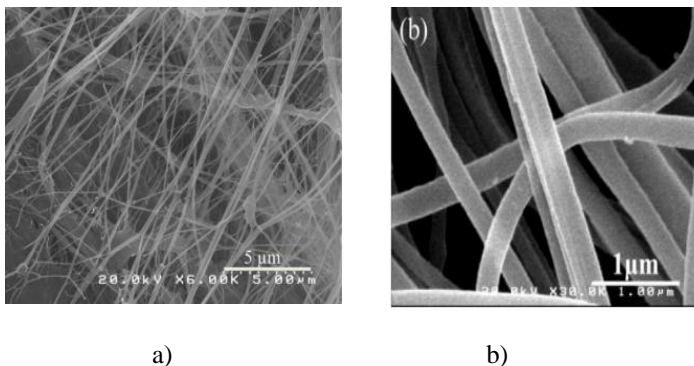
<center>Fig. 1.11. Electron micrographs of PTFE (a) and PBTF (b) nanofibers</center>

Microfibrillar morphology in polymer mixtures is currently realized for many pairs of polymers by methods of extrusion, blowing, uniaxial stretching and 3D forming. For the formation of a matrix-fibrillar morphology, the liquid droplets of the dispersed phase must deform and merge in the direction of the flow and maintain a constant shape until the moment of solidification, i.e., the processes of deformation, capillary instability, coalescence, as well as the extent and properties of the transition layer are important. Fundamental studies of microfibrillar structure formation were first conducted at the Kyiv National University of Technology and Design. As a result, the mechanism of this phenomenon was proposed and experimentally confirmed [134]. On the equipment used for processing polymers, there are zones where the melt flows from a wide tank to a narrow one. The transition can be smooth (convergent channels) and sharp (flat entrance with an entrance angle of 180^0). With such a flow geometry, longitudinal and shear deformation are superimposed on each other, the flow lines converge, forming a cone. Only tensile stresses act on the

<center>58</center>

flow axis, which originate far from the entrance to the forming hole, grow in magnitude and reach a maximum already in the hole itself [3,68]. Using the example of a polyoxymethylene/copolyamide (POM/SPA) mixture, it is shown that as tensile stresses arise in the viscosymmetric tank, the POM drops begin to deform and orient in the direction of the flow lines in the SPA matrix. The elongated shape of the droplets leads to their contact through thin layers of the polymer-matrix and the formation of liquid jets (fibrils), the deformation and thinning of which continues until the tensile stresses reach their maximum value. This happens when the distance to the entrance to the channel is (0.2-0.3) of its diameter. Later, the tension relaxes, which is accompanied by a slight increase in the diameters of the microfibrils and a violation of their parallelism. In the channel of the forming hole, under the action of shear stresses, the jets are stretched again and become parallel. Thus, a structure is formed, which is a continuous phase of the dispersion medium, filled with tens of thousands of thin jets of the dispersed phase (Fig. 1.12) [27].
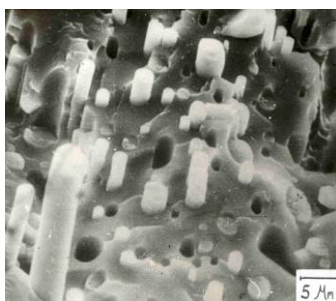
Fig. 1.12. Electron micrograph of a cross-section of an extrudate of a polyoxymethylene/copolyamide mixture

The formation of microfibrils from individual droplets of the dispersed phase in the entrance zone of the forming hole was also confirmed by microscopic studies of longitudinal sections from the zone of the viscometric reservoir of the POM/ethylene copolymer with vinyl acetate (SEVA) mixture flow (Fig. 1.13) [27].
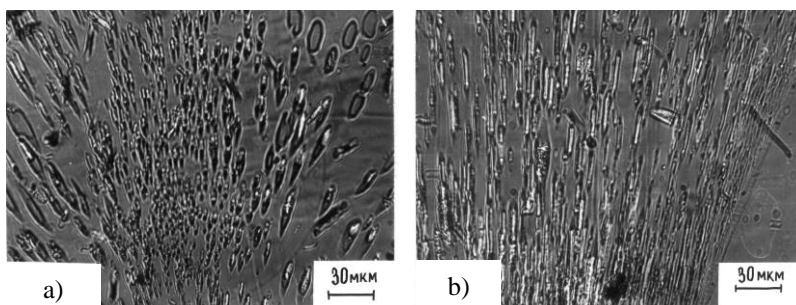
Fig. 1.13. Micrographs of longitudinal sections of extrudates of the
POM/SEVA mixture:
a) at the initial stage; b) closer to the entrance to the spinning mill

As can be seen from fig. 1.13a, the polymer droplets of the dispersed phase are oriented and deformed in the direction of the flow, when tensile stresses begin to arise in the tank. The deformation reaches maximum values on the flow axis and decreases as the angle between the flow direction and the axis of rotation of the ellipsoid (deformed POM droplet) increases. The degree of deformation increases with the approach of POM drops to the entrance to the forming hole of the die (Fig. 1.13b). The different degree of deformation of POM droplets in the downstream flow is one of the reasons, along with aggregation, for the formation of POM microfibrils with a wide distribution of diameters.

1.3.2. Factors affecting the formation of microfibrillar structure

1.3.2.1. Chemical nature of polymers. One of the most effective factors for regulating the parameters of the phase structure is the affinity (compatibility) of the components, that is, the ability of polymers to spontaneously mix with each other at the level of macromolecules. Low affinity leads to high interfacial tension and complicates the dispersion and deformation of components during melt processing. If they are fully compatible, homogeneous homogeneous melts are formed. The best compatibility is achieved not between polymers of similar chemical structure, but when the macromolecules of the components have functional groups that complement each other and can form hydrogen, ion-dipole, dipole-dipole bonds, etc. These types of intermolecular interactions were called specific interactions [135]. For MFC formation, incompatible polymers with a certain degree of interaction between their macromolecules are chosen, which will ensure the formation of a transition layer of sufficient length and the transfer of stresses from the matrix to the dispersed phase. Table 1.1 shows the results regarding the influence of the chemical nature of the polymers on the average diameter of microfibrils of the dispersed phase (d) in the matrix and the mass fraction of the types of structures formed during the melt flow of the mixture [27]. Of the investigated mixtures, the microfibrillar structure is worst realized in the PE/SPA melt flow: polyethylene fibrils have the maximum diameter, while other types of structures (particles, short fibrils, films) are present in the extrudates. This is due to a significant difference

in the chemical nature of the indicated polymers, which causes the insignificant length of the interfacial layer and the weak interaction between PE and SPA macromolecules.

Table 1.1. The influence of the chemical nature of the components of the polymer mixture on the formation of microfibrillar morphology

The name of the mixture	Microfibrils		The fate of other types of structures, weight %		
	d, μm	share, weight %	short fibrils	particles	films
PE/SPA	9,0	81,2	1,6	0,2	17,0
POM/PS	8,1	98,6	-	-	1,4
POM/SEVA	5,5	100	-	-	-
POM/PVS	5,0	68,0	-	-	32,0
POM/SPA	3,9	86,5	3,0	0,5	10,0

For the POM/SPA pair, strong hydrogen bonds between their functional groups contribute to sufficiently high compatibility of the components at the phase separation boundary, so the microfibrils have the smallest average diameter. At the same time, it can be the reason for the formation of short fibrils and particles during the flow of the melt of this mixture. The most perfect morphology is formed in the POM/SEVA mixture, in which POM microfibrils are the only type of structure. As for the POM/PVA mixture, both of its components are polar polymers, specific interactions can form between their macromolecules, and the interfacial layer has a sufficient length, which causes the formation of current fibrils (d = 5.0 μm).

Thus, changing the chemical nature of polymers allows controlling the processes of structure formation during their flow due to the influence on the interaction of components in the interphase layer and the intensity of deformation. For the formation of microfibrillar composites, mixtures with specific interactions between the macromolecules of the original polymers are best suited.

1.3.2.2. Rheological properties of component melts. The formation of matrix-fibrillar morphology is significantly influenced by a number of microrheological processes, namely: deformation, capillary instability, and coalescence. Classical studies of the deformation of a droplet in a matrix environment showed that it depends on the ratio of the viscosities of the polymer droplet of the dispersed phase (η) and the matrix (μ) ($K = \eta/\mu$), as well as the Weber number: $We = \mu \gamma r / \gamma_{\alpha\beta}$ (γ – local shear stress, r - is the radius of the droplet, $\gamma_{\alpha\beta}$ - is the interfacial tension). For polymer melts, an additional factor is the elasticity of the components, which is indirectly characterized by the amount of equilibrium swelling of the extrudates (B) [68]. The deformation of drops of one polymer in the matrix of another is determined by shear stresses, which are caused by viscosity, as well as by the distribution of pressure around the drop, which occurs due to the elasticity of the components of the mixture. According to the theory of classical hydromechanics, the ratio of viscosities of the components should be close to unity, and its deviation in one direction or another contributes to an increase in the size of the dispersed particles. In the melts of polymer dispersions, a change in the ratio of the viscosities of the melts of the

dispersed phase and the matrix (η/μ) and their elasticities (B_1/B_2) can shift the equilibrium in the processes of deformation and coalescence of droplets and the disintegration of liquid cylinders [27]. Experimental data on the influence of the rheological properties of the polymers of the mixture on the formation of the microfibrillar structure are shown in Table 1.2.

Table 1.2. The influence of the rheological characteristics of the components of the polymer mixture on the formation of microfibrillar morphology

The name of the mixture	η/μ	B_1/B_2	Microfibrils		The fate of other types of structures, mass. %		
			d, μm	share, weight %	short fibrils	particles	films
POM/SEVA	0,65	0,92	6,9	89,0	-	-	11,0
POM/SEVA	1,05	0,92	5,5	100	-	-	-
POM/SEVA	1,67	0,92	6,2	80,0	-	-	20,0
POM/SEVA	8,64	0,92	8,5	75,1	-	0,1	24,8
POM/SEVA	10,77	0,92	10,2	4,7	52,3	43,0	-
POM/PVS	0,31	0,80	5,0	68,0	-	-	32,0
PE/SPA	1,00	2,4	9,0	81,2	1,6	0,2	17,0

Quantitative microscopic studies of the influence of the ratio of viscosities of mixed polymers on the formation of microfibrils in the matrix were carried out for many mixtures [27]. This issue was studied in the most detail on POM/SEVA mixtures with a composition of 20/80 wt. %. The ratio of viscosities of the polymer of the dispersed phase and the matrix varied widely (0.65÷10.77) and was achieved by using POM with different molecular weight and SEVA with different

content of acetate groups. Analysis of table data. 1.2 shows that the most clearly studied phenomenon is expressed by the η/μ ratio close to unity: the average diameter of microfibrils is minimal, there are no undesirable types of structures (films, particles, short microfibrils).

Provided that the viscosity of the polymer melt of the dispersed phase is an order of magnitude higher than μ of the matrix, only a small part of the POM forms continuous microfibrils, and the rest of it is in the extrudate in the form of short fibers and particles. In this case, POM drops, passing through the entrance zone, are slightly deformed and almost do not form continuous microfibrils, but retain their original dimensions in the extrudate. This is consistent with theoretical generalizations and experimental results regarding the important role of the viscosity of the dispersion medium in the formation of the morphology of polymer compositions [68]. For the PE/SPA mixture, even with the best ratio of melt viscosities ($\eta/\mu = 1$), the degree of deformation of the dispersed phase is 1.7 times lower, compared to the POM/SEVA system. This is due to the high elasticity of the polyethylene melt ($B = 2,4$) and the associated resistance to stretching and shifting of drops. A significant difference in the viscosities of the POM and SEVA melts contributes to the radial migration of dispersed phase droplets to the walls of the capillary and the formation of a large number of films (32 wt. %).

Thus, the ratio of viscoelastic properties and the absolute values of viscosities and elasticities of melts of mixed polymers are important factors for the formation of

microfibrillar morphology in thermodynamically incompatible polymer mixtures.

1.3.2.3. Composition of the mixture. Numerous studies of the processes of structure formation in thermodynamically incompatible mixtures of polymers show that the in situ formation of microfibrils of one polymer in the matrix of another is significantly influenced by the ratio of their components. At the same time, the content of the component of the dispersed phase can be within wide limits - (10.0÷50.0) wt. % and is determined by the chemical nature and rheological properties of the ingredients [24,27,29,136]. The results of the study of the influence of the composition of the mixture on the microstructure of extrudates are shown in Table 1.3.

For all the investigated mixtures, the process is most clearly realized with a ratio of dispersed phase and matrix of 20/80 by mass. %: microfibrils are the predominant type of structure in the extrudates, and their diameters are minimal. For a composition of 30/70 wt. % in the mixtures, aggregation processes increase, which leads to an increase in the diameters of fibrils, as well as the proportion of films. If the polymer concentration of the dispersed phase is further increased in PP/SPA and POM/SEVA mixtures, along with rather thin fibrils, more than 50 wt. % of layered structures, i.e. there is a phase inversion that occurs in the range of 40/60 and 50/50 mass ratios. %. At the same time, for the PET/PP mixture, the microfibrillar structure is formed at a PET content of ≤ 30.0 wt. %, which is clearly visible from electron micrographs of PET residues after PP extraction from extrudates of PET/PP mixtures of different composition (Fig. 1.14).

Table 1.3. Dependence of the microstructure of extrudates of mixtures on their composition and the chemical nature of the components

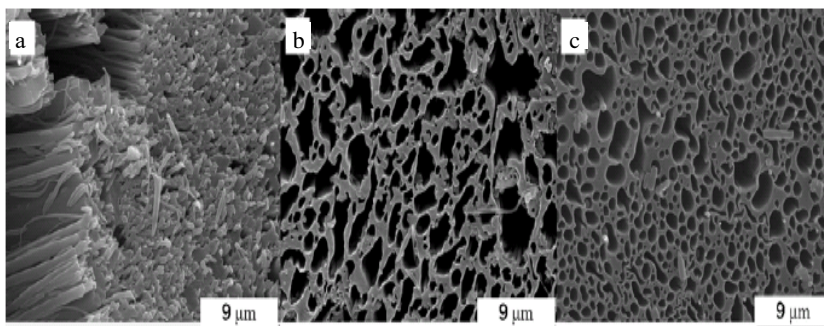| Ratio of components, mass. %	Types of structures			
	Microfibrils		particles, weight %	films, weight %
	d, μm	share, weight %		
PP/SPA mixture				
20/80	3,6	86,4	6,4	7,2
30/70	4,0	82,7	8,3	9,0
40/60	7,8	45,7	1,9	52,4
50/50	The microfibrillar structure is not realized			
PP/PVA mixture				
20/80	3.0	89,5	3,2	7,3
30/70	3.5	86,5	3,8	9,7
40/60	4.0	84,0	3,7	12,3
50/50	3.5	81,9	4,0	14,1
POM/SEVA mixture				
10/90	5,2	100	-	-
20/80	5,5	100	-	-
30/70	8,0	96,7	-	3,3
40/60	9,5	93,3	-	6,7

Fig. 1.14. Electron micrographs of PET residues after extraction of PP from extrudates of PET/PP mixtures of composition, wt. %: a) 30/70; b) 40/60; c) 50/50

For mixtures of compositions 40/60 and 50/50 wt. %, it is difficult to determine which of the polymers is the dispersed phase, and which is the dispersion medium [29].

At the same time, it should be emphasized that in the PP/PVA mixtures, the microfibrillar morphology occurs for the entire studied range of compositions, including the phase change region. According to the content of polypropylene (20÷50) wt. %, microfibrils with an average diameter of (3.0÷4.0) μm are formed, which may be caused by the competing influence on the degree of polypropylene dispersion of its concentration and microrheological processes. PP/PVA mixtures contain glycerin, which can act not only as a PVA plasticizer, but also as a compatibilizer of this system. Obviously, the reduction of the interfacial tension contributes to the slowing down of the coalescence processes and the increase in the stability of the dispersion. Under these conditions, an increase in the content of polypropylene can contribute to the formation of microfibrils with smaller diameters. This is confirmed by the method of mathematical modeling of the processes of mixing and homogenization of melts of mixtures, as a result of which it was proved that the degree of dispersion should increase with an increase in the volume concentration of the dispersed phase [137].

Thus, the ratio of the components of the mixture plays an important role in the formation of the morphology of the polymer dispersion. For low polymer concentrations of the dispersed phase, the most typical structure is microfibrillar, even with significant differences in the chemical nature and rheological properties of the mixed polymers. From the point

of view of obtaining microfibrils of continuous length, the polymer content of the dispersed phase should be (20÷30) wt. %.

1.3.2.4. Stability of microfibrils and their disintegration into droplets. The final morphology of the polymer dispersion is the result of a balance between such microrheological processes as deformation and disintegration, migration and coalescence of droplets of the dispersed phase. Destruction takes place both at the stage of preparation of the composition and during processing into products and can occur under the condition that the spherical drop has deformed and formed an ellipsoid or thread-like liquid cylinder. At the same time, the forces of surface tension, which tend to maintain the spherical shape of the drop, cannot counteract the forces that deform and destroy it. Establishing the regularities of the disintegration of liquid jets (microfibrils) is important for controlling the mixing processes and the formation of the microfibrillar structure in composites. In order to preserve the formed morphology, it is necessary to slow down the decay of the microstreams.

The first theoretical study of the disintegration of a liquid cylinder was performed by Tomotica on systems in which the dispersed phase and the dispersed medium were Newtonian fluids [138]. Having analyzed the hydrodynamic stability of the jet, he showed that the cause of its disintegration is the occurrence of wave-like disturbances on the surface, the amplitude of which increases exponentially with time:

$$a = a_0 \exp(q \cdot t_{\text{ж}}), \qquad (1.1)$$

where: a_0 – the initial amplitude of the disturbance, q – coefficient of instability, $t_{\text{ж}}$ – jet lifetime.

Коефіцієнт The instability coefficient is a complex function of the wave number and the ratio of phase viscosities (*K*). The jet collapses under the condition that the magnitude of the perturbation amplitude becomes equal to its radius. The life time is directly proportional to the viscosity of the liquid, the radius of the cylinder and inversely proportional to the surface tension:

$$t_{\text{ж}} = \eta R / \gamma_{\alpha\beta} \qquad (1.2)$$

By its nature, the destruction of a liquid cylinder is a transient phenomenon. Before its disintegration, thickening and thinning are formed, which leads to an increase in surface energy, and destruction is the result of the system's desire to decrease it. According to Tomotika's theory, each value of the viscosity ratio (*K*) corresponds to a certain wavelength at which the liquid cylinder is maximally unstable. The stability of the jets in the flow increases by several orders of magnitude, which is due to the uneven growth of the amplitude of the destructive wave [138].

For viscoelastic liquids, the shape and stability of droplets in the flow are determined not only by shear stresses that arise during viscous flow, but also by stresses caused by the distribution of pressure around the droplet, that is, by their elasticity. Studies of the laws of the disintegration of polymer liquid jets have shown that, as for Newtonian fluids, the mechanism of their destruction also consists in the formation of wave-like disturbances on the surface, and the variables that

control the deformation of the drop also determine the critical conditions for the destruction of the formed cylinder. Such variables are the ratio of viscosities of melts of mixed polymers and the Weber number [27,139].

The stability of a liquid polymer jet in the matrix of another is determined by the instability coefficient, which is a complex function of the wave number (X), the ratio of the viscosities of the dispersed phase and the dispersion medium ($K = \eta/\mu$) and the value of the interfacial tension between the cylinder and the matrix ($\gamma_{\alpha\beta}$) [139]:

$$q = \left(\frac{\gamma_{\alpha\beta}}{2\eta R} \right) F(X, K)$$

(1.3)

To study the regularities of the disintegration of liquid jets of one polymer in the matrix of another, a technique was developed [139,140], based on the measurement of the growth rate of capillary waves, in accordance with the classical theory of Tomotics. Longitudinal sections of extrudates of the mixtures were placed on the heating table of the microscope, the temperature was increased at a rate of 0.6 degrees/sec, and various stages of the decomposition process were photographed. An individual microfibril can be viewed as a liquid cylinder in a matrix polymer melt that is thermodynamically unstable due to an unfavorable surface-to-volume ratio. At the appropriate temperature, it begins to break down in places of reduced cross-section under the action of interfacial tension forces and disintegrates into a chain of droplets (Fig. 1.15) [140].
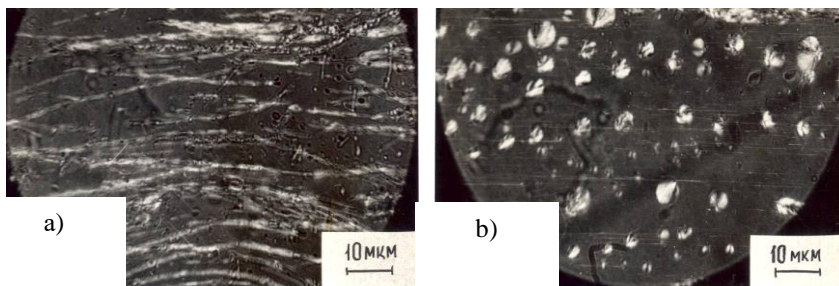
Fig. 1.15. Photomicrographs of longitudinal sections of extrudates of the POM/SEVA mixture at temperatures of ^{0}C: a – 150; b – 165

The diameters of initial microfibrils (d_0) and varicose thickenings ($d_в$), droplet radii (r) and the maximum disturbance wavelength (λ_m) were determined from the obtained photographs, as the distance between the centers of neighboring drops. After that, the initial radius of the jet (R), the wave number ($X = 2\pi R / \lambda_m$), the reduced lifetime ($t_ж /R$), the instability coefficient (q) and the surface tension ($\gamma_{\alpha\beta}$) at the phase separation boundary were calculated. The decay time ($t_ж$) was taken as the term during which the main mass of the jets in the section was destroyed. The lowest temperature at which almost all microfibrils disintegrated was recorded. This temperature determines the field of operation of products made from them, obtained by processing this mixture of polymers.

Using the methodology [140], the regularities of the disintegration of viscoelastic polymer jets in systems with different chemical nature, the ratio of viscosities and elasticities of component melts (Table 1.4) were investigated [27,32-35,79].

Table 1.4. Dependence of the parameters of the kinetics of liquid jet disintegration and interfacial tension on the chemical nature and rheological properties of the mixture components

The name of the mixture	Ratio		Coeffi-cient of instability	Lifetime , s	Reduced lifetime, s/μm	Surface tension, mN/m
	of visco-sities	of elasti-cities				
POM/SEVA	0,91	0,93	0,0243	120	46,9	1,30
POM/SEVA	1,67	0,93	0,0196	300	195,0	1,90
PP/SPA	0,33	1,31	0,0398	32,6	38,9	2,36
PP/SPA	0,51	1,57	0,0418	56,2	47,4	2,60
PP/PVA	0,83	1,43	0,0375	317	259	0,73

From the table 1.4, it can be seen that the viscoelastic properties have a significant influence on the patterns of destruction of liquid jets. For the same pair of polymers, the lifetime increases with increasing viscosity of the component of the dispersed phase, which is consistent with equation (1.2), i.e., if the droplet is highly viscous, it can be elongated to a cylinder of small radius, which will remain stable for a long time time. Systematic studies on the influence of the chemical nature of the components on the stability of liquid jets have shown that the viscoelastic properties of the dispersion medium have a greater influence on their stability than the characteristics of the dispersed phase [27].

The chemical nature of mixed polymers also determines the stability of polymer cylinders in the matrix (Table 1.4). Thus, the lifetime of microfibrils in POM/SEVA and PP/PVA

mixtures is almost 5 times higher than in PP/SPA, which is due to the different degree of interaction between the components in the transition layer. An indirect characteristic of the compatibility of polymer macromolecules in the zone of their contact is the value of the interfacial tension ($\gamma_{\alpha\beta}$), which can be used to judge the surface energy, structure, and length of the transition layer. Experimental measurement of $\gamma_{\alpha\beta}$ in polymer mixtures (especially in melts) is very difficult. Using the theory of destabilization of a liquid cylinder under the action of destructive excitation waves, a method was developed to determine the interfacial tension in the melt of two polymers, one of which is in the form of liquid jets in the matrix of the other. To determine the value of the surface tension, a formula was proposed [139]:

$$\gamma_{\alpha\beta} = \frac{q\mu\, d_0}{\Omega\, f\,(X,K)} \qquad (1.4)$$

where: q – the tangent of the slope angle of the dependence curve $ln(2(d_s - d_0)/d_0)$ on the duration of heating;

Ω – tabulated function, which is determined from the dependence curve $X = f(\lg K)$.

The value of $\gamma_{\alpha\beta}$, calculated on the basis of the kinetics of decay, reaches the highest values in PP/SPA mixtures (Table 1.4). This is due to the low affinity between segments of macromolecules of non-polar polypropylene and polar co-polyamide at the boundary of phase separation. The formation of specific interactions between the functional groups of POM and SEVA causes the formation of an interfacial layer of sufficient length and reduces the surface tension. As can be

seen from equation 1.3, there is a direct relationship between the resistance of liquid jets to destruction and the value of the interfacial tension, that is, a decrease in the values of $\gamma_{\alpha\beta}$ (other things being equal) will increase their stability.

Conducted studies show that the theoretical regularities regarding the stability of liquid jets established for Newtonian fluids are qualitatively confirmed for viscoelastic systems as well. At the same time, there are significant differences in the dimensional characteristics of the decay parameters, namely: the wavelength of the disturbance and the size of the formed droplets for polymer mixtures are larger than for Newtonian ones [27,139]. The growth of the amplitude of the destructive wave slows down in the final stages of decay. Calculated according to formula 1.2 and experimentally determined life time values of the polymer cylinder differ by (2÷3) orders of magnitude. The high elasticity of the melts of the components of the dispersed phase and the matrix complicates the formation of microfibrils of one component in the matrix of another.

1.3.2.5. Technological parameters of mixture processing. The morphology of polymer dispersions can also be controlled by varying their flow conditions. The amount of shear stress (τ) is one of the determining parameters for the implementation of the process of forming microfibrils of one polymer in the matrix of another. At low values of τ, the droplets of the dispersed phase are weakly deformed and fibrils are not formed. Significant shear stresses also adversely affect the formation of the microfibrillar structure. There is an optimal value of τ at which microfibrils are the only or

predominant type of structure in the extrudate [27]. When processing melts of polymer mixtures on extrusion equipment, the formation of jets of the dispersed phase in the matrix occurs under the action of shear and tensile stresses in the zone of transition of the melt from a wide reservoir to a narrow one. The stability of the shape of fibrils is determined by the time of their disintegration, as they are thermodynamically unstable, and the duration of their stay in the forming hole [141]. The tensile stress field deforms the particles to a greater extent than the shear flow, but with a high shear rate gradient, the amount of deformation also increases [26,142]. In work [26], using the polylactide/polyvinyl alcohol mixture as an example, it was shown that spherical and ellipsoidal PL particles are elongated and merge in the jet as the extrusion speed increases. At the same time, coalescence between larger drops occurs more intensively, and drops with diameters smaller than 150 nm practically do not merge. The transition of rod-like particles of the dispersed PL phase into continuous thin fibrils in the PVA matrix occurs at the point where the axial velocity gradient reaches its maximum value. The amount of stress during the processing of the PP/SPA mixture on a single-screw extruder was adjusted by changing the size of the cells in the filtration grids and the pressure value [143]. It is shown that the most perfect morphology (the ratio between the number and size of PP microfibrils and the number of unwanted structures is the best) is formed at a pressure of $70 \cdot 10^5$ Pa and a cell size of 30 μm. An increase in shear and tensile stresses at a pressure of $90 \cdot 10^5$ Pa causes a decrease in the diameters of the fibrils.

However, at the same time, the number of particles in the strands increases, which is the result of the disintegration of the jets due to their capillary instability, which increases with a decrease in the diameter of the fibrils. The change in shear stress along the radius of the forming hole significantly affects the inhomogeneity of the microstructure of the extrudate, which manifests itself in the formation of a fibrous shell of continuous length filled with microfibrils [27].

In order to preserve the formed structure during the flow through the capillary of the forming hole, its dimensional characteristics play an important role. Thus, using the example of a mixture of polyamide/liquid crystal polymer, it was established that jets are formed in the area of the narrowing of the forming hole, which maintain the stability of the shape during extrusion through a capillary with a ratio of length to diameter (L/D) = 10 [141]. For the capillary with L/D=40, the deformation of the particles of the dispersed phase and the formation of jets were not observed. The absence of a fibrillar structure of the dispersed phase during the flow along a long capillary is associated with high shear stresses, which cause the destruction of liquid cylinders on the drop. This is due to the fact that the time of disintegration of the fibrils of the dispersed phase is significantly shorter than the average period of their stay in the capillary. An important factor influencing the formation of the matrix-fibrillar structure is coalescence. The intensive interaction of particles, which occurs at a high concentration of the dispersed phase or due to geometrical restrictions, causes their numerous collisions and subsequent

aggregation. This process leads to a change in the shape and size of the droplets of the dispersed phase.

Channels with a conical entrance zone (convergent channels) are widely used for processing polymer mixtures into products, as this allows for a more uniform distribution of stresses and the elimination of high local velocity gradients. Using the example of POM/SEVA mixtures, the influence of the angle of entry into the die (40, 60, 90, 120 and 180^0) on the formation of the microfibrillar structure was investigated [27]. It was established that POM microfibrils are formed at all investigated angles of entry into the capillary. However, its value significantly affects the quantitative parameters of the process: the microfibrils have the minimum diameter and the highest uniformity of diameter distribution at the entrance angle of 120^0. This is explained by the fact that in the convergent channel there is a more accelerated flow, compared to the flat entrance, that is, the voltages increase by as the melt flows from the tank to the entrance zone, where maximum velocities are reached [68]. In addition, at this entrance angle, there are no stagnant zones in which the melt is retained and the size of the droplets of the dispersed phase increases due to aggregation.

The formation of fibers and films from polymer melts is always associated with their longitudinal deformation at the exit from the forming hole, which is estimated by the value of the spinneret extraction (Φ) and calculated according to the ratio:

$$\Phi = (v_1/v_2)100 \ (\%) \qquad (1.5)$$

where v_1 – thread pick-up speed; v_2 – flow velocity of the melt from the forming hole

Studies of mixtures of polymers of different chemical nature confirmed a significant change in the microstructure of the extrudates in the field of the longitudinal velocity gradient: further deformation of already formed jets and fibrillization of films and coarse microfibrils occur [27]. Depending on the composition and nature of the polymers, new films can be formed as a result of a decrease in the distance between the fibrils. Longitudinal deformation contributes to the reduction of the diameter of the extrudate and its rapid cooling, which leads to a decrease in the content of particles and short fibrils. The degree of longitudinal deformation of the polymer in the mixture is determined by the intensity of interaction with another component at the boundary of the phase separation. In case of insufficient interaction of the polymers during the longitudinal deformation of the melt of the mixture, one of them may be destroyed, if the elongation ratio exceeds the permissible value for this polymer. Studies of the structure of a composite monofilament from a POM/SPA mixture have established that after longitudinal deformation, it retains a microfibrillar structure, that is, a SPA matrix reinforced with POM microfibrils with diameters of ≈ 100 nm [27]. Using the example of POM/SEVA and POM/SPA mixtures, it is shown that in the range of values of $\Phi = (0 \div 1000)$ %, the average diameter of microfibrils varies inversely proportional to the square root of the multiplicity of spinneret drawing [27]. This indicates that the components are drawn with the same multiplicity in the field of the longitudinal velocity gradient,

despite the large difference in the ability to deform the melts of each of them. Deformation of PET/PP strands at a temperature of 85 ^{0}C achieved the maximum orientation of PET fibrils in the PP matrix, reducing their diameters and increasing their length [29]. When studying the matrix-fibrillar structure in PP/PS and PE/PA-6 mixtures, it was shown that in the field of a longitudinal deformation gradient, dispersed PS formed highly oriented fibrils in the PP matrix, which migrated to the surface of the composite strand, and PA-6 microfibrils in the PE matrix, on the contrary, moved to its center. The phenomenon of migration was not observed for unextracted samples [144,145].

The temperature of their processing is an important factor that determines the morphology formed during the flow of melts of mixtures. Thus, it was shown that incompatible POM/SPA, POM/SEVA, and POM/PS systems are capable of flow at temperatures lower than the melting temperature of the dispersed phase polymer [27]. At the same time, the extrudate contains POM particles of the original size. For these mixtures, at the extrusion temperature (175÷220) ^{0}C, a microfibrillar morphology is formed, and the number of particles and films significantly depends on the temperature of the melt. At a temperature of 190 ^{0}C, only fibrils with an average diameter of 5.5 μm are formed in the POM/SEVA extrudate. An increase or decrease in the processing temperature determines the deterioration of the structure of the extrudate - a certain amount of polyoxymethylene forms short microfibrils and particles.

Thus, for the formation of comnosite with a microfibrillar structure, the fulfillment of the following

conditions is necessary and sufficient:

- the choice of thermodynamically incompatible polymers capable of specific interactions between the macromolecules of the components in the processing process, in which fine dispersion of one polymer in the mass of another is achieved and a transition layer of sufficient length is formed;

- the content of the dispersed phase component must be ≤ 30.0 wt. %

- the ratio of viscosities and elasticities of the melts of the ingredients should be close to unity;

- ensuring the stability of liquid currents (microfibrils) in the matrix after the exit of the melt from the forming hole;

- the use of extrusion equipment with a certain geometry of forming devices for the realization of specified shear and tensile stresses;

- selection of optimal processing parameters (temperature, duration, degree of longitudinal deformation, etc.).

1.3.2.6. New materials based on polypropylene microfibers and technological recommendations for their production.

Properties of complex threads from polypropylene microfibers. In this section, the properties of complex yarns (CY) made of PP microfibers formed from compatibilized PP/SPA mixtures were investigated, and their comparison with the characteristics of yarns produced by traditional technologies was carried out.

Complex threads from PP microfibers were obtained by forming composite monofilaments from binary, three- and

four-component melts of PP/SPA mixtures on a UFTP extrusion type spinning machine and extracting matrix polymer (SPA) from them. Studies of the mechanical properties of complex PP threads showed that the implementation of specific fiber formation in compatibilized mixtures of PP/SPA with a composition of 50/50 wt. % makes it possible to obtain threads with the strength of textile threads formed by traditional technology (Table 1.5). The latter indicates that the polypropylene microfibers are continuous or at least of considerable length.

Table 1.5. Mechanical properties of complex threads from PP microfibers formed from compatibilized PP/SPA mixtures of 50/50 wt. %

A mixture of polymers	Linear density, tex	Strength, sN/tex	Disconti-nuous elonga-tion, %
PP/SPA *	18	30	21
PP/SPA /5% SEVA	24	28	24
PP/SPA /3% oleate Na	25	33	22
PP/SPA /0,5% PES -5	24	38	21
PP/SPA /3% oleate Na /5% SEVA	24	42	22
PP/SPA /3% oleate Na /0,5% PES-5	23	48	21
PP/SPA /5%SEVA /0,5%PES-5	24	45	23
Textile PP thread **	30	25-45	15-30

*Threads from a mixture of composition 30/70 wt. %
** According to regulatory documents

From the table 1.5 shows that the nature of the compatibilizer affects the strength of ultra-thin PP threads: the introduction of sodium oleate and organosilicon additive PES-5 into the PP/SPA mixture improves the mechanical properties of

the threads. The addition of a binary mixture of compatibilizers is more effective in terms of increasing strength. It is known that the properties of threads are related to their structure. Detailed quantitative microscopic studies showed that the polymer of the dispersed phase (PP) in all cases forms mainly ultra-thin fibers of continuous length. This is a necessary condition for obtaining complete threads. The extrudates of the mixtures contain small amounts of other types of structures: films, particles, short fibers. The mixture of compatibilizers improves fiber formation, which contributes to the growth of the strength of complex strands of PP fibers. When studying the properties of POM microfiber threads obtained by processing the POM/SEVA binary mixture, it was shown that the thinner the microfibers and the greater their number, the higher the strength of the threads. The presence of films sharply reduces their mechanical properties. The specified regularity was also obtained by us for complex threads from PP microfibers formed from compatibilized PP/SPA mixtures. Reducing the average diameter of microfibers and the number of films in complex threads when using binary additives of compatibilizers increases the strength of the threads (Table 1.5).

It is known from the literature that PP threads are resistant to abrasion and in this respect they are inferior only to polycaproamide threads. The results of the study of the resistance of complex threads made of PP microfibers to abrasion are shown in Table 1.6.

Table 1.6. The influence of the nature of compatibilizers on

83

resistance to abrasion and shrinkage of complex PP threads

A mixture of polymers	The number of thousands of cycles to erasure	Shrinkage, % provided:	
		100^0C	120^0C
PP/SPA *	90	7,4	9,9
PP/SPA /5% SEVA	134	9,8	11,0
PP/SPA /3% Na oleate	228	9,5	12,0
PP/SPA /0,5% PES-5	1238	6,8	7,2
Textile PP thread **	516	5-6	-

*Threads from a mixture of composition 30/70 wt. %
** According to regulatory documents

The low resistance to abrasion of complex PP threads obtained from binary mixtures of PP/SPA and with additives of SEVA and sodium oleate is obviously related to the presence of microfibrils on the surface of microfibers (Table 1.6). If the PES-5 siloxane liquid is used, the number of cycles to erasure increases dramatically. The latter can be explained by the fact that after extraction of the matrix polymer, organosilicon liquids remain on the surface of the fibers and, as good lubricants, reduce the coefficient of friction [27]. This fact was established for the first time and is of great practical importance, as it makes it possible to expand the range of goods based on the investigated threads.

In order to determine the operating temperature limits of PP microfiber threads, their shrinkage was evaluated when boiling in water and at 120^0C. As can be seen from the Table. 1.6, shrinkage depends on the nature of the compatibilizer and is minimal for samples formed with PES-5 additives.

To evaluate the hygienic properties of complex threads made of PP microfibers, their capillarity, hygroscopicity, and

specific surface area were studied. It is known that polypropylene is a hydrophobic polymer with an equilibrium water absorption of $0.1 \div 0.2\%$. For PP microfibers, the hygroscopicity increases in $20 \div 39$ times (Table 1.7).

Table 1.7. Dependence of the hygienic properties of complex PP threads on the composition of the mixture

A mixture of polymers	Capillarity, $M \cdot 10^{-3}$	Hygrosco-picity, %
PP/SPA/sodium oleate; 50/50/3,0	2,1	3,5
PP/SPA/PES-5; 50/50/0,5	1,7	2,0
PP/SPA/sodium oleate /SEVA; 50/50/3,0/5,0	2,7	3,9
Textile PP thread	1,8	0,1

In our opinion, the established regularity is determined by the unusual structure of the microfiber surface. Fiber formation in the polymer matrix provides the latter with a unique surface structure that even natural fibers do not have, namely: each fiber is covered over the entire surface with ultra-thin microfibrils [27]. Capillarity and hygroscopicity depend on the chemical structure of the compatibilizer. Hydrophilic sodium oleate significantly increases these PP indicators of microfibers.

The study of the process of nitrogen sorption by fibers showed that the sorption isotherms (curves of dependence of the volume of sorbed nitrogen on its relative pressure) are S-like curves, typical for capillary-porous bodies with a developed structure of micropores (Fig. 1.16).
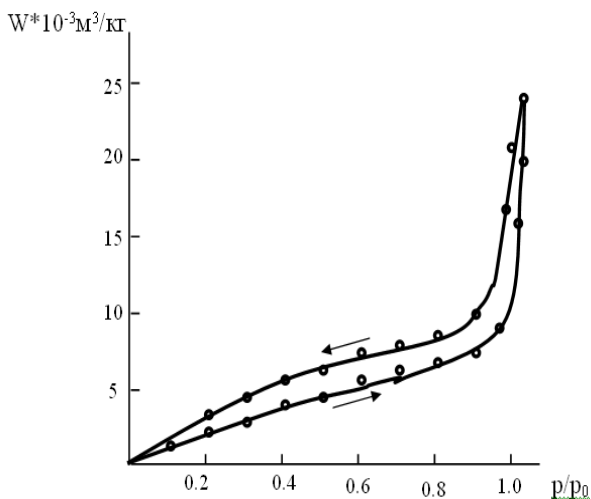
Fig. 1.16. Sorption and desorption isotherms of nitrogen by PP microfibers

A characteristic feature of isotherms is the presence of a hysteresis loop. Significant hysteresis in the entire range of relative pressures indicates unevenness of pores in diameter. It was established that PP microfibers have a mesoporous structure with a pore size of 100-1000Å. Their share is more than 90% (Table 1.8). The values of the specific surface of microfibers exceed by several orders of magnitude S_{ss} fibers with a smooth surface obtained by traditional technology, and differ among themselves, which is connected with the use of different theoretical approaches for their calculations.

Table 1.8. Characteristics of the pore structure of PP microfibers from compatibilized PP/SPA mixtures

Compatibilizer		Specific surface area, m^2/g			The volume of por, sm^3/g	
name	quan-tity, wt. %	according to the BET equation	according to the Langmuir method		summa-ry	meso-pore
			sorption	desorption		
PES-5	0,3	12,64	11,38	12,03	0,0335	0,0328
Oleate Na	3,0	12,83	8,82	12,90	0,0503	0,0494
SEVA/ PES-5	5,0/ 0,3	16,07	9,33	15,28	0,0427	0,0401
Textile thread*		0,69	0,56	0,12	0,0005	0,0002

* formed according to traditional technology

The developed specific surface provides fibers with high sorption properties. This is confirmed by the ability of polypropylene microfibers to absorb petroleum products at the level of natural sorbents (Table 1.9).

Table 1.9. Absorption capacity (kg/kg) of PP microfibers

Microfibers from a mixture of polymers	Diesel			Motor oil					
				original			worked out		
	Duration of contact, hours								
	1	16	24	1	16	24	1	16	24
PP/SPA; 30/70	3,3	3,4	3,5	3,5	3,7	3,7	3,8	3,9	4,0
PP/SPA /PES-5; 50/50/0,5	4,8	4,9	5,0	5,2	5,3	5,2	5,2	5,2	5,4
Mineral sorbent - glauconite	4,5	4,7	4,7	4,5	5,6	5,6	4,2	5,1	5,1

The sorption process ends in the first hour and does not change with contact duration of 16 and 24 hours, which indicates a high rate of sorption of mineral oils. The sorption effect is the same for clean and used oils.

Conducted studies have shown that ultra-thin PP fibers, like fibers formed by traditional technology, have a negative electrostatic charge. In terms of magnitude, it exceeds the charge of natural skin and is (-0.3) mV. All this once again confirms that the formation of microfibers from melts of polymer mixtures makes it possible to obtain fibers and threads that have new, unique properties.

New filter materials based on ultra-thin polypropylene fibers

Today, the issue of protecting people from the harmful effects of the environment is acute. One of the most simple, reliable and economically feasible methods of cleaning water, atmospheric air and process gases from highly dispersed aerosols is microfiltration through thin fiber filters. In practice, filter materials (FM), which are called Petryanov filters (FP) have been used for a long time and are widely used. They are characterized by high cleaning efficiency and productivity with low aerodynamic resistance. However, the technology of their production is complex, expensive and environmentally very harmful, since FPs are obtained by molding from polymer solutions. In recent years, new methods of manufacturing thin-fiber FM from polymer melts have been widely developed: high-speed extraction of fibers from the melt (melt-spinning), aerodynamic spraying of the melt in the form of fibers with a jet of compressed air (melt-blowing), and the formation of

ultra-thin synthetic fibers by processing the melt of the polymer mixture.

KNUTD has created a fundamentally new technology for the production of highly efficient precision thin-fiber FM by processing melts of polymer mixtures [27]. The technology is distinguished by the simplicity of processes, high productivity, low energy consumption, and the absence of harmful emissions into the atmosphere, soil and water bodies. The resulting filter materials are precision fiber depth filters that do not have the main drawback of fiber FMs, namely: erosion of the filter layer and leaching of short fibers by filtrate.

In this section, the results of the study of the properties of FM formed from compatibilized PP/SPA mixtures (Tables 1.10, 1.11) are given.

Table 1.10. Efficiency of atmospheric air filtration FM from the mixture PP/SPA/PES-5 composition 35.0/64.9/0.1 wt. %*

Particle size, μm	Concentration of particles, pcs./dm^3		Efficiency,%
	before the filter	after the filter	
1,5	765	0	100
1,0	1129	0	100
0,8	1935	0	100
0,6	2645	0	100
0,5	3239	1	99,97
0,4	4864	2	99,95
0,3	15270	11	99,92

*Results of tests on the AZ-5 meter

In earlier studies [27], it was shown that the introduction of sodium oleate or SEVA into the PP/SPA mixture in amounts of 3 and 5% of the PP mass, respectively, made it possible to create FM with a fineness of cleaning of 0.45; 0.3 μm by processing melts of mixtures of composition 40/60; 50/50 wt. %. The results of this work show that similar effects can be obtained when using 0.1 wt. % siloxane liquid of the PES-5 brand (Table 1.10). The latter is explained by the high efficiency of PES-5 from the point of view of the implementation of specific fiber formation. As expected, filter materials formed from four-component mixtures have even greater efficiency (Table 1.11). It is known that filtration through precision fiber filters occurs according to the following mechanism: polluted air passes through the FM, particles larger than 5 micrometers get "stuck" in the gaps between the fibers of the upper layer of the filter. This is the so-called "sieve" effect, which does not play a decisive role in the precise purification of gases.

Table 1.11. Efficiency of atmospheric air filtration from particles with a size of 0.3 microns FM based on PP microfibers *

Mixture of polymers	The number of particles after the filter, pcs./dm^3	Efficiency, %
PP/SPA/Na Oleate/SEVA; 50/50/3/5	3	99,98
PP/SPA/SEVA /PES-5; 50/50/5/0,5	0	100
PP/SPA/Na Oleate /PES-5; 50/50/3/0,5	0	100

*Results of tests on the AZ-5 meter

Therefore, further precision filtration takes place due to a number of physical and chemical processes - the effect of contact, adsorption, Brownian diffusion.

Analysis of table data. 1.10, 1.11 shows that the FMs developed by us effectively retain particles in a wide range of sizes, which is due to the high uniformity of the structure of the filter layer. The latter is due to the orientation of the microfibers in the direction of the flow, a decrease in their diameter and an increase in the density of FM due to an increase in the PP content up to 50 wt. % in compatibilized mixtures.

Comparative tests on air purification, conducted at the Institute of Electric Welding named after E.O.Paton of the National Academy of Sciences of Ukraine showed that the effectiveness of the retention of the solid component of welding aerosol (TSZA) by the developed FM is the same as that of the Petryanov filters (Table 1.12). The sizes of toxic aerosols are tenths and hundredths of a micrometer. The obtained result confirms that filtration through these FMs is not purely "sieve" in nature, but is also carried out due to adsorption and electrostatic interaction. The presence of a negative charge on the filter material strengthens the intermolecular interaction in the particle-fiber system and thereby improves filtration.

Table 1.12. Effectiveness of atmospheric air filtration from
welding aerosol contamination

Name of filter material (FM)	The mass of the TSZA filter, kg $\cdot 10^{-3}$	Efficiency, %
Petryanov filter	0,4859	99,90
FM from a mixture of PP/SPA/PES-5 composition 35,0/64,9/0,1	0,4847	99,65
FM from a mixture of PP/SPA/SEVA/ PES-5 composition 50/50/5.0/0.3	0,4863	99,92

To evaluate the properties of FM in cleaning liquid media, the dependence of productivity (Q) on pressure (P) was studied (Fig. 1.17).
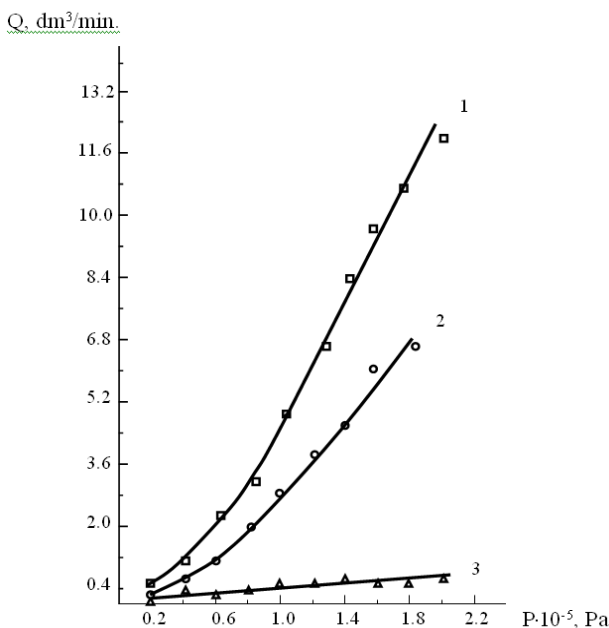

Fig. 1.17. Dependence of productivity on pressure for FM from mixtures
of PP/SPA/oleate Na/PES-5 composition:
50/50/3.0/0 (1); 50/50/0/0.5 (2); 50/50/3.0/0.5 (3)

The dependence $Q = f(P)$ is nonlinear, which indicates a change in the FM structure under the influence of pressure. This is natural for thin-fiber depth filters that do not have pores with a clear size. The nature of the compatibilizer significantly affects the value of productivity under the conditions of all investigated pressures. Sodium oleate gives hydrophilicity to the filter layer made of PP microfibers, therefore curve (1) lies much higher than curve (2). If PES-5, which is hydrophobic, is used, the ability to wetting deteriorates, which is manifested in a drop in productivity. The introduction of a binary mixture of compatibilizers made it possible to obtain a fundamentally new FM, which has cleaning efficiency and productivity close to the similar characteristics of the polyvinyl alcohol membrane "Hemofil" with a pore diameter of 0.25 micrometers.

Studies performed in the bacteriology laboratory of the Institute of Veterinary Medicine of the Ukrainian Academy of Veterinary Sciences showed that FM obtained from compatibilized mixtures of PP/SPA/PES-5 with a composition of 50/50/0.3 and PP/SPA/SEVA/PES-5 with a composition of 50/50/1.7/0.3 wt. % provide sterilization of solutions containing the causative agent of anthrax and Pasteurella.

Thus, the introduction of compatibilizers into binary mixtures of PP/SPA makes it possible to obtain more precise (up to membrane) FMs, which are characterized not only by high filtering properties, but also by sorption properties. This once again confirms that polymer materials with new unique characteristics can be obtained by forming microfibers from melts of polymer mixtures.

Technological schemes for the formation of PP microfibers from compatibilized PP/SPA mixtures

The production of polypropylene fibers in the world is developing at an accelerated pace. Due to the complex of valuable mechanical characteristics, their preservation in a wet state, high chemical and biological resistance, polypropylene fibers and threads are widely used. Modification of the properties of PP fibers by creating microfibers allows you to strengthen their unique characteristics - to improve the mechanical indicators and the neck of the fibers, to ensure the necessary comfort.

According to the results of previously performed research, technological schemes for obtaining complex threads and filter materials based on microfibers were proposed [27]. Their main stages are: drying of matrix polymer granules, mixing of fiber-forming and matrix components in a melt to obtain mixture granules, drying of the latter, formation of composite films or threads from a mixture of polymers, and matrix polymer extraction.

The influence of the parameters of mixing the components of the mixture on the realization of the phenomenon of specific fiber formation. One of the important conditions for the implementation of specific fiber formation is the dispersed type of the structure of the initial mixture of polymers with the optimal size of the droplets of the dispersed phase. According to the classical theory of [183], there is a critical size of droplets below which they are resistant to shear and stretching and are unable to deform. This degree of dispersion corresponds to droplet diameters of several

micrometers and is determined by the nature of the polymers [27]. If the degree of dispersion is insufficient, the phenomenon of specific fiber formation is also not realized; this is due to the fact that during the flow of the melt, the stresses that arise in the matrix do not have time to deform the drop into a jet. In addition, with an increase in the size of the droplets, the probability of their aggregation increases, and when such a mixture flows, films will form. It is known from the general theory of mixing that the elementary act of this process consists in the deformation of droplets of the dispersed phase into thin strips (streams). Since the liquid cylinder is thermodynamically unstable due to an unfavorable surface-to-volume ratio, the jet breaks up into drops much smaller than the initial ones. The most common method is mixing polymers in the melt using extrusion equipment. Twin-screw and combined worm-disc extruders were used in our research.

   Mixing on a worm-disc extruder. Its main working body is a pair of discs, one of which rotates and the other is stationary. In the gap between the disks, significant tensile and shear stresses occur, under the influence of which dispersion occurs. The size of the gap between the moving and stationary disks of the extruder (H) determines the value of tensile and shear stresses in this zone. The smaller the gap, the greater the resulting stresses and the higher the degree of dispersion of the dispersed phase polymer. Data on the effect of the size of the gap between the discs of the LHP-25 polymer granulation line on the mixing quality of the PP/SPA mixture with a composition of 20/80 wt. % are given in the Table. 1.13. They allow us to conclude that mixing should be carried out at gap

values $(4.5 \div 6.0) \cdot 10^{-3}$ m. At lower H, microfibers and particles with a degree of dispersion close to the critical are formed. An increase in the size of the gap increases the inhomogeneity of the extrudate structure, a significant number of films are formed in it along with microfibers.

Table 1.13. The effect of the size of the gap between the LHP-25 disks on the processes of structure formation*

H 10^{-3} m	Types of structures						
	continuous fibers		short fibers		particles		films
	d, μm	numb. %	d, μm	numb. %	d, μm	numb. %	numb. %
2,5	1,5	40,8	1,6	32,9	1,2	26,3	-
4,5	3,5	45,4	3,3	30,2	3,0	22,0	2,4
6,0	3,8	47,5	3,5	27,1	3,4	22,4	3,0
7,0	4,3	35,1	3,8	33,4	3,6	21,2	10,3
14,0	5,2	25,4	4,9	19,8	5,0	34,9	19,9

* under the condition Q = 10.0 kg/h.; Fv=200%

Besides the value of *H*, fiber formation is also significantly affected by the performance of the extruder (*Q*) and the spinneret extraction ($\varPhi_в$). The performance of the extruder is equivalent to the influence of the magnitude of the shear stress (τ). Low values of τ do not promote either dispersion or fiber formation. At high shear stresses, the negative effect of elasticity on structure formation is manifested. Due to the swelling of the jets coming out of the forming hole, the processes of aggregation are strengthened and, as a result, the heterogeneity of the structure increases. Table data. 1.14 confirm the effect of productivity on the realization of the phenomenon of specific fiber formation: with

an increase in Q from 10.0 to 22.0 kg/h. thinner fibers are formed, their number increases, and the number of particles decreases. But with high productivity due to the effect of elasticity, film formation increases. Recommended values of Q lie in the range of $10.0 \div 15.5$ kg/h.

Table 1.14. Impact of LHP-25 extruder performance on processes of structure formation*

Q, kg/hour	Types of structures						
	continuous fibers		short fibers		particles		films
	d, µm	numb. %	d, µm	numb. %	d, µm	numb. %	numb. %
10,0	4,3	38,1	3,8	37,4	3,8	21,2	-
15,5	3,3	51,5	3,7	23,6	3,4	17,6	7,3
22,0	2,8	60,2	3,5	20,2	3,0	9,6	10,0
27,5	2,0	48,2	2,1	21,2	2,1	12,7	17,9

* on the condition that H = 6.0·10-3 m; $\Phi_в$ =200%

As expected, spinneret extraction also significantly affects the processes of structure formation (Table 1.15). With the growth of $\Phi_в$, the diameter of microfibers naturally decreases and their number increases. However, when $\Phi_в = 400\%$, the degree of dispersion of polypropylene approaches the critical one, so further increase in the size of the spinneret hood is impractical.

Thus, the following parameters are recommended for mixing polypropylene and co-polyamide on the LHP-25 worm-disc extruder: $H = (4.4 \div 6.0) \cdot 10^{-3}$ m; $\Phi_в = 200 \div 400\%$; $Q = 10 \div 15$ kg/h.

Table 1.15. The influence of the amount of spinneret extraction on the processes of structure formation*

$\Phi_{\scriptscriptstyle{6}}$, %	Types of structures						
	continuous fibers		short fibers		particles		films
	d, μm	numb. %	d, μm	numb. %	d, μm	numb. %	numb. %
100	4,8	37,4	4,0	46,8	3,4	10,2	5,6
200	3,5	45,4	3,3	30,2	3,0	22,0	2,4
400	3,0	52,2	3,2	19,1	3,0	27,7	1,2

* on the condition that $H = 4.5 \cdot 10^{-3}$ m; $Q = 10.0$ kg/h.

The conducted studies showed that the introduction of compatibilizers in the PP/SPA mixture does not significantly change the technological scheme and the main parameters of microfiber production. The only difference is that in order to ensure a fine dispersion of the components of the mixture and an even distribution of additives, the latter are pre-introduced into the melt of the matrix polymer (SPA) on a worm-disc extruder. The temperature regimes of mixing SPA with various compatibilizers and their binary mixtures are given in Table. 1.16.

Granules of the PP/SPA/compatibilizer mixture are obtained by repeated extrusion on the LHP-25 line (Table 1.17).

Table 1.16. Temperature regimes of SPA extrusion with
compatibilizers on the line LHP-25

Name and content of the compatibilizer, wt. %			Temperature in the extruder zones, ^{0}C			
SEVA	oleate Na	PES-5	T_1	T_2	T_3	T_4
5,0	-	-	140	185	192	195
-	3,0	-	140	183	190	194
-	-	0,3	132	180	190	192
5,0	-	0,3	135	205	188	188
-	3,0	0,3	130	200	184	184
5,0	3,0	-	130	200	180	182

Q=15 kg/h, $\Phi_в$ =200%, H=4.8·10^{-3} m

Table 1.17. Temperature regimes of extrusion of the PP/SPA
mixture with a composition of 50/50 wt. % with additions of
compatibilizers

Name and content of the compatibilizer, wt. %			Temperature in the extruder zones, ^{0}C			
SEVA	oleate Na	PES-5	T_1	T_2	T_3	T_4
-	-	-	130	190	186	186
5,0	-	-	130	188	190	192
-	3,0	-	130	188	190	192
-	-	0,3	130	186	190	190
5,0	3,0	-	132	180	188	188
5,0	-	0,3	132	180	186	190
-	3,0	0,3	132	184	184	188

Mixing of components on a twin-worm extruder. Technological parameters of the processing of the mixture of PP/SPA/compatibilizer composition 50/50/0.5 wt. % are given in the table. 1.18. PMS-100 polymethylsiloxane liquid was used as a compatibilizer. Significantly higher temperatures in the zones of the twin-screw extruder, in comparison with the worm-disk extruder, are due to the short stay of the polymers in the melt.

Table 1.18. Technological parameters of mixing on a twin-screw extruder

Parameter name	Value
Temperature in the extruder zones, $^{\circ}C$	
T_1	245-249
T_2	251-254
T_3	260-268
T_4	258-266
T_5	238-240
T_6	222-230
The amount of rarefaction in the 1-st and 2-nd degassing zones, N/m^2	1,2
Pressure of the melt at the entrance to the head, $Pa \cdot 10^5$	6,0
Productivity, kg/h	40,0
Diameter of the forming hole of the die, $m \cdot 10^{-3}$	2,0
Number of strands, pcs.	10
Strand diameter, $m \cdot 10^{-3}$	$2 \div 3$
The temperature of the water in the bath, $^{\circ}C$	$16 \div 18$

The results of microscopic studies showed that during the processing of the PP/SPA/PMS-100 mixture on a twin-screw extruder, the phenomenon of specific fiber formation is

realized. At the same time, the share of microfibers of continuous length is ≈ 90%, and their average diameter is 4.5 micrometers. It should be especially emphasized that the required degree of PP dispersion is achieved without prior mixing of SPA with compatibilizer, and the presence of two degassing zones makes it possible to process mixtures without drying SPA under vacuum. Low molecular weight substances and moisture are removed from the melt in the degassing zones. This is very important, as the technological process is simplified by reducing the number of operations, namely: there is no need to dry the original SPA and its granules with compatibilizer additives and mix SPA with the compatibilizer on the LHP-25 line.

Development of technological parameters for obtaining FM and complex threads from compatibilized PP/SPA mixtures. The main technological operation that determines the structure and properties of FM and complex threads based on PP microfibers is the formation of a composite film or monofilament from a polymer melt. Composite films were formed on a ChP-45 worm press with the following technological parameters (Table 1.19; 1.20).

Thus, as a result of the research, the compositions of the compositions and the technological parameters of the production process of filter elements with FM based on polypropylene microfibers with a cleaning fineness of 0.3 μm and sterilizing ones were determined.

Table 1.19. Technological parameters of composite film formation

Parameter name	The value of the parameter	
	FM 0.3 μm	FM sterilizing
The composition of the PP/SPA mixture, wt. %	35,0/64,9	50,0/50,0
Compatibilizer	ПЕС-5	ПЕС-5/СЕВА
Additive amount, wt. %	0,1	0,3/1,7*
Extrusion temperature on LHP-25, ^{0}C	$184 \div 192$	$184 \div 190$
The size of the gap between the discs, m$\cdot$10^{-3}	4,8	4,5
Extrusion temperature on ChP-45, ^{0}C	$153 \div 210$	$153 \div 210$
Spindle hood, %	400	400
Composite film thickness, m $\cdot$10^{-3}	0,35	0,35

* from the mass of PP

Table 1.20. Temperature regime of formation of composite films on ChP-45

Temperature by zones,^{0}C	T_1	T_2	T_3	T_4	T_5	T_6	T_7	T_8
	153	188	210	210	200	195	190	190

Composite threads from melts of PP/SPA mixtures with additives of compatibilizers were formed on a research and industrial spinning machine UFTP-2, drawn on an extraction stand. The technological parameters of the formation of composite threads are given in the table. 1.21.

Table 1.21. Technological parameters of the formation of composite threads

Parameter name	The value of the parameter
The composition of the PP/SPA mixture, wt. %	35,0/64,9
Compatibilizer - PES-5, wt. %	0,1
Temperature, ^{0}C	150-192
The temperature of the water in the bath, ^{0}C	5-10
Spindle hood, %	1000
Extraction temperature, ^{0}C	150
Multiplicity of extraction	4-5

Filter materials and complex threads made of PP microfibers were obtained after the extraction of the matrix polymer from composite films and threads.

1.3.3. Micro- and macrorheological processes in polymer mixtures with additives

1.3.3.1. *Physico-chemical regularities of obtaining ultrafine microfibers from melts of polymer mixtures*. At the Kyiv National University of Technology and Design, fundamental research was carried out in the field of physico-chemistry of melts of polymer mixtures, which made it possible to create the scientific basis for the formation of ultra-thin synthetic fibers and to develop technologies for the production of a number of new thin-fiber materials based on them [1,127,135]. One of the important conditions for the realization of the phenomenon of specific fiber formation is the optimal degree of compatibility of the components in the melt.

This ensures the formation of a transition layer of sufficient length and the possibility of transferring the stresses that arise in the dispersion medium to the polymer drops of the dispersed phase. It is known that polymer mixtures are a specific class of colloid systems of the "polymer in polymer" type. Their feature is the formation of an interphase transition layer between the two components of the mixture. A developed interphase layer is characteristic only for polymer dispersions, and it largely determines the physicochemical and mechanical properties of polymer mixtures and their products [27].

According to Taylor's theory [183], a dispersive medium during flow acts on a drop dispersed in it with a force T_η which is proportional to the gradient of the shear rate dV_x/dy, the viscosity (μ) of the medium and is a function of the ratio of the viscosities of the components:

$$T_\eta = C \, (dV_x/dy) \, \mu f \, (\mu/\eta)$$

where η – viscosity of the dispersed phase polymer;

C – constant value

The T_η force will not be able to be transmitted to the drop and deform it if there is no interaction between the two polymers of the mixture, namely, a transition layer of the appropriate length and a sufficient degree of connection of the components in it. A drop of dispersed phase polymer resists deformation with force

$$T_\gamma = 2 \, \gamma_{\alpha\beta} / r$$

where $\gamma_{\alpha\beta}$ – interphase tension;

r –   the radius of the polymer droplet of the dispersed phase

Under conditions when $T_\eta = T_\gamma$, the radius of the droplet, and therefore of the microfiber, is determined by the following equation:

$$r = [C *\gamma_{\alpha\beta}] \, / \, [\, (dV_x/dy) \, \mu f \, (\mu/\eta)] \qquad (1.6)$$

It follows from equation (1.6) that microfibers will be thinner, the higher the viscosity of the matrix polymer, the greater the shear rate gradient, and the lower the viscosity of the fiber-forming polymer and the interfacial tension.

It is known that due to the very small entropy of mixing, most polymers in mixtures are thermodynamically incompatible. Weak intermolecular interactions in the interfacial layer lead to low adhesion at the interface of phase separation both in the melt and in the solid state. Thus, Utraki [3] estimated the value of the interfacial viscosity, which turned out to be 100 times lower than the melt viscosity of the mixture as a whole. That is why "property-composition" dependences for polymer mixtures usually have a negative deviation from additivity. It follows from the above that it is necessary to improve the compatibility of the components of the polymer mixture (compatibilization). In the studies carried out in the problem laboratory of KNUTD, it was shown [12,27,30-39,41-42] that specific interactions are realized between the macromolecules of the following pairs of polymers: POM/SPA, POM/SEVA and SEVA/SPA. Their formation causes the emergence of an interphase layer of sufficient length and provides the possibility of transferring forces from the matrix to the polymer regions of the dispersed phase. Due to this, the kinetic stability of the polymer

dispersion increases, the degree of dispersion and specific fiber formation is clearly realized. Of particular interest is the method of introducing an additional component into the binary mixture, acting as a compatibilizer.

Previously performed studies showed that in binary mixtures of polymers, the phenomenon of specific fiber formation is most clearly realized when the ratio of fiber-forming and matrix polymers is 20/80; 30/70 wt. % [27]. The introduction of compatibilizers contributes to the formation of microfibers with a higher content of the fiber-forming component.

In this section, the results of the study of the effect of additives of organosilicon liquids on the phenomenon of specific fiber formation in melts of polypropylene / co-polyamide mixtures are presented. The problem of compatibility emerges acutely in the case of using PP/SPA mixtures for the production of PP microfibers. Polypropylene and co-polyamide are dramatically different in chemical structure, which is why they are incompatible.

The objects of the study were: PP, SPA, their binary mixtures of composition 20/80; 30/70; 40/60; 50/50 wt. % and ternary mixtures with 0.1 additives; 0.3; 0.5; 1.0 wt. % of organosilicon liquids by mass of PP.

1.3.3.2. The influence of siloxane additives on the processes of structure formation in PP/SPA mixtures. Processes of structure formation in the extrudates of the mixtures were evaluated qualitatively - by examining transverse and longitudinal sections, and quantitatively - by counting the number of all types of structures under a

106

microscope and determining their sizes. Analysis of microphotographs of longitudinal sections and PP residues washed from SPA showed that specific fiber formation occurs for all compositions of PP/PA mixtures with additives of different brands of organosilicon liquids. On the basis of detailed quantitative microscopic studies, the possibility of clearly realizing the phenomenon of specific fiber formation was shown for PP/SPA mixtures compatibilized by siloxane liquids with a ratio of components related to the phase change region (40/60 and 50/50 wt. %). In the absence of siloxane liquids for PP/SPA mixtures of the indicated compositions, fiber formation of PP in the SPA matrix has no place (Table 1.22; 1.23; 1.24). Such a regularity during the introduction of siloxanes was established by us for the first time [27].

Table 1.22. The influence of PES-5 additives on the microstructure of extrudates of PP/SPA mixtures with a composition of 50/50 wt. %

Quanti-ty of add., wt. %	Continuous fibers			Short fibers		Particles		Films % numb.
	d*, μm	% numb	δ^2	d*, μm	% numb.	d*, μm	% numb	
0	Fiber formation is not realized							
0,1	5,6	80,2	19,3	5,4	5,4	6,3	5,8	8,6
0,3	3,8	89,4	3,2	3,2	4,2	3,7	3,3	3,1
0,5	4,1	72,0	5,0	4,3	12,6	4,5	9,3	6,1
1,0	6,3	73,0	32,0	6,0	14,9	7,1	7,6	4,5

*d – average diameter of fibers and particles

Table 1.23. The influence of PMS-100 additives on the
microstructure of extrudates of mixtures
PP/SPA composition 50/50 wt. %

Quanti-ty of add., wt. %	Continuous fibers			Short fibers		Particles		Films % numb.
	d*, µm	% numb	δ^2	d*, µm	% numb.	d*, µm	% numb	
0	Fiber formation is not realized							
0,1	7,4	82,2	28,0	7,2	5,1	7,6	3,9	9,0
0,3	4,5	87,0	8,8	4,0	5,1	4,9	4,1	4,1
0,5	4,9	74,7	7,9	4,4	11,3	5,1	5,9	8,7
1,0	5,7	71,0	24,3	5,9	13,9	6,3	6,5	9,4

*d – average diameter of fibers and particles

Table 1.24. The influence of PMS-500 additives on the
microstructure of extrudates of PP/SPA mixtures
composition 40/60 wt. %

Quanti-ty of add., wt. %	Continuous fibers			Short fibers		Particles		Films % numb.
	d*, µm	% numb	δ^2	d*, µm	% numb.	d*, µm	% numb	
0	Fiber formation is not realized							
0,1	7,4	64,5	11,2	8,5	15,1	6,8	15,1	5,3
0,5	4,2	82,9	9,0	3,1	5,3	3,0	7,0	4,8
1,0	6,5	80,4	12,4	6,0	7,6	6,3	7,8	4,2

*d – average diameter of fibers and particles

From the Tables 1.5-1.7 it can be seen that the predominant type of structure in the extrudates of PP/SPA mixtures with a composition of 40/60 and 50/50 wt. % with additives are PP microfibers, the share of which is 82.9 89.4 numerical %. The chemical structure of siloxanes significantly affects the processes of structure formation during the flow of PP/SPA melts. PES-5 is a more effective compatibilizer than polymethylsiloxanes: the diameters of microfibers are minimal, their number is maximal; curve of distribution of fibers of

continuous length by diameter for a mixture of PP/SPA composition 40/60 wt. %, which contains 0.5 wt. % PES-5, narrower than for the same amount of PMS-100 (Fig. 3.1). The latter is explained by the different length of hydrocarbon radicals and the degree of branching of siloxane macromolecules.

The evaluation of the morphology of the extrudates showed that the introduction of organosilicon liquids also affects the processes of structure formation in PP/SPA mixtures with a composition of 30/70 and 20/80 wt.%. PES-5 additives increase the degree of dispersion of polypropylene in the SPA matrix and improve specific fiber formation: the number of continuous fibers increases from 43 52% in the original mixtures to 87 90% for mixtures containing PES-5 (Table 1.25; Fig. 1.18; 1.19) .

Table 1.25.The influence of PES-5 additives on the microstructure of extrudates of the PP/SPA mixture

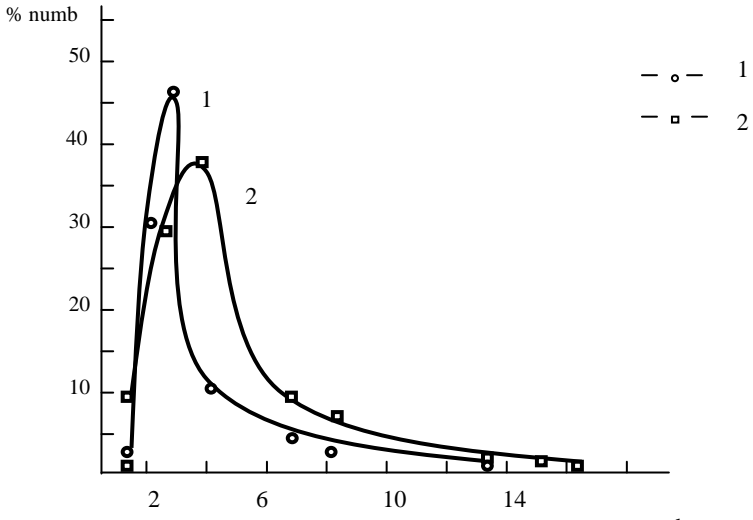| Composi-tion of the mixture, wt. %	Amount of additi-ves, wt.%	Continuous fibers		Short fibers		Particles		Films % numb.
		d, µm	% numb	d, µm	% numb	d, µm	% numb	
30/70	0	5,7	43,1	3,7	34,9	12,6	17,2	4,8
30/70	0,1	3,8	64,0	3,6	20,0	4,5	9,4	2,1
30/70	0,5	2,6	87,3	3,2	7,1	3,7	4,0	1,6
30/70	1,0	4,0	73,6	4,1	10,0	3,7	10,4	6,0
20/80	0	3,6	52,0	3,2	19,1	4,4	27,1	1,2
20/80	0,5	1,8	90,3	2,5	5,2	3,5	4,5	-

Fig. 1.18. Experimental curves of distribution of PP microfibers by diameters in extrudates of PP/SPA/siloxane mixtures of composition 40/60/0.5 wt. % depending on the brand of siloxane liquid: 1 - PES-5; 2 - PMS-100
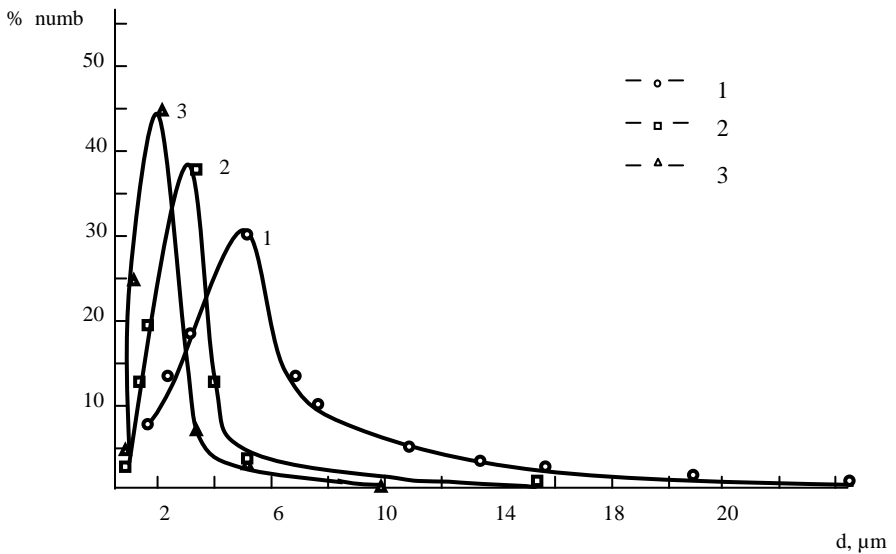

Fig. 1.19. Experimental curves of distribution of PP microfibers by diameter in extrudates of PP/SPA/PES-5 mixtures of composition: 30/70/0 (1); 30/70/0.1(2); 30/70/0.5(3)

The analysis of the distribution curves of fibers of continuous length by diameters shows that PES-5 additives improve PP fiber formation in the SPA matrix. With an increase in the content of PES-5 to 0.5 wt.%, the average diameter of microfibers decreases, their number and uniformity increase (Fig. 1.18; 1.19; Table 1.25). The processing of the results by the methods of mathematical statistics [160] showed that the experimental curves of the distribution of fibers by diameters are not described by normal, as well as log-normal distribution laws, which are often found in the case of dispersed systems, judging by the Pearson and Kolmogorov matching criteria.

As already noted, polypropylene and co-polyamide are thermodynamically incompatible with each other, but their separation is hindered by the high viscosity of both components. When flowing in a round channel, a less viscous liquid tries to reach the wall, forming a relatively low-viscosity wall layer, which is manifested by the presence of a thin fibrous outer shell of PP in the structure of the extrudate (Table 1.22-1.25). This is true for all compositions of polymer mixtures and all brands of siloxane liquids tested.

Analysis of the obtained results shows that the formation of other types of structures depends on the amount of siloxane liquid and its brand. From the point of view of the implementation of specific fiber formation, it is recommended to recommend organosilicon liquid PES-5 in the amount of 0.3 0.5 wt.%. It is known that when compatibilizers are introduced into the original polymers or their mixture, the interfacial surface tension decreases, the stress concentration around the

polymer droplets of the dispersed phase and the rate of coalescence and migration of the polymer droplets decrease, i.e., the kinetic stability of the dispersion in the melt increases. Obviously, this is the mechanism of action of the addition of siloxane liquids in the processing of melts of PP/SPA mixtures. The found regularity is of great practical importance, as it allows to increase the content of fiber-forming polymer (PP) in the mixture by 2.5 times and to reduce energy costs for the extraction and regeneration of the matrix polymer (SPA). It is very important that with such a high content of PP, the predominant type of structure is microfibers of continuous length, and the films are a thin outer fibrous shell.

1.3.3.3. Rheological properties of melts of PP/SPA mixtures

The effect of additives of organosilicon liquids. Taking into account that the processing of polymers is carried out through the melt, the rheological properties of the original polymers and their mixtures were studied. The obtained results indicate that siloxane additives have different effects on the viscosity of PP and SPA melts (Table 1.26).

Thus, if the viscosity of PP melts with the introduction of 0.1 1.0 wt.% siloxanes decreases in the entire range of studied concentrations, then in the case of SPA the nature of the dependence "η - siloxane content" is more complex: the introduction of 0.1 wt.% siloxane causes a significant - 1.7-1.8 times increase in η of the SPA melt. With a further increase in the content of the additive, the viscosity of the SPA melt decreases, while remaining higher than the η of the original co-polyamide melt.

Table 1.26. The influence of siloxane additives on the viscosity
of PP and SPA melts

Name of siloxane	Amount of siloxane, wt.%	Viscosity, Pa · s at $\tau=5{,}69 \cdot 10^4$ Pa	
		PP	SPA
PES-5	0	480	950
PES -5	0,1	420	1700
PES -5	0,3	420	1520
PES -5	0,5	400	1130
PES -5	1,0	380	1090
PMS -100	0,1	420	1840
PMS -100	0,3	400	1640
PMS -100	0,5	350	1150
PMS -100	1,0	310	1070
PMS -500	0,5	430	1270

In our opinion, the mechanism of effect of siloxanes on η of the SPA melt is twofold: on the one hand, siloxane can structure the melt due to the formation of hydrogen bonds, on the other hand, it acts as an interstructural plasticizer. The formation of hydrogen bonds between the oxygen of the siloxane and the -NH- group of SPA is confirmed by the change in the frequencies of the absorption bands of the valence vibrations of the -NH- groups of the co-polyamide, namely, the shift to the low-frequency region from $\gamma_{NH} =3335$ cm^{-1} to $\gamma_{NH} =3320$ cm^{-1} (Fig. 1.20).

The joint action of the two specified mechanisms determines the value of η of the SPA melt. The flow regime and elasticity of PP and SPA melts change slightly in the presence of additives. The same frequency shift of the -NH- band occurs for the PP/SPA/PES-5 mixture.
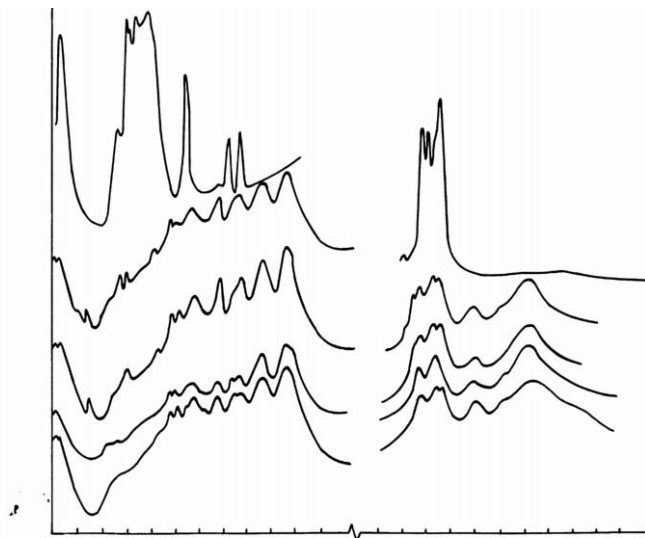
Fig. 1.20. IR - transmission spectra: 1 – SPA; 2 – SPA/PES-5; 3 – PP/SPA; 4 – PP/SPA/PES-5; 5 – PES-5.

From the table 1.26 it can be seen that the effective viscosity of SPA is almost 2 times higher than η PP. However, when they are mixed, systems are formed, the viscosity of which is significantly lower than the viscosity of the original components, as well as additive values (Table 1.10). This is a characteristic property of melts of polymer mixtures, between the macromolecules of which there are no specific interactions, and it is explained by the deformation and orientation of the droplets of the dispersed phase in the direction of the flow.

It has been shown theoretically and experimentally [171] that a smaller pressure drop (corresponding to a lower viscosity) is required for the realization of the melt flow of a mixture with deformable drops than for the flow of melts of individual polymers. The introduction of even small additives

of organosilicon liquids causes a further decrease in the viscosities of the melts of the studied mixtures (Table 1.27). On the "η - additive content" curves, there is a minimum at 0.3 wt. % of siloxane (Fig. 1.21).

Table 1.27. The effect of the addition of 1.0 wt.% organosilicon liquids on the viscosity of melts of PP/SPA mixtures

Composi-tion of the mixture, wt.%	Additive viscosity, Pa·s	Viscosity of the binary mixture, Pa·s	Viscosity of the mixture with additives of siloxane liquid, Pa·s		
			PES-5	PMS-100	PMS-500
20/80	892	340	270	-	300
30/70	803	290	240	-	260
40/60	754	200	195	200	210
50/50	705	230	200	220	220
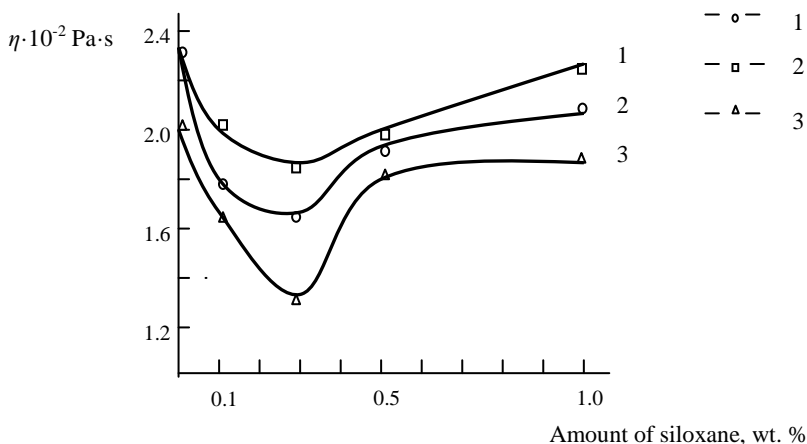
Fig. 1.21. The influence of siloxane additives on the viscosity of melts of PP/SPA mixtures of composition, wt. %: 1 – 50/50/PMS-100; 2 – 50/50/PES-5; 3 – 40/60/PES-5.

The established nature of the dependence can be explained by the influence of additives on the processes of structure formation of the dispersed phase polymer. It is known [27,30-35] that the realization of the phenomenon of specific fiber formation is accompanied by a decrease in the viscosity of the melts of the mixtures. Thus, the minimum on the dependence curve "η - additive content" at 0.3 wt. % of siloxane correlates with the results of microscopic studies and confirms that it is small amounts of organosilicon liquids that have the greatest effect on fiber formation of PP in the SPA matrix. The further increase in viscosity is associated with the formation of hydrogen bonds between siloxane macromolecules and SPA.

One of the important rheological features of melts of polymer mixtures is increased elasticity in comparison with the same indicator for the original polymers. High elasticity is expressed in the fact that the swelling "B" of the extrudates of the mixtures is much higher than the additive values. This regularity is explained by the development of large elastic deformations and normal stresses during the flow of the melt mixture due to the orientation and deformation of the polymer droplets of the dispersed phase in the direction of the flow. For melts of polymer mixtures, the value "B" also depends on the type of structure formation of the polymer of the dispersed phase. Thus, it was shown [27] that swelling correlates with specific fiber formation: the thinner the microfibers that are formed and the greater their number, the higher the "B" value. Fig. 1.22 presents data on the influence of siloxane additives on the elasticity of the melts of the investigated PP/SPA mixtures.
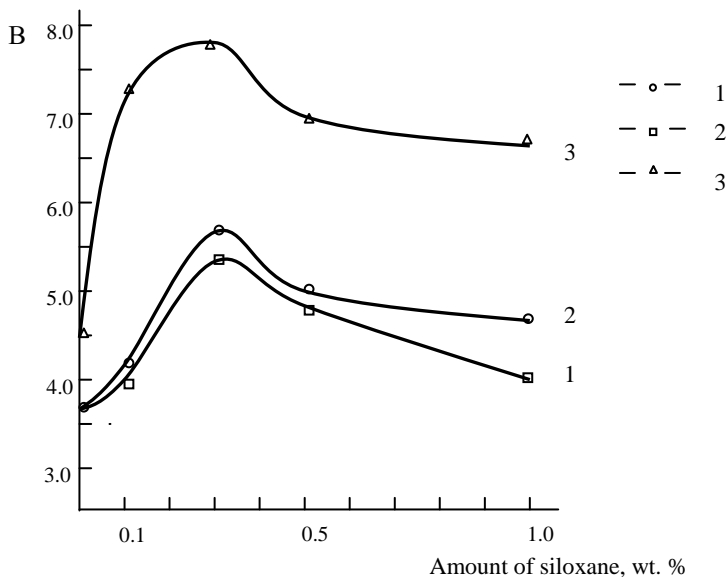
Fig. 1.22. The influence of siloxane additives on the swelling of extrudates of PP/SPA mixtures of composition, wt. %: 1 – 50/50/PMS-100; 2 – 50/50/PES-5; 3 – 40/60/PES-5.

The data of microscopic studies (Tables 1.22-1.25) and the nature of the dependence of the amount of swelling on the content of the additive (fig. 3.6) indicate that the introduction of organosilicon liquids in the PP/SPA mixture improves specific fiber formation in the entire range of studied concentrations. Yes, if the PP/SPA ratio is 40/60 and 50/50 wt. % microstructure of the extrudates is a layered morphology consisting of rough films, then for ternary mixtures there is fiber formation of PP in the mass of SPA. For this reason, the swelling of extrudates containing siloxanes increases by more than 1.5 times. The maximum on the dependence "B - siloxane content" falls on 0.3 wt. % additive when the swelling value reaches 7.6 against 5.3 for the binary mixture.

Effect of temperature. We have shown that the addition of siloxane liquid affects the viscosity of the original PP: it decreases in the entire temperature range. The temperature dependence of the viscosity of the melt for the original SPA and with the addition of siloxane is more complex. In the temperature range of 180-190 ^{0}C, the introduction of PES-5 leads to an increase in the η of the SPA melt, and at temperatures of 200-220 ^{0}C, the viscosity of the SPA melt with the addition of PES-5 decreases compared to the *η* of the original SPA (Fig. 1.23).

$\eta \cdot 10^{-2}$ Pa·s
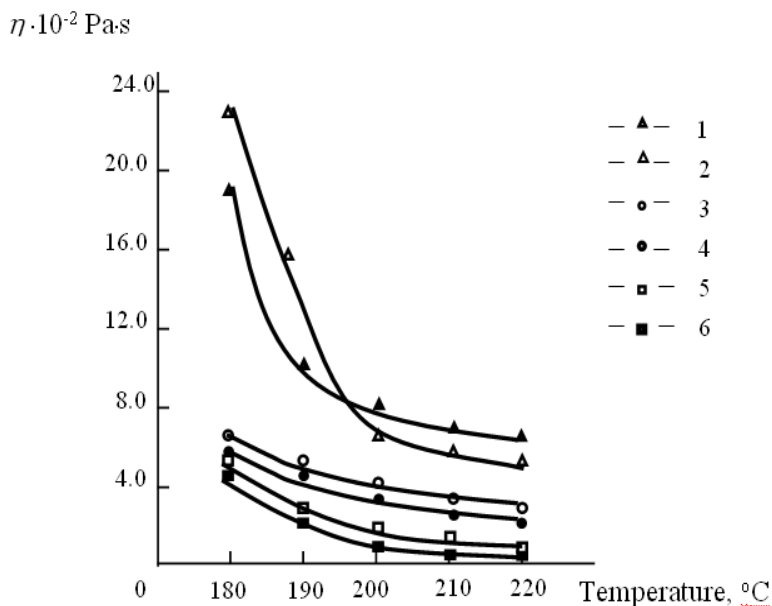
Fig. 1.23. Dependence of melt viscosity on temperature:
1 – SPA; 2 – SPA+0.3 wt. % PES-5; 3 – PP;
4 – PP+0.3 wt.% PES-5; 5 – PP/SPA; 6 – PP/SPA+0.3 wt.% PES-5

The established regularity is related to the competing effect of two factors: the structuring of the melt due to the formation of hydrogen bonds between the polymer and the additive and their destruction with increasing temperature. In the first named temperature range, structuring processes prevail, and in the second, an increase in temperature causes the breaking of intermolecular bonds and makes it possible for the plasticizing effect of the siloxane liquid on the SPA melt to manifest itself. The latter is confirmed by the decrease in the activation energy of the viscous flow (E) of the investigated melts (Table 1.28).

Table 1.28. Dependence of the activation energy of the viscous flow on the shear stress

The name of the polymer, mixture of polymers	E, KJ/mol at $\tau \cdot 10^{-4}$ Pa		
	5,69	4,20	1,98
PP	42	42	44
PP+0,3% PES-5	38	39	40
SPA	64	67	70
SPA+0,3% PES-5	58	60	67
PP/SPA	67	70	71
PP/SPA+0,3%PES-5	61	61	63

The plasticizer, as a rule, leads to a decrease in E due to a decrease in the interaction between polymer macromolecules. The tendency for E to decrease with increasing shear stress is generally known and natural.

For all investigated shear stresses, the dependence of the viscosity of melts of PP/SPA mixtures on the content of siloxane liquid at a temperature of 190 ^{0}C is expressed by

curves with a minimum when the concentration of the additive is 0.3 wt. % (Fig. 1.24). A similar nature of dependence occurs at other temperatures.
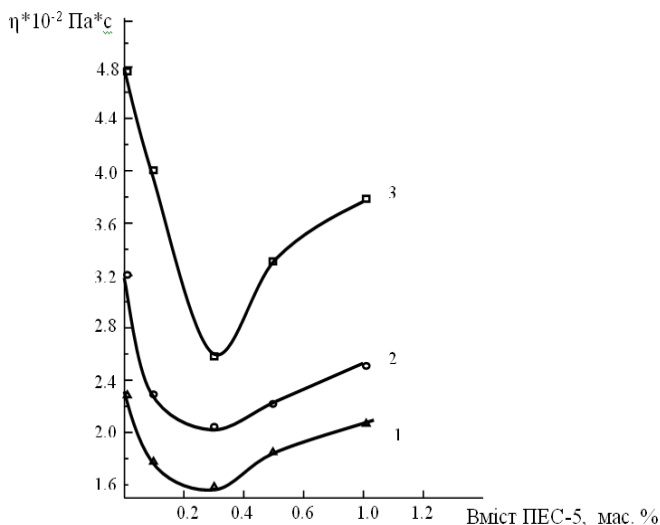

Fig. 1.24. Dependence of the viscosity of melts of the PP/SPA mixture composition 50/50 wt. % of PES-5 content at $\tau \cdot 10^{-4}$ Pa: 5.69 (1); 4.20 (2); 2.72 (3)

As already noted, one of the important rheological characteristics of polymer melts is their elasticity, which is manifested in the swelling of the extrudate. The "B" value of extrudates for melts of polymer mixtures also depends on the type of structure formation of the polymer of the dispersed phase and is an indirect characteristic of specific fiber formation. Table 3.8 shows data on the effect of siloxane liquid additives on the elasticity of melts of PP, SPA and a mixture of PP/SPA with a composition of 50/50 by mass. % at different temperatures. The analysis of the data in Table 1.29 shows that

the elasticity of the melts of the original polymers and their mixture is determined by the temperature and the presence of additives. For mixtures of PP/SPA and PP/SPA/PES-5, the effect of temperature is manifested through a change in the structure formation processes of the dispersed phase polymer.

Table 1.29. Dependence of the swelling of extrudates on the processing temperature

The name of the polymer, a mixture of polymers with a composition of PP/SPA 50/50 wt. %	The amount of swelling at temperatures, ^{0}C				
	180	190	200	210	220
PP	2,3	2,2	2,1	2,1	2,0
PP+0,3 wt.% PES-5	2,3	2,2	2,1	2,0	2,0
SPA	1,4	1,3	1,2	1,1	1,0
SPA+ 0,3 wt.% PES -5	2,0	1,9	1,9	1,8	1,7
PP / SPA	3,0	3,7	3,8	3,6	3,2
PP /SPA+0,3 wt.% PES -5	3,5	5,5	5,4	4,3	3,9

Taking into account that the value "*B*" correlates with specific fiber formation, a temperature of 190-200 ^{0}C should be recommended for the formation of PP microfibers from the studied mixtures, since the swelling is maximum at this time.

1.3.3.4. Influence of additives of organosilicon liquids and temperature on the directivity of melts of PP/SPA mixtures

The formation of fibers, films and other products from polymer melts is necessarily associated with the longitudinal deformation of the melt as it exits the forming nozzle. The degree of longitudinal deformation can be measured by the value of the maximum spinneret elongation, therefore, the effect of additives of siloxane liquids and temperature on the ability to process melts of PP, SPA and their mixtures was

estimated by the value of Fmax of the melt jet formed through the cylindrical hole (Table 1.30, 1.31).

Table 1.30. The influence of PES-5 additives and temperature on the directivity of PP melts, SPA and mixtures of PP/SPA composition 50/50 wt. %

The name of the polymer, a mixture of polymers	Φ_{max}, % at temperature, ^0C				
	180	190	200	210	220
PP	23180	15110	14100	12320	3850
PP +0,3 wt.% PES-5	24700	25650	20090	17490	12870
SPA	66780	72500	55250	42870	19400
SPA +0,3 wt.% PES -5	85780	174480	98500	38500	17620
PP /SPA	3480	3700	4080	3090	2280
PP /SPA+0,3 wt. % PES -5	4350	5910	4970	3770	2710

Table 1.31. The influence of additives of organosilicon liquids on the directivity of PP melts, SPA and PP/PA mixtures

Найменування силоксану	Amount of siloxane, wt. %	Φ^*_{max}, %			
		PP	SPA	PP /SPA 40/60	PP /SPA 50/50
PES-5	0	15110	72500	6910	3700
PES -5	0,1	24700	109780	7380	4150
PES -5	0,3	25650	174480	7750	5910
PES -5	0,5	27500	140170	6900	4100
PES -5	1,0	34520	92660	6300	3540
PMS -100	0,1	25600	136130	-	4170
PMS -100	0,3	25990	191380	-	4810
PMS -100	0,5	29150	147480	-	4680
PMS -100	1,0	36080	101300	-	4450

* at a temperature of 190 ^0C

The results of our research showed that PP and SPA have different ability to longitudinal deformation in the entire temperature range: the values of Φ_{max} differ by 1.3-2.3 times [170]. Co-polyamide deforms much better in the field of longitudinal forces.

The ability to process the melt of the binary mixture significantly deteriorates, which is associated with its two-phase nature and the presence of a transition layer with weakened interphase intermolecular interaction. Introduction of $0.1 \div 1.0$ wt. % siloxane liquid significantly improves the ability to process both the original components and their mixtures, which is explained by the influence of siloxanes on interfacial phenomena. Siloxane liquids are not compatible with most organic substances and are already pushed to the surface when they are introduced in an amount of $\approx 10^{-4}$ %. Due to their low viscosity and high surface activity, they are finely dispersed in the melt, located at the interface, reduce surface energy and interfacial surface tension, and thereby improve processability. The nature of the dependences "Φ_{max} - siloxane content" and "B - additive content" are the same, that is, the implementation of specific fiber formation contributes to the growth of melt directivity. The better straightness of the mixture at temperatures of $190 \div 200$ ^{0}C can also be explained by fiber formation, that is, the formation of anisotropic structures in the form of ultra-thin fibers. The presence of such structures facilitates the extraction of fibers and films from two-phase mixtures.

1.4. Microfibrillar nanofilled polymer composites and thin fiber products based on them

1.4.1. Formation of microfibrillar structure in nanofilled polymer dispersions. The formation of microfibrils (microfibers) of one polymer in the medium of another (matrix) is a fundamentally new process of forming ultrafine fibers, in which the diameter and number of filaments do not depend on the number of holes in the spinneret, but are determined by the chemical nature, rheological properties of the components of the mixture, and phenomena on boundaries of phase separation. From the point of view of thermodynamics, the spherical shape of droplets is the most stable, and their formation in the melt of a mixture of polymers is conditioned by the minimization of the phase separation surface, and the dimensional characteristics depend on the ratio of the viscosities of the components of the mixture and the amount of interfacial tension [146]. The introduction of nanofillers into melts of polymer mixtures contributes to the formation of a developed transitional layer, which significantly affects microrheological processes during their flow (deformation of droplets, merging into liquid jets and disintegration, migration of the dispersed phase along the radius of the forming hole, etc.), which opens up a wide range of possibilities for regulating morphology polymer dispersions.

The addition of NPs in a small amount makes it possible to obtain stable non-spherical forms of the component of the dispersed phase: microstreams, coalescent clusters, chains, laces. Thus, for the mixture of polyamide-6/polystyrene

and polylactide/polyurethane polymers, the possibility of regulating the shape and stability of the particles of the dispersed phase over time due to the introduction of all (1÷3) wt. % of nanosilica [72,147,148]. At the same time, the irregular shape of individual domains and fibrils remains unchanged for one hour after stopping the flow. The authors explain the established stabilization of the dispersion structure by the limitation of relaxation processes in polymer chains due to the presence of NPs in them or the formation of network structures and discrete domains of irregular shape due to the high ability of silica nanoparticles to combine into chains and cover the surface of droplets, contributing to their adhesion.

The shape of the particles of the dispersed phase can be controlled most effectively if the nanoadditive is preferentially localized at the boundary of the polymer/polymer interface. At the same time, the intensity of interaction between drops changes, which can either merge into liquid jets or partially merge with the formation of irregularly shaped domains. Coalescence of liquid droplets in the presence of interfacially adsorbed spherical silicon dioxide nanoparticles occurs in incompatible polymer mixtures when they accumulate in the interfacial layer closer to the matrix [149,150]. Most often, the clustering of dispersed phase droplets covered with nanoparticles occurs when they are more closely related to the matrix component. Selective localization of clay NPs at the boundary of the phase separation in the PS/polymethyl methacrylate mixture contributes to the formation of a finer droplet-matrix morphology [151]. Layered nanoclays are

effective modifiers that allow changing the morphology of the mixture regardless of the saturation of the transition layer with a nano additive. This may be due to the fact that the flat shape of clay particles allows them to better adapt to the structure of the interphase layer. At the same time, anisotropic particles, such as carbon nanotubes, are able to influence the shape of droplets of the dispersed phase only if the transition layer is fully saturated [152].

Studies on the formation of a microfibrillar structure in a mixture of polyethylene terephthalate (PET)/PP filled with titanium oxide nanoparticles showed that the morphology of the system is determined by the content and size of NPs, the sequence of mixing with the ingredients (pre-dispersion in a dispersed phase or matrix component or simultaneous mixing) and process parameters [27,153,154]. Table 1.32 shows data on the influence of the concentration of titanium dioxide nanoparticles with diameters of 300 nm on the dimensional characteristics of polyethylene terephthalate fibrils in a polypropylene matrix. Increasing the content of nano additives in the mixture helps to reduce the average diameter of the fibrils and increase the homogeneity of their distribution. Nanoparticles of titanium dioxide exhibit a modifying effect regardless of their location, but it becomes maximal when they are preferentially localized at the boundary of phase separation.

Fundamental studies of the influence of nanofillers on the micro- and macrorheological properties of melts of thermodynamically incompatible polymer mixtures have been conducted at KNUTD for many years.

Table 1.32. Effect of titanium dioxide content on diameters
of PET microfibrils

Composition of the mixture PET/PP/TiO$_2$, vol. %	Microfibrils	
	average diameter, μm	range of diameters, μm
30/70/0	5,4	2,0÷9,2
24,5/73,5/2,0	1,4	1,6÷5,6
24,0/72,0/4,0	1,1	0,6÷4,5

For the modification of PP/SPA and PP/PVA mixtures, the following nanofillers were used: carbon nanotubes [12,155], silicas with different specific surface areas and functional groups [27,28,79-81] and complex substances TiO$_2$/SiO$_2$ [34,36], Ag/Al$_2$O$_3$ and Ag/SiO$_2$ [35]. It was established that in the presence of all investigated nanoadditives, the character of flow and structure formation do not change: in nanofilled systems, as in the original ones, the component of the dispersed phase (polypropylene) forms microfibrils in the SPA and PVA matrix. In fig. 1.25, as an example, electron micrographs of transverse and longitudinal chips of the extrudate of the PP/SPA/SiO$_2$ mixture with a composition of 30/70/1 weight %, which indicate the formation of a microfibrillar structure during its flow [36]. At the same time, the diameters of microfibrils and the ratio between other types of structures in the extrudate (particles, films) depend on the chemical nature of mineral nanoadditives.
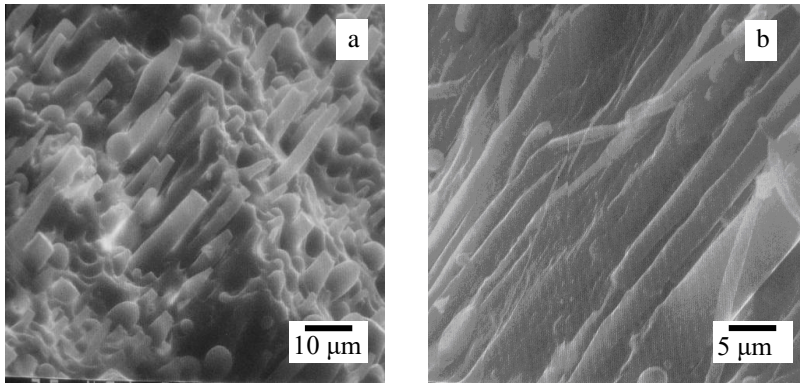
Fig. 1.25. Electron micrographs of transverse (a) and longitudinal (b) chips
of the extrudate of the PP/SPA/ SiO$_2$ mixture

The influence of the type of nanofiller on the morphological characteristics of extrudates of PP/SPA and PP/PVA mixtures with a 30/70 ratio of components, which contain 1.0 wt. % additives are given in table 1.33. Data of Table 1.33 show that all investigated nanofillers have a modifying effect - the average diameter of PP microfibrils decreases by almost 2 times, and their mass fraction increases to $\geq$ 90.0 wt. %. A significant effect is due to the predominant localization of NPs in the transition layer. Filling the phase separation boundary with nanoparticles was achieved, first of all, by using two-stage mixing of the ingredients, as well as by the lack of interaction of nonpolar PP macromolecules with the polar surface of mineral NPs.

Table 1.33. The influence of the chemical nature of
nanoadditives on the characteristics of the microstructure of
extrudates of polymer mixtures

The name of the nano additive	Types of structures		particles, weight %	films, weight %
	microfibrils			
	đ, мкм	weight %		
PP/SPA mixture				
without additives	4,0	82,7	8,3	9,0
silica	2,0	91,0	0,1	8,9
methylsilica	2,6	84,4	2,1	13,5
titanium oxide/silica	1,8	95,0	1,2	3,8
silver/silica	2,7	94,2	1,2	4,6
silver/alumina	2,2	95,2	1,3	3,5
carbon nanotubes	3,2	93,4	1,2	5,4
PP/PVA mixture				
without additives	3.5	86,5	3,8	9,7
methylsilica	1,7	94,0	2,3	3,7
silver/silica	1,6	90,6	3,3	6,1

Interphase-adsorbed nanoadditives improve the
compatibility of components in the transition layer, which is
evidenced by a decrease in the surface tension (Table 1.34). A
decrease in interfacial tension naturally leads to a decrease in
the diameters of microfibrils due to the minimization of energy
costs for the formation of new surfaces of the dispersed phase.
The change in the ratio between the types of structures towards
an increase in the number of PP microfibrils is the result of an
increase in the resistance of liquid cylinders to droplet
disintegration.

Table 1.34. The influence of the chemical nature of nanoadditives on the value of interfacial tension and the resistance of liquid jets to disintegration

The name of the nano additive	Surface tension, mN/m	Coeffi-cient instability	Life-time, s	Reduced lifetime, s/µm
PP/SPA mixture				
without additives	2,60	0,0418	56,2	47,4
silica	0,60	0,0143	67,4	54,7
methylsilica	0,75	0,0250	75,0	62,4
titanium oxide/silica	0,41	0,0180	154,3	75,9
silver/silica	0,54	0,0216	47,5	31,6
aluminum oxide	0,49	0,0157	158,2	83,9
silver/alumina	0,32	0,0193	55,2	38,9
CNT	0,32	0,0186	52,4	46,3
PP/PVA mixture				
without additives	0,73	0,0375	317	259
methylsilica	0,47	0,0198	390	330
silver/silica	0,38	0,0211	390	378

As is known (see equations 1.2 and 1.3), the value of the surface tension is directly proportional to the lifetime of the jets and their instability coefficient. The formation of thinner microfibrils is also due to the fact that the solid nanoparticles in the PP jets prevent the thinnest ones from breaking up into drops. It can be seen from the electron micrographs (Fig. 1.26) that when TiO_2/SiO_2 nanoparticles are introduced into the PP/SPA mixture, the dimensional characteristics of the microfibrils change, and they acquire the correct cylindrical shape [34].
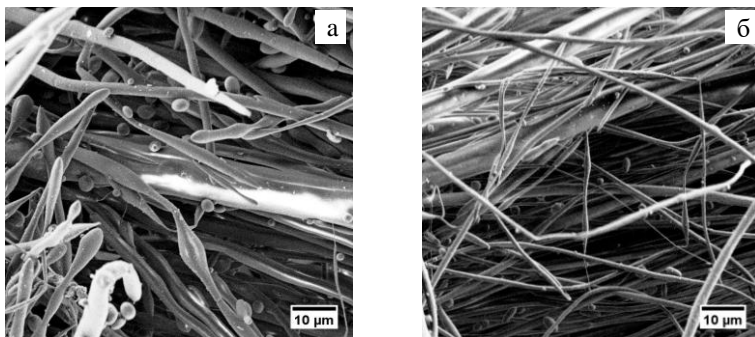
Fig. 1.26. Electron micrographs of PP microfibrils from a mixture of
PP/SPA/ TiO$_2$/SiO$_2$ composition, wt. %: 30/70/0 (a); 30/69/1 (b)

At the same time, the so-called "varicose" fibers, which are formed as a result of incomplete disintegration of liquid jets, are practically absent.

The morphology of incompatible polymer mixtures is also influenced by the content of nanofiller in the composition. Thus, studies of the microstructure of extrudates of the PP/SPA mixture filled with NPs of mixed oxide showed that the introduction into the system of (0.1÷3.0) wt. % additive helps to increase the degree of dispersion and homogeneity of the distribution of polymer particles of the dispersed phase in the dispersion medium (Fig. 1.27) [34].
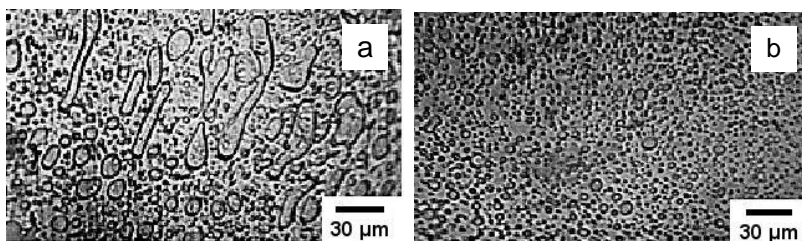
Fig. 1.27. Photomicrographs of cross-sections of extrudates of mixtures of
PP/SPA/ TiO$_2$/SiO$_2$ composition, wt. %: 30/70/0 (a); 30/69/1 (b)

The analysis of PP residues after SPA extraction shows that during the flow of melts of nanofilled mixtures there is an effect of phase distribution of components: the polymer of the dispersed phase forms thin jets that remain in the form of a bundle of microfibrils after the dissolution of the matrix polymer. Quantitative microscopic studies showed that along with microfibrils of continuous length, other types of structures are formed: particles, films, short microfibrils (Table 1.35).

Table 1.35. Microstructure characteristics of extrudates of PP/SPA/ TiO_2/SiO_2 mixtures *

Content of TiO_2/SiO_2 wt. %	Microfibrils					Particles		Films, wt. %
	continuous			short				
	d, μm	share, wt. %	σ^2, μm^2	d, μm	share, wt. %	d, μm	share, wt. %	
0	4,0	79,5	2,6	3,2	10,8	4,1	2,7	7,0
0,5	2,7	82,7	1,2	2,4	9,0	2,9	2,6	5,7
1,0	1,8	94,0	1,2	2,0	1,1	2,4	1,2	3,8
1,5	2,2	89,9	1,7	2,1	2,3	2,6	3,4	4,4
3,0	2,5	85,4	1,9	2,3	4,7	3,1	5,8	4,1

* за напруги зсуву $\tau = 5{,}69 \cdot 10^4$ Па

The obtained data confirm the improvement of the *in situ* formation of PP microfibrils at all investigated concentrations of TiO_2/SiO_2 - the average diameter of microfibrils of continuous length decreases from 4.0 μm (for the original mixture) to (1.8÷2.7) μm (depending on the concentration additives), their homogeneity in diameters increases, judging by the value of the dispersion of the distribution (σ^2). At the same time, the concentration of the nanofiller significantly affects the dimensional characteristics of the fibrils and the relationship between them and other structures in the extrudate. The diameters of microfibrils reach minimum values, and their

number becomes maximum at an additive content of 1.0 wt. % (Table 1.35).

The formation of a more perfect morphology at all investigated concentrations of the mixed oxide is the result of a decrease in the surface tension at the phase separation boundary (Table 1.36).

Table 1.36. The influence of the TiO_2/SiO_2 content in the PP/SPA mixture on the kinetics of the disintegration of polypropylene jets in the co-polyamide matrix

Content of TiO_2/SiO_2, wt. %	Surface tension, mN/m	Coefficient of instability	Lifetime, s	Reduced lifetime, s/µm
0	2,60	0,0347	32,6	24,5
0,5	0,87	0,0159	128,1	59,5
1,0	0,41	0,0180	154,3	75,9
3,0	1,52	0,0247	130,2	62,3

Data of Table 1.36 show that in the presence of a nanofiller, the surface tension decreases, a developed transition layer is formed at the boundary of the separation of the components of the mixture, and the stability of liquid jets increases. The maximum effect of the nanoadditive on the morphology of the extrudate occurs at a minimum value of the interfacial tension. At the same time, the value of γαβ decreases to 0.41 mN/m against 2.60 mN/m in the original mixture, and the average diameter of microfibrils decreases more than twice (tables 1.35, 1.36). A further increase in the amount of mixed oxide in the system leads to an increase in the interfacial tension and, accordingly, in the microfibril diameters. This can be explained by the fact that when the critical content is reached, the nano-

additive (compatibilizer) separates into a separate phase, and its surface activity decreases. The decrease in the diameters of microfibrils is also facilitated by an increase in their resistance to decay: the instability coefficient decreases, and the life time increases (Table 1.36).

Thus, the influence of fillers on the formation of morphology in melts of thermodynamically incompatible polymer mixtures is manifested by the occurrence of a number of processes: a decrease in the value of surface tension at the boundary of phase separation and the free surface energy of mixing, changes in the ratio of viscosities and elasticities of phases, the occurrence of significant interactions between polymer macromolecules and solid particles of the additive, counteracting the coalescence of drops due to their physical shielding. Regarding the mechanism of formation of microfibrils of the component of the dispersed phase in the matrix, the views of scientists differ somewhat. Some of them believe that the formation of PET microfibrils in the PP matrix in PP/PET mixtures filled with TiO_2 nanoparticles occurs at the stage of drawing the composite extrudate [154]. The results of the research carried out at KNUTD show that the type of structure of polymer dispersions is laid already in the entrance zone of the forming hole: when passing from a wide reservoir to a narrow droplet of the dispersed phase, they deform and merge into liquid jets. The compatibilizing action of nanofillers improves this process. In our opinion, orientational stretching ensures further reduction of microfibril diameters. An additional factor leading to the improvement of the microfibrillar morphology of nano-filled systems is the

increase in the thermodynamic stability of jets of small diameters due to the fact that the amplitude of the destructive disturbance wave is extinguished on the nanoparticles [34,36]. However, the mechanisms of influence of nanofillers (especially of different geometric shapes) on the morphology of mixtures still remain a subject of debate and require further research and theoretical generalizations.

Based on the above, it can be concluded that the influence of nanoparticles on the formation of microfibrillar morphology of thermodynamically incompatible mixtures is determined by a combination of the following factors:

• chemical nature of the ingredients and composition of the composition;

• content and morphometric characteristics of nanofiller;

• rheological properties of the components and the ratio of their viscoelastic indicators;

• the value of surface tension at the boundary of phase separation;

• degree of compatibility of polymers of the mixture and interphase interaction;

• conditions of the process of mixing ingredients;

• • predominant localization of nanoparticles in the volume of one of the components or at the border of their separation.

1.4.2. Effect of nano-additives on the properties of thin-fibrous microfibrillar materials. Reducing the diameters of filaments to micro- and nano-size significantly improves the quality of products based on them. The formation of thin

fibrous materials (complex threads and filters) by processing melts of polymer mixtures allows you to adjust their characteristics both due to the influence on the process of structure formation of the component of the dispersed phase in the matrix, and due to the unique properties of the nanofillers themselves.

The technology of obtaining materials from ultrafine fibers by processing melts of polymer mixtures involves two main stages: the formation of composite products (films, monofilaments) with a given structure (isotropic matrix filled with micro- or nanofibrils of the second component) and the extraction of the matrix polymer with an inert solvent [27].

1.4.2.1. Nano-filled complex microfibrillar threads. A significant advantage of textile materials made of ultrafine fibers is that they fully preserve all the positive properties of traditional synthetic fibers: high strength, shape and wear resistance. At the same time, due to the very small diameter of individual filaments, there are many pores in the materials based on them, thanks to which free air circulation can occur between the human skin and the external environment, and products made from them are characterized by increased comfort ("breathe") [19].

The conducted studies showed that the melts of nano-filled mixtures of PP/SPA and PP/PVA are stably processed into threads and films on the existing extrusion equipment. Complex threads from nano-filled PP microfibrils were obtained by extracting the matrix polymer (SPA) with an aqueous solution of ethyl alcohol from composite monofilaments. Carbon nanotubes [12], silica nanoparticles

[27] or complex substances based on it [34,35] were used as modifiers. In the process of processing melts of mixtures, solid nanoparticles do not prevent the deformation of PP drops and their merging in the longitudinal direction. The formed microfibrils have an almost continuous length, their strength and elongation at break are within the limits for textile polypropylene threads formed by traditional technology. Complex threads from nano-filled microfibrils are characterized by increased mechanical parameters, and the degree of their growth is determined by the chemical nature of the nano additive (Table 1.10).

As can be seen from the table. 1.10, modified silicas are more effective nano additives than original SiO_2. The introduction of carbon nanotubes provides the maximum values of tensile strength, which is the expected result. At the same time, the properties of nano-filled complex threads, as well as those formed from melts of unmodified mixtures, are largely determined by the type of structures of the dispersed phase in the matrix: the thinner the microfibers and the smaller the number of films, the higher their strength and resistance to deformation [27]. The worse mechanical indicators of complex threads obtained from mixtures with silica additives (compared to other nano additives) are due to the fact that there is a significant amount of films in their structure (Table 1.33, 1.37).

Table 1.37. The influence of the chemical nature of
nano-additives on the mechanical properties of complex
threads made of PP microfibrils

The name of nano additives	Linear density, tex	Tensile strength, MPa	Elongation at break, %
without additives	4,2	170	13,3
silica	4,2	210	12,9
methylsilica	4,0	230	12,3
titanium oxide/silica	4,1	240	12,6
silver/silica	3,9	250	11,1
carbon nanotubes	4,0	290	10,4

Table 1.38 shows the results of the study of the influence of the content of mixed oxide (TiO_2/SiO_2) on the properties of complex threads made of nano-filled PP microfibrils.

Table 1.38. The influence of TiO_2/SiO_2 additives on the
properties of complex threads

Content of TiO_2/SiO_2, wt. %	Strength, MPa	Initial modulus, MPa	Elongation, %	Specific surface area, m^2/g
0	160	2800	13,3	84
0,5	190	3500	11,8	135
1,0	240	3800	12,6	190
3,0	220	3400	11,7	210

The obtained results indicate that their tensile strength and initial modulus largely depend on the concentration of the additive: its increase to 1.0 wt. % leads to an increase in these indicators by 1.5 and 1.3 times, respectively. The maximum values are achieved with an additive content of 1.0 wt. %, when the most perfect microfibrillar morphology is formed. A

further increase in the content of TiO_2/SiO_2 nanoparticles is accompanied by some deterioration of the mechanical characteristics of the threads, which is associated with a change in the dimensional characteristics of microfibrils and an increase in the share of other types of structures (Table 1.38).

Polypropylene is a hydrophobic polymer and absorbs $(0.01 \div 0.02)$ wt. % of moisture. The hygroscopicity of PP microfibers, determined by the value of equilibrium water absorption, is more than an order of magnitude higher compared to traditional textile polypropylene threads (Table 1.39).

Table 1.39. The influence of the chemical nature of nanoadditives on the specific surface area and hygroscopicity of polypropylene microfibers

The name of additives	Specific surface area, m^2/g	Hygroscopicity, %
without additives	84	0,17
SiO_2	244	0,35
Ag/SiO_2	230	0,31
TiO_2/SiO_2	190	0,48
CNT	270	0,24

This is due to the fact that the microfibers formed in the polymer matrix have an unusual surface structure - it is not smooth, but uniformly covered with nanofibrils along the entire length [27]. Such a structure provides them with a developed specific surface ($S_{пит}$) and high sorption properties. In nano-filled microfibrillar materials, the value of $S_{пит}$ increases, compared to unmodified microfibers, and depends on the content of the additive and its chemical nature (Table 1.38,

1.39). Increasing the specific surface area of nano-filled fibers improves their hygienic and sorption properties. Thus, the adsorption of bacteria from aqueous solutions by modified microfibers is at the level of silica, which is known to be an effective adsorbent and is widely used in medicine [27].

The introduction of bactericidal nanoadditives into the structure of fibrils provides microfibrillar threads with antimicrobial properties that depend on the chemical nature of the additive [12,36]. Carbon nanotubes give threads weak biological activity. The use of combined silver-containing substances helps to delay the growth of many reference and clinical strains of microorganisms. The most effective are nanoadditives in which silver NPs are applied to the surface of mineral sorbents (silica, alumina), as they combine the antimicrobial effect of silver in the nanostate with high sorption and antitoxic properties of the base. Complex threads filled with Ag/Al_2O_3 nanoparticles are the most effective due to the fact that aluminum oxide itself exhibits high antimicrobial activity against strains of microorganisms [23]. Materials based on nano-filled complex threads are able to protect against pathogenic microflora and can be used to create new products with improved hygienic properties, including protective suits for medical workers.

1.4.2.2. Modified thin fiber filter materials. Composite films were also formed by processing melts of nanofilled PP/SPA/nanoadditive mixtures on a ЧП-45 worm press through a flat-slit fishtail head [27,36]. After the matrix polymer was extracted from them, non-woven sweatpants were obtained, the main structural unit of which is nano-filled PP

microfibrils of continuous length. Silica and bifunctional substances based on it were used as a nanofiller - silver/silica and titanium oxide/silica, which were introduced in the amount of 1.0 wt. %. In fig. 1.28a shows an image of a sample of non-woven material stretched in the transverse direction, from which it can be seen that the microfibers in the layer are located parallel to each other and maintain their orientation in the direction of extrusion.
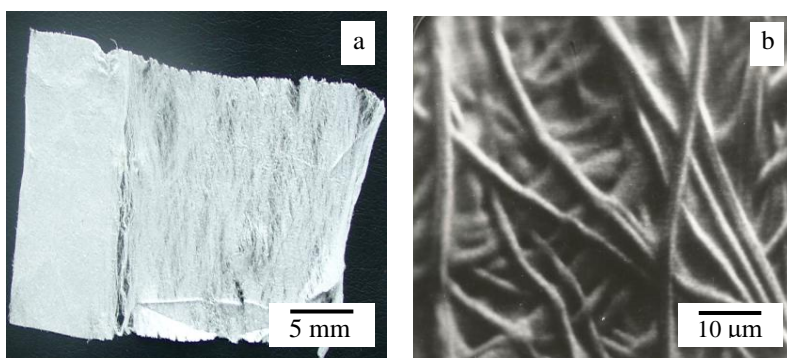

Fig. 1.28. Microphoto of a sample of non-woven material (a)
and electronic image of its surface layer (b)

At the same time, in the surface layer during the SPA extraction process, they partially lose parallelism (Fig. 1.28b). Fibrous materials with such an ordered, homogeneous structure can be used as precision filters. The main parameters characterizing filter materials (FM) are their retention capacity and productivity. The results of the evaluation of the efficiency of cleaning the atmospheric air from mechanical particles with a size of (0.3÷1.0) microns through modified materials show that the introduction of nano additives into the structure of polypropylene microfibers improves their operational

characteristics, compared to FM from the original mixture (Table 1.40).

Table 1.40. The influence of the chemical nature of nanoadditives on the efficiency of air purification and the performance of filter materials

The name of additives	Efficiency, % (by particle size, μm)						Producti-vity, $dm^3/m^2 \cdot h$ *
	0,3	0,4	0,5	0,6	0,8	1,0	
без добавок	78,6	83,5	85,9	87,8	91,9	99,4	4050
SiO_2	99,9	100	100	100	100	100	10650
Ag/SiO_2	99,3	99,9	100	100	100	100	10840
TiO_2/SiO_2	99,9	100	100	100	100	100	12230

* at a pressure of $0,5 \cdot 10^5$ Pa

As can be seen from the table. 1.40, the efficiency and precision of modified FMs increase dramatically, especially when cleaning from small particles. The increase in the retention capacity of the filters is due, firstly, to the improvement of the structure of the filter layer (a decrease in the average diameter of nano-filled PP microfibrils by almost 2 times, an increase in their number and a more correct geometric shape) (Table 1.33, Fig. 1.26). This is natural, since the size of the pores in the filter layer is lower, the smaller the size of its components, and their shape is more uniform, the more uniform and perfect the shape of the structures forming the filter layer is [158]. The second important factor that ensures the improvement of the efficiency of modified fine-fiber FM is that precision filtration (cleaning of media from impurities ≤ 1.0 μm in size) occurs not only by the so-called "sieve" effect, but also due to a number of physico-chemical processes - the

effect of touching, adsorption, Brownian diffusion [158]. Thanks to this, the fine-fiber filter material can retain particles with diameters 5 times smaller than the pore size. The decisive importance of the adsorption process is evidenced by a sharp increase in the specific surface area up to 84 m^2/g for original and up to (190÷244) m^2/g for nano-filled PP microfibers, compared to fibers formed by classical technology (Table 1.38, 1.39).

The permeability of filters is determined by the pressure difference on both sides of the filter partition and the resistance of the material in relation to the filtered medium. Studies of the productivity of FM in distilled water showed its increase for samples in the structure of which there are nanoparticles of the original and modified silicas (Table 1.13). This is an important unexpected result, since increasing the precision and efficiency of filters of any class, as a rule, is accompanied by a decrease in their permeability. The increase in productivity is obviously caused by a decrease in the hydraulic resistance of the filter layer due to better hydrophilicity of nano-filled PP microfibers (Table 1.39). An additional factor that ensures the maximum performance of FM modified by mixed oxide is obviously the ability of materials with TiO_2 nanoparticle additives to self-clean like plant leaves, insect wings, etc. [19].

Depending on the fields of application, filter materials, in addition to the specified basic indicators, must meet a number of additional requirements. In some cases, it is necessary that the filter layer is not a source of growth of microorganisms, has antimicrobial properties, withstands

sterilization, etc. The adsorption capacity of nano-filled filter materials in relation to bacteria is at the level of A300 silica. They also exhibit high antimicrobial and antifungal activity against reference and museum test strains of microorganisms and fungi [27,36].

The developed nano-filled polypropylene filter materials have sufficient strength, withstand 20 times sterilization with hot steam and chemical reagents (water-alcohol solutions and hydrogen peroxide) and are regenerated by reverse current by 80%.

An important advantage of the method of obtaining thin-fiber filter material by extracting the matrix polymer from a composite film with a microfibrillar structure is the possibility of increasing the working surface of the filter. At the same time, it should be emphasized that, unlike other methods, in this case, a corrugated film (that is, a semi-finished product) is crimped, and not a ready-made filter material, which prevents mechanical damage and contamination of the filter layer and deterioration of its properties. Filters based on nano-filled PP microfibrils effectively purify drinking water, pharmaceuticals, technological environments of the food industry and medicine, air, etc.

Thus, the creation of polymer nanocomposites, regulation and research of their properties is one of the most important areas of development in the field of nanotechnology. Significant interest in such materials is due to the fact that they combine low cost with a set of unique characteristics that are not inherent in the original polymers. The introduction of nanofillers into melts of thermodynamically incompatible

polymer mixtures is one of the most effective factors in regulating the structure formation process of the dispersed phase polymer in the matrix. This is achieved due to the effect of nano-additives on the rheological properties of the initial components and interphase phenomena: a decrease in the surface tension, an increase in the degree of dispersion and deformation of the polymer droplets of the dispersed phase, and the stabilization of jets of smaller diameters. The established regularities make it possible to determine the key factors that ensure the formation of micro- and nano-sized microfibrils uniform in diameter of continuous length as the predominant type of structure of polymer nanocomposites.

CHAPTER 2
MATHEMATICAL MODELING AND SOFTWARE FOR THE STUDY OF MICRO-AND MACRO-RHEOLOGICAL PROCESSES IN MELTS OF INCOMPATIBLE POLYMER MIXTURES

2.1. Mathematical methods of modeling the structure and rheological behavior of polymer dispersion systems

The study of flow characteristics of polymer dispersion systems is in the center of attention of researchers of many developed countries of the world, as it allows controlling micro- and macro-rheological processes during their processing and creating products with predetermined properties. To date, a significant amount of experimental data has been accumulated and a number of empirical dependencies have been formulated that describe with sufficient accuracy the features of the rheological behavior of melts of polymer mixtures, however, in general, in the mechanics of dispersed systems, there is a noticeable lag between theoretical studies and experimental ones. Mathematical modeling methods play an important role in solving many scientific and practical problems of predicting and controlling the phase morphology of polymer systems.

Any theoretical research on the creation of mathematical models begins with the establishment of rheological equations of state, which connect the stress tensor in the suspension with the kinematic characteristics of the flow and make it possible to close the system of equations of motion obtained on the basis of the general laws of mechanics. Phenomenological (macroscopic) and structural (microscopic)

approaches are used to construct the rheological equations of state of dispersed systems, and in recent years, their unification – structural-phenomenological. The phenomenological approach is based on the assumption that the environment is continuous and homogeneous. Equations of state under this approach are created on the basis of the general laws of classical mechanics and phenomenological thermodynamics under certain assumptions regarding the properties of the environment (instability, isotropicity, elasticity, etc.). The use of modern methods of mathematics - tensor analysis, group theory, functional analysis allows obtaining the dependence of the stress tensor on kinematic parameters and other characteristics that determine the nature of the flow in a fairly general form, which is undoubtedly a strong point of the phenomenological approach [159-161]. The structural approach describes the rheological properties of systems based on the study of the flow behavior of their constituent elements. At the same time, the macroscopic characteristics of dispersions are expressed by averaging the parameters of the microstructure and the dispersion medium. The first work in which a structural approach was used to study the behavior of dilute suspensions was a study by Einstein [162]. He proposed an equation for determining the effective viscosity ($\mu_{e\phi}$) of the suspension:

$$\mu_{e\phi} = \mu \, (1 + 2{,}5 \, \varPhi) \qquad (2.1)$$

where μ – liquid viscosity; $\varPhi$ – volume concentration of suspended particles

147

Einstein's energy approach was widely used by other authors to determine the $\mu_{e\phi}$ of dilute suspensions with particles of different geometric shapes [163,164]. The disadvantage of this method is that, by determining the scalar function - viscosity, it is impossible to answer the main question - what is the form of the rheological equation of the state of the suspension.

The dynamic Landau method is also used to study the behavior of dispersed systems from the standpoint of a structural approach [165]. At the same time, velocity and pressure disturbances introduced into the flow of the dispersion medium by a suspended particle are used to find the stress tensor caused by these disturbances. Using this method, the rheological equations of state of dilute suspensions of hard spherical particles [166] and concentrated dispersed systems with hard and deformable particles [167,168] were obtained. The most widespread hydrodynamic models of the microstructure of suspensions of rigid particles are balls, one-dimensional "dumbbells", cylindrical sticks, ellipsoids, disks, and for deformable suspended particles - elastic and viscoelastic spheres and ellipsoids [169,170]. The strength of the structural approach is that, with the selected particle model, all quantities included in the rheological equation of state are determined theoretically as functions of the parameters characterizing the microstructure and dispersion medium. At the same time, the structural approach has its weaknesses. Einstein's energy method allows you to find only the effective viscosity of a dispersed system in the simplest flow. The dynamic Landau approach leads to rather cumbersome

equations and calculations, which makes it ineffective when constructing the equations of state of systems that have a complex microstructure.

The positive aspects of the considered methods mutually complement each other, that is, there is an expediency of combining them when creating rheological equations of state of complex environments [170-175]. The structural-continuum approach is based on the use of phenomenological models of the structural continuum, which contain the necessary number of internal parameters to describe the behavior of the microstructure of the dispersed system. The structural continuum is a model of a continuous medium in which, under the basic assumptions of continuum mechanics (continuity, inseparability of functions characterizing the movement and state of the medium), the peculiarities of changes in the microstructure of the dispersed phase and their influence on the rheological properties of the dispersion are taken into account. If in classical mechanics each point of the continuum is characterized by density, speed and pressure, then in the structural continuum, along with the listed indicators, there are also so-called internal parameters. Thus, unlike the continuum of classical mechanics, the structural continuum has additional degrees of freedom, which are used to take into account the peculiarities of the behavior of the dispersion microstructure. Internal parameters can be scalars, vectors, tensors, and their number and type are determined by the nature of the morphology of the dispersed phase. Thus, when building phenomenological models of the structural continuum for suspensions of rigid and deformable particles, the choice of

internal parameters is determined by the need to introduce into the rheological equations the influence of the orientation of suspended particles, their hydrodynamic interaction and deformation on the behavior of the suspension. In the case of dilute suspensions, the orientation and deformation of particles that have symmetry relative to an axis and a plane perpendicular to it are modeled by only one internal parameter, a vector [176]. The location of the vector in space characterizes the dependence of the rheological properties of the medium on the direction (anisotropy), and the modulus of the vector is the deformation of the particles during the flow. In [171], a deformable ellipsoid of rotation with internal viscosity and elasticity was considered as a model of a suspended particle. At the same time, it was assumed that in the process of interaction with the dispersion medium, the particle changes its size, but its shape remains an ellipsoid of rotation, which retains its volume. Conducted studies of the behavior of a deformable ellipsoidal particle under the inhomogeneous flow of a Newtonian fluid showed that the ability of a suspended particle to deform complicates the rheological equations of state of dilute suspensions. Although the form of the equations is close to the rheological equations of state of rigid particles, they differ significantly in content. Instead of rheological constants, these equations contain rheological functions that are included in the quantities to be averaged.

A dilute suspension of ellipsoidal particles is the most common hydrodynamic model of deformable asymmetrically elongated particles in a Newtonian fluid. Under the condition of a non-Newtonian dispersion medium and another (more

complex) geometric shape of a dispersed particle, the possibility of obtaining rheological equations of state of such dispersions is complicated by the need for an analytical solution to the problem of hydrodynamic interaction of the particle with the environment. Therefore, the authors of [175] proposed to use a deformable triaxial dumbbell as a hydrodynamic model of the particle. Such models are three-dimensional and do not have the disadvantages of classic models. When using the specified models, rheological equations of state of dilute suspensions of deformable particles were obtained, which can be extrapolated to dispersed systems with particles of more complex geometry. Thus, the structural-phenomenological approach makes it possible to describe the rheological properties of polymer dispersions in a fairly general way, taking into account their microrheological characteristics.

A number of mathematical models have been developed that predict the possibility of regulating the types of phase structures in multicomponent polymer mixtures due to changes in the surface tension and free interfacial energy [177,178]. The introduction of the third polymer component into the binary mixture significantly increases the number of possible phase structures. Hobbs [177] proposed theoretical relations that make it possible to predict the type of morphology of phases B and C in matrix A by determining the spreading coefficient (λ_{ij}). If λ_{BC} and λ_{CB} are negative, then phases B and C will form separate dispersions in matrix A. Phase C encapsulates phase B in the case when $\lambda_{BC} \succ 0$, and, conversely, a positive value λ_{CB} leads to encapsulation of component C by phase B.

The authors of [178] created a more advanced model that allows predicting the types of phase structures and changing them, based on the fact that the thermodynamically favorable morphology of a multicomponent system is determined not only by surface tension, but to a greater extent by free interfacial energy. The theory is based on the principle that when mixing, systems with the lowest free energy are formed. To determine the Gibbs free energy (G) of multiphase polymer systems, the following equation was proposed:

$$G = \sum_i n_i \mu_i + \sum_{i \neq j} A_i \gamma_{ij} \qquad (2.2)$$

where: n – the number of molecules; μ – chemical potential; A – the area of the interfacial region; γ – interphase tension

For a ternary system where two interfaces coexist, there are nine possible types of phase structures. The authors [178] calculated the interphase free energy of the system for different phase structures using the following mathematical model

$$\left(\sum A_i \gamma_{ij}\right)_{B+C} = (4\pi)^{1/3}[n_B^{1/3} x^{2/3} \gamma_{AB} + n_C^{1/3} \gamma_{AC}](3V_C)^{2/3}$$

$$\left(\sum A_i \gamma_{ij}\right)_{B/C} = (4\pi)^{1/3}[n_B^{1/3} (1+x)^{2/3} \gamma_{AB} + n_C^{1/3} \gamma_{BC}](3V_C)^{2/3} \qquad (2.3)$$

$$\left(\sum A_i \gamma_{ij}\right)_{C/B} = (4\pi)^{1/3}[n_B^{1/3} x^{2/3} \gamma_{BC} + n_C^{1/3} (1+x)^{2/3} \gamma_{AC}](3V_C)^{2/3}$$

where: $x = V_B/V_C$; n_B; n_C – number of B and C phase particles; V – total volume

The adequacy of this model was tested on three-component mixtures of polyethylene / polypropylene / polystyrene (PE/PP/PS) and PE/PS/PMMA (polymethyl methacrylate) of different compositions. Calculations

performed using equations (2.3) showed that for PE/PP/PS mixtures of 70/20/10 wt. % minimum free energy occurs when PS particles are encapsulated by the polypropylene phase, i.e. the theory predicts the formation of just such a morphology. The results of experimental studies coincided with the types of structures predicted by the specified authors. Similar confirmation by theoretical prediction was also obtained for PP/PE/PS mixtures of 70/20/10 mass. %. For this system, the minimum calculated interfacial energy occurs for structures in which PE and PS form separate dispersed phases in the PP matrix. Exactly this type of structure was obtained experimentally.

The dependence of the types of morphology of the components of the mixture on the free interfacial energy allowed Guo and co-authors [178] to conclude that the structure of such systems can be changed by increasing or decreasing the interfacial tensions between the components. Experimental reduction of interfacial tension in PE/PP/PS mixtures was achieved by adding (0.5 2.0) wt. % of the interphase-active diblock copolymer of styrene and ethylene (C-E). When introducing 2.0 wt. % C-E, the encapsulated type of structure (PP/PS) changes to dispersed (PP+PS), as predicted by the proposed model. Similar results were also obtained when adjusting the structure of the PE/PS/PMMA mixture with a ratio of 70/15/15 components by introducing 3.0 wt. % block copolymer of ethylene with methyl methacrylate.

The model, which allows predicting the type of structure in three-component systems, was applied to four-component polymer mixtures containing PE, PP, PS, and

PMMA in different ratios [179]. Calculations made on the model show that the interphase voltages play a major role in the formation of the phase structure, and the surface area of the dispersed phase has a much smaller effect. The predicted structures were compared with experimental data. In most cases, the correspondence between the predicted and experimentally obtained morphology is shown. In addition, it was established that the structure of the four-component system can be changed from one phase morphology to another, for example, when using surface-active block copolymers. The presented studies show the possibility of predicting and establishing the desired morphology of phases in multicomponent systems. However, despite all the importance of the theoretical studies performed, the above-mentioned theories do not describe the entire variety of types of phase structures that are formed in polymer mixtures, and, which is especially important for multicomponent polymer compositions, do not distinguish between dispersed and microfibrillar morphology.

2.2. Mathematical model and software of the process of formation of microfibrillar structure in melts of polymer mixtures

2.2.1. Mathematical modeling by the structural-continuum method of the deformation of droplets of the dispersed phase component during the flow of melts of mixtures. As shown in section 1.3.1, a microfibrillar structure is formed during the flow of melts of thermodynamically

incompatible polymer mixtures. The study of factors affecting the dimensional characteristics of microfibrils of one component in the matrix of another is of significant scientific and practical interest, as it allows obtaining polymer composites with adjustable morphology and properties. By extracting the matrix component from them, thin fibrous materials with micro- and nano-sized filament diameters are obtained. A number of authors attempted to describe the process of microfibril formation during the flow of a binary mixture melt, but in their research, the main attention was paid to the deformation of a polymer drop in the channel of the forming hole or after exiting it and during subsequent thermal orientation drawing. However, the mechanism of microfibrillar structure formation was previously formulated and experimentally confirmed, the essence of which is that the in situ formation of microfibrils of the dispersed phase component in the matrix mass occurs in the field of shear and tensile stresses that arise in the melt during its flow from a wide reservoir to a narrow [134].

Theoretical studies of the rheological behavior of polymer dispersion systems are associated with significant difficulties. To understand the processes that take place in the dispersion flow, it is necessary to determine the influence of many factors: the viscoelastic properties of the components, the volume concentration of the dispersed phase, the shape and size of the particles, their interaction, etc. Detailed consideration of these indicators is possible within the framework of a structural (microscopic) approach. The latter found particularly successful development in the study of

relatively simple environments, such as dilute suspensions with round or oval-shaped particles. The possibility of using the structural method in the rheology of dispersions is limited by their variety and complexity of morphology. The structural-continuum approach proposed by the authors [170-172] combines phenomenological and structural methods and makes it possible to take into account all the main provisions of continuum mechanics (the integrity of the medium, the inseparability of the functions characterizing its movement and state) and the peculiarities of the behavior of the dispersed phase. Thus, in the structural continuum model, each dispersion point is characterized by density, velocity, and pressure (as in classical mechanics) and, in addition, by so-called internal parameters. In the case of dilute suspensions of deformable particles, one internal parameter is introduced into the rheological equation of state - a vector that takes into account the influence of orientation, hydrodynamic interaction and deformation of suspended particles on the behavior of the medium. At the same time, the coordinates of a particle in space, which are described by a vector, determine the dependence of the rheological properties of the suspension on the orientation of the particles (anisotropy), and the modulus of the vector is the amount of deformation during the flow [171].

To create a model of the deformation of the polymer droplets of the dispersed phase in the matrix form, the droplets were taken as an ellipsoid, which changes its size in the process of interaction with the dispersion medium, but at the same time retains its volume. The dispersion medium was modeled with a Newtonian fluid in order to simplify the mathematical

expressions and the possibility of solving the obtained equations.

The system of equations describing the isothermal movement of a continuous medium consists of uniaxial tensile flow equations, flow continuity, and the rheological equation of the liquid state. To analyze the velocity field in the entrance zone, a cylindrical coordinate system was used, since the streamlines at the entrance to the channel have a radial velocity component (Fig. 2.1).
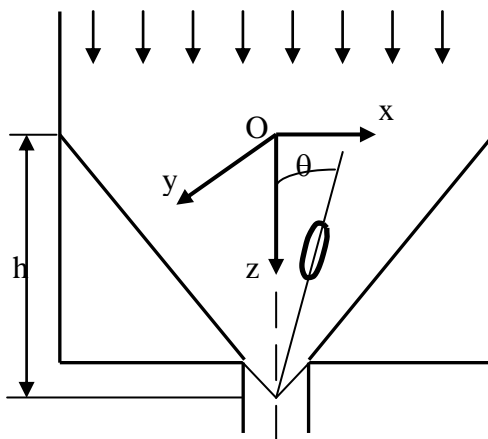

Fig. 2.1. Schematic representation in the cylindrical coordinate system of the melt flow of the mixture during the transition from a wide reservoir to a narrow one

Such a flow field arises as a result of superposition of the longitudinal deformation of the melt on its shear flow. The vectors of local velocities are directed along the generating cone and have three components: the velocity in the direction of the flow V_z and in the perpendicular directions V_x, V_y. The first of them gives tensile deformation, and the other two -

shear. The velocity field in this case can be described as follows:

$$V_x = -u/2x; \qquad V_y = -u/2y; \quad V_z = uz; \qquad (2.4)$$

where: u – flow intensity of uniaxial tension $(u = V/h)$;

V – the rate of descent of the upper layer of the melt mixture;

h – the height of the melt layer of the mixture

The strain rate tensor (d_{ij}) of uniaxial tension is determined from the dependence [172]:

$$d_{ij} = \begin{pmatrix} -u/2 & 0 & 0 \\ 0 & -u/2 & 0 \\ 0 & 0 & u \end{pmatrix} \qquad (2.5)$$

At the same time, it is assumed that there is no circulation current. The flow continuity equation in the case of constant density has the form: $u_{i,i} = 0$.

The rheological state of the investigated dispersion was described by an equation derived from the structural-continuum approach for dilute suspensions with ellipsoidal deformable particles [172]. This equation has one internal parameter $\vec{n}_i$ - the vector , which is related to the element of the microstructure - the weighted deformable particle. The vector $\vec{n}_i$ depends on the nature of the medium flow and can change in space and time. The direction of the vector coincides with the vector of the axis of symmetry of the ellipsoid, and its modulus coincides with the length of the semi-axis of rotation (a), i.e. $= |\vec{n}_i| = a$. The rheological equation describing an anisotropic liquid has the following form:

158

$$\dot{n}_i = \lambda_1 n_i + \lambda_2 d_{km} n_k n_m n_i + \lambda_3 d_{ij} n_j \qquad (2.6)$$

where: $\dot{n}_i$ – похідна derivative of the orientation vector ($\vec{n}_i$) in time, taken at the corresponding point and at the corresponding moment;

d_{km} – elements of the strain rate tensor of uniaxial tension;

$n_k \ n_k, \ n_m, \ n_i$ – vector coordinates

Values $\lambda_1, \ \lambda_2, \ \lambda_3$ characterize the rheological properties of the system. Expressions for their definition are obtained in the work [173]:

$$\lambda_1 = \frac{-2ab^2 \beta_0^{"} G \dfrac{a}{a_0}(1-\dfrac{q}{q_0})}{\mu(2+3ab^2 \beta_0^{"}\dfrac{\eta}{\mu})}(1-M\varPhi)$$

$$\lambda_2 = \frac{2+(N-2M)\varPhi}{a^2(2+3ab^2\beta_0^{"}\dfrac{\eta}{\mu})} - \frac{a^2-b^2+\dfrac{15(a^2-b^2)(\alpha_0+\beta_0)+4(a^2+b^2)(\beta_0-\alpha_0)}{6ab^2\beta_0^{'}B}\varPhi}{a^2+b^2+\dfrac{15(a^2-b^2)+4(a^2+b^2)^2}{6ab^2B}\varPhi}$$

$$\lambda_3 = \frac{a^2-b^2+\dfrac{15(a^2-b^2)(\alpha_0+\beta_0)+4(a^2+b^2)(\beta_0-\alpha_0)}{6ab^2\beta_0^{'}B}\varPhi}{a^2+b^2+\dfrac{15(a^2-b^2)^2+4(a^2+b^2)^2}{6a^2bB}\varPhi} \qquad (2.7)$$

where:

$$M = \frac{4}{ab^2(2+3ab^2\dfrac{\eta}{\mu}\beta_0^{"})} * \{ \frac{5}{6(\alpha_0+2\beta_0-2\beta_0^{'}(a^2+b^2))} -$$

$$-\frac{100\beta_0' a^2 (2\beta_0' a^2 - \alpha_0 - 2\beta_0)}{(\alpha_0 + 2\beta_0)(\alpha_0 + 2\beta_0 - 2\beta_0'(a^2 + b^2))} * \left[\frac{1}{24a\beta_0} - \frac{1}{2\beta_0'^2 a^2 - (\alpha_0 + 2\beta_0)} \right] \Big\}$$

$$N = \frac{4}{ab^2} \left[\frac{10}{18\beta_0''} + \frac{5\beta_0''}{8b^4 \alpha_0'^2} - \frac{10(\beta_0'' - \alpha_0'')(2b^2 \alpha_0' + 3\beta_0'')}{72b^4 \alpha_0'^2} \right]$$

$$B = a^2 \alpha_0 + b^2 \beta_0$$

where a, b, a_0, b_0 – semi-axis of the ellipsoid in the deformed and undeformed state;

G, Φ – modulus of elasticity and volume concentration of the dispersed phase;

μ, η – viscosity of the dispersion medium and the dispersed phase;

$$q = \frac{a}{b}; \quad q_0 = \frac{a_0}{b_0} \quad -\ \text{deformation values.}$$

The values α_0, β_0, a_0', β_0', α_o'', β_o''– are defined in [163]. In the equations used, the dot means the full time derivative; repeating indices – addition from 1 to 3 by this index..

To solve equation (2.6) with respect to the amount of deformation and orientation of the ellipsoid (polymer droplet) in the flow, it was decomposed along the coordinate axes *x, y, z:*

$$\begin{cases} \dot{n}_x = \lambda_1 n_x + \lambda_2 \dfrac{u}{2}(-n_x^2 - n_y^2 + 2n_z^2)n_x + \lambda_3(-\dfrac{u}{2})n_x \\[2mm] \dot{n}_y = \lambda_1 n_y + \lambda_2 \dfrac{u}{2}(-n_x^2 - n_y^2 + 2n_z^2)n_y + \lambda_3(-\dfrac{u}{2})n_y \quad (2.8) \\[2mm] \dot{n}_z = \lambda_1 n_z + \lambda_2 \dfrac{u}{2}(-n_x^2 - n_y^2 + 2n_z^2)n_z + \lambda_3 u n_z \end{cases}$$

In the cylindrical coordinate system, the vector $\vec{n}_i$ coordinates can be defined as follows:

$$\begin{cases} n_x = a\cos\varphi \\ n_y = a\sin\varphi\sin\theta \\ n_z = a\cos\varphi \end{cases} \quad (2.9)$$

where: φ – кут the angle between the Ox axis and the projection of the rotation axis of the ellipsoidal particle onto the Oxy plane;

θ – the angle between the flow direction and the axis of rotation of the ellipsoid

Taking the derivatives of the left and right parts of (2.9), equating the right parts of the corresponding equations (2.8) and (2.9) and making the necessary transformations, a system of differential equations was obtained:

$$\begin{cases} \dot{\varphi} = 0 \\[2mm] \dot{\theta} = -\dfrac{3}{4}u\lambda_3 \sin(2\theta) \\[2mm] \dfrac{\dot{a}}{a} = \lambda_1 + \dfrac{u}{2}(\lambda_2 a^2 + \lambda_3)(2 - 3\sin^2\theta) \end{cases} \quad (2.10)$$

where: $\dfrac{\dot{a}}{a}$ – the rate of deformation of the ellipsoid

The presented system of differential equations (2.10) is a mathematical model of the deformation of the droplets of the dispersed phase component during the flow of the melt of the polymer mixture in the entrance zone of the forming hole [37,38,180]. The model allows determining the amount of deformation and the orientation of droplets in the flow depending on the rheological properties of the components of the mixture and the volume concentration of the dispersed phase.

For the convenience of solving the system of equations (2.10), we switched to dimensionless variables in the equation for determining the rate of deformation. In the new variables, the system of equations (2.10) can be written as follows:

$$\begin{cases} \dot{\varphi} = 0 \\ \dot{\theta} = -\dfrac{3}{4}u\lambda_3 \sin(2\theta) \\ \dfrac{\dot{q}}{q} = \dfrac{3}{2}(\lambda_1 + \dfrac{u}{2}(\lambda_2 r_0^2 q^{4/3} + \lambda_3)(2 - 3\sin^2\theta)) \end{cases} \qquad (2.11)$$

The latter system of differential equations was solved numerically by the Runge-Kutta method with the help of a specially written program (listing - see the appendix) in the Delphi environment in the Object Pascal language [190, 192].

The adequacy of the created model was checked by comparing the values of drop deformation calculated using the obtained equations with experimental results. For this purpose,

we used data from work [181], in which, on the example of mixtures of polyoxymethylene/copolymer of ethylene with vinyl acetate (POM/SEVA) with a composition of 20/80 wt. % the effect of the ratio of the viscosities of the mixture components on the formation of POM microfibrils in the SEVA matrix was investigated. With the help of the model, the deformation and orientation of the POM droplet in the flow as it moved to the entrance to the forming hole was calculated. The depth of descent of the drop along the height of the entrance zone was determined from the equation: $h(t) = h_0(e^{ut} - 1)$, where h_0 is the initial height of the melt of the mixture; t - is time.

The obtained results show that the magnitude of deformation (q) significantly depends on the distance to the entrance to the capillary and the angle of orientation of the drop in the flow (Fig. 2.2). The obtained theoretical results correspond to the conclusions of [182] regarding the melt flow rate during the transition from a wide reservoir to a narrow one. In such channels, the melt moves at an accelerated rate: the speed increases as it approaches the entrance to the die, and its maximum value is reached on the axis line. The values of q calculated using the model also agree with the experimental data on the deformation of the droplets in the inlet zone, shown in Fig. 1.13 (see section 1.3). The polymer droplets of the dispersed phase are deformed in the direction of the flow, when tensile stresses begin to arise in the tank (Fig. 1.13a, 2.2). The quantity q increases as the drop approaches the entrance to the forming hole. It becomes maximum on the axis of the flow ($\theta = 0$) and decreases as the angle θ - between the direction of

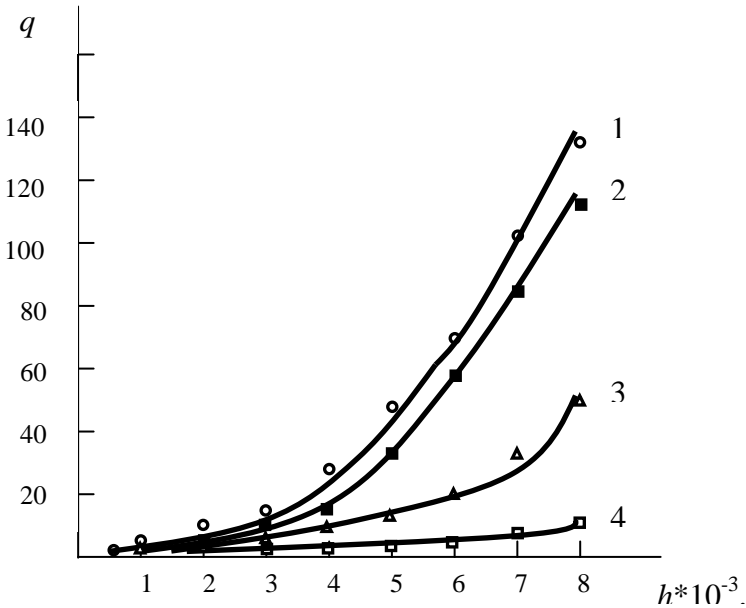the flow and the axis of rotation of the ellipsoid increases (Fig. 1.13b, 2.2).

Fig. 2.2. Dependence of the amount of deformation of the dispersed phase drop on the depth of immersion and the orientation angle θ, radian: 0 (1), 0.2 (2), 0.4 (3), 0.7 (4), under the condition $\eta/\mu = 1.0$

The experimentally established wide distribution of microfibrils in terms of diameters [27,181] is due to the different degree of deformation of the polymer droplets of the dispersed phase in the flow behind the flow in the extrusion equipment.

In sections 1.2, 1.3 it was shown that the microstructure of extrudates of polymer mixtures is formed during the flow and is determined by such microrheological processes as deformation, disintegration, coalescence and

migration of polymer droplets of the dispersed phase. The degree of manifestation of one or another of the listed processes depends to a large extent on the ratio of viscosities of the polymer of the dispersed phase and the matrix (η/μ). Calculations of the amount of deformation of a polyoxymethylene drop depending on the ratio of the viscosities of POM and SEVA performed with the help of the model show that the value of q decreases with an increase in $\eta_{\text{pom}}/\mu_{\text{seva}}$ (Fig. 2.3).
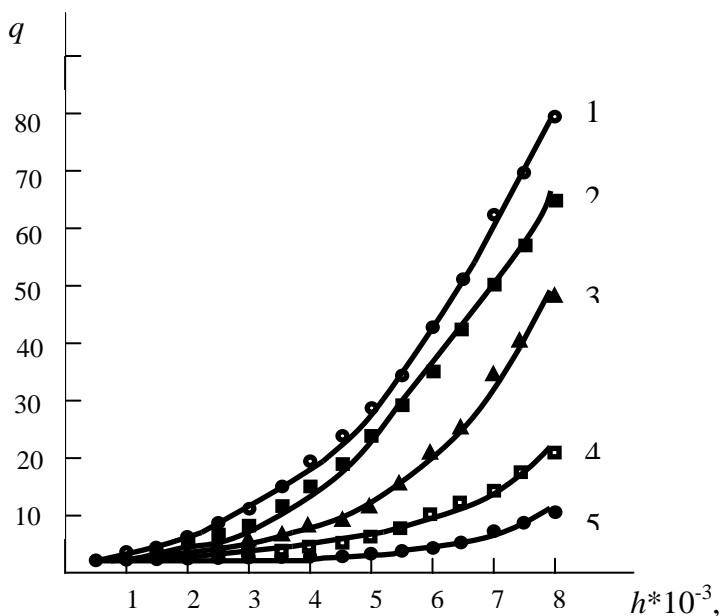
Fig. 2.3. The dependence of the amount of deformation of a dispersed phase droplet on the depth of immersion and the ratio of viscosities η/μ: 0.65 (1); 0.85 (2); 1.05 (3); 4.14 (4); 10.77 (5) at θ=0.4 radian

The latter is completely natural and has been confirmed experimentally [27,181]. In the case when the viscosity of the polymer melts is the same, the component of the dispersed phase is deformed to the same extent as the continuous phase. In the case when the viscosity of the polymer melts is the same, the component of the dispersed phase is deformed to the same extent as the continuous phase. Provided that η of the dispersed phase is smaller than that of the medium, the droplets deform better. An increase in η/μ is accompanied by a deterioration of the deformation of the dispersed phase component [68].

A comparison of the experimental results, which reflect the influence of the ratio of the viscosities of the components of the dispersed phase and the matrix on the dimensional characteristics of POM microfibrils in the SEVA matrix [181] with POM drops of size q calculated using the model, are shown in Table 2.1.

Table 2.1. Deformation values of droplets of the dispersed phase component

$H_{pom}/$ μ_{seva}	Experimental diameters of microfibrils*, µm			The values of q, calculated:					
				from experimental $đ_{cp}, d_{min}, d_{max}$ microfibrils			using the model at different angles θ, rad		
	$đ_{cp}$	d_{min}	d_{max}	q_{cp}	q_{min}	q_{max}	0	0,4	0,7
0,65	6,9	2,6	31,2	22,5	2,3	97,3	249,1	76,9	11,2
0,85	4,9	1,7	20,8	37,6	4,3	184,0	207,8	64,9	10,1
1,05	5,5	2,1	26,0	31,6	3,1	134,0	138,7	48,1	7,0
4,14	7,3	2,6	100	20,7	0,4	97,3	112,5	19,7	3,8
8,64	8,5	5,2	31,2	16,5	2,3	97,3	103,4	14,3	2,0
10,77	10,2	5,2	31,2	12,5	2,3	34,4	57,9	9,5	1,3

* $đ_{cp}; d_{min} d_{max}$ – average, minimum and maximum diameters

The analysis of the results shows that the developed mathematical model describes the real process of deformation of a polymer droplet of the dispersed phase in the entrance zone. Thus, the calculated deformation values are a function of the ratio of the viscosities of the mixed polymers. For values of $\eta_{pom}/\mu_{seva} > 1$, the deformation worsens, and for $\eta_{pom}/\mu_{seva} < 1$, q first increases and then decreases. The experimentally determined increase in the average diameter of POM microfibrils and drop in q under the condition of $\eta_{pom}/\mu_{seva} = 0.65$ contradicts theoretical conclusions [137]. A possible reason for this is the migration of droplets of a low-viscosity dispersed phase to the walls of the capillary. As a result, the center of the flow is impoverished, and a larger fraction of the dispersed phase is deformed on the periphery, where the deformation rates are much smaller than on the axis of the flow. For the values of q calculated using the model, there is a natural dependence of the deformation values on the viscosity ratio: when $\eta_{pom}/\mu_{seva} < 1$, the degree of deformation increases, and when $\eta_{pom}/\mu_{seva} > 1$, it decreases.

It is known that in addition to the ratio of the viscosities of the components of the mixture, their absolute values also make a significant contribution to microrheological processes during the flow of melts of polymer mixtures. The latter is confirmed by the results of calculations using the model of deformation values of droplets of the dispersed phase for cases when $\eta/\mu = 1$ (Table 2.2).

Table 2.2. The influence of the absolute values of the viscosities of the initial components on the amount of deformation*

$h*10^{-3}$,m	q provided:				
	$2\eta/2\mu$	$1,5\eta/1,5\mu$	η/μ	$0,75\eta/0,75\mu$	$0,5\eta/0,5\mu$
2	1,2	1,5	1,8	4,9	13,2
4	3,1	4,4	7,1	31,2	61,1
8	9,4	24,5	48,1	79,2	102,9

* provided θ = 0.4 radians умови

Calculations performed using the developed model show that the smaller the absolute values of component viscosities, the greater their deformation. So, for example, at $0,5\eta/0,5\mu$ and h = 8, the amount of deformation is 102.9, and at $2\eta/2\mu$ it is only 9.4. As expected, a decrease in the absolute values of η and μ leads to an increase in deformation. However, minimum viscosities are limited by the ability of polymers to be processed into fibers or films, as well as by the strengthening of coalescence processes. Obviously, there are optimal viscosities of the initial polymers for which the maximum values of the deformation of the droplets of the dispersed phase can be achieved under the condition that η/μ = 1. Thus, the choice of the absolute values of the viscosities of the polymers of the mixture can be one of the methods of regulating structure formation with the aim of obtaining fibrils with nanosized diameters.

It is known that there is a competing influence of the rheological properties of mixed polymers and the composition of the mixture on the microstructure of extrudates [27,68,137].

Calculations of the amount of deformation using the model with an increase in the concentration of the polymer of the dispersed phase from 4 to 16% by volume showed an increase in the value of q. This is consistent with Starita's theory [137], according to which the degree of deformation increases with an increase in the volume concentration of the dispersed phase. However, this conclusion is not always confirmed in practice for polymer mixtures, especially in the case of the formation of microfibrillar morphology [27], since Starita's theory does not take into account coalescence processes, which are intensified when the content of the dispersed phase in the mixture increases.

Вплив The influence of the elasticity of the fiber-forming polymer melt on its deformation in the developed model was taken into account through the modulus of elasticity G. The determination of the value of q shows that the proposed model correctly describes the influence of the specified factor on the degree of deformation of the droplets. Increasing elasticity worsens their deformation, that is, they are more resistant to stretching and shearing.

In the classical works of Tomotica and Taylor [138,183], using the example of low-molecular emulsions, it was established that the deformation of spherical drops of one liquid in the flow of another is determined by the ratio of their viscosities and the value of surface tension ($\gamma_{\alpha\beta}$). The first theory regarding high molecular weight substances was Van Owen's theory, which linked the interfacial tension and rheological properties of polymers with the processes of structure formation in their binary mixtures [184,185].

According to this theory, the phase with higher elasticity always forms droplets in the phase with lower elasticity. A component with less elasticity will form layers (stratify). Thus, if the phase β forms layers in the phase α, it will be α in the phase β in the form of drops, and the structures of the extrudates of the composition $10\alpha/90\beta$ and $10\beta/90\alpha$ should be opposite (complementary).

Термодинамічно Thermodynamically, surface tension is defined as the work of forming a unit area of a new surface by stretching the previous one. By reducing $\gamma_{\alpha\beta}$, it is possible to reduce the work of forming new surfaces, that is, to facilitate the dispersion and deformation of the component of the dispersed phase. Deformation of the drop is counteracted by its resilience (elasticity). Under the condition of equilibrium of the forces of internal elasticity and surface tension, the rheological constant $\lambda 1$ (2.7) will have the following form [37]:

$$\lambda_1 = \frac{-2ab^2\beta_0^{"} \dfrac{\gamma_{\alpha\beta}}{R_0} \dfrac{a}{a_0} q^{\frac{2}{3}}}{\mu(2 + 3ab^2\beta_0^{"}\dfrac{\eta}{\mu})}(1 - M\varPhi) \qquad (2.12)$$

where: R_0 – the initial radius of the droplet

Calculations regarding the influence of the surface tension on the ability of a drop of a dispersed phase to deform are given in table. 2.3 and Fig. 2.4. As can be seen from the table. 2.3, the degree of deformation of a polymer droplet of the dispersed phase depends on the amount of surface tension: a decrease in $\gamma_{\alpha\beta}$ is accompanied by an increase in the q value.

170

Table 2.3. Dependence of the deformation of the dispersed
phase drop on the surface tension

$h \cdot 10^{-3}$,m	q^*, provided:				
	$\gamma_{\alpha\beta} =0,1$	$\gamma_{\alpha\beta} =0,5$	$\gamma_{\alpha\beta} =1,0$	$\gamma_{\alpha\beta} =2,0$	$\gamma_{\alpha\beta} =3,0$
2	2,4	2,1	2,0	1,9	1,8
4	70,8	44,8	32,0	21,1	11,3
8	228,4	67,5	40,4	29,0	17,7

* provided $\theta = 0,4$ radian; $\eta / \mu = 1$

The created model realistically describes the indicated process:
q values increase as the drop approaches the entrance to the
die, and their maximum values are reached at minimum surface
tension (Fig. 2.4). The results calculated using the model are in
good agreement with the experimental data on the study of
structure formation in polymer mixtures in which the surface
tension was adjusted by introducing compatibilizers.
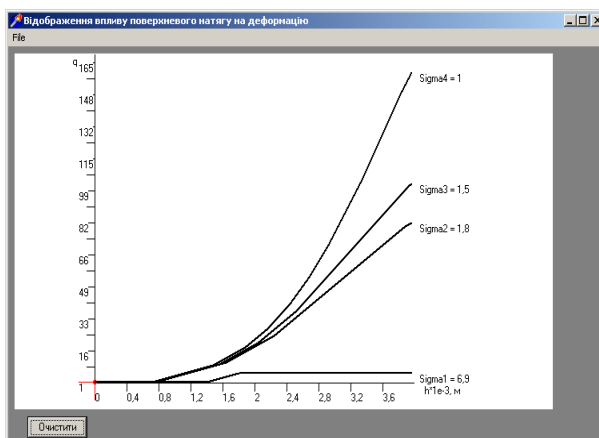
Fig. 2.4. Software image of the dependence of the degree of deformation of
a droplet of the dispersed phase on the depth of immersion and the value of
the interfacial tension, provided η/μ=1.0

Reduction of interfacial tension in modified mixtures of polyethylene terephthalate (PET)/PP [29], PP/SPA [30-31,33] and PP/polyvinyl alcohol (PVA) [32] contributes to the formation of polyester and polypropylene microfibrils with smaller diameters.

Thus, for the first time, using the structural-continuum method, a mathematical model was created and software was developed to calculate the deformation of a polymer droplet of a dispersed phase during the flow of a polymer mixture melt from a wide reservoir into a narrow one. The model makes it possible to determine the amount of deformation of a polymer droplet of the dispersed phase in the flow depending on its viscosity and elasticity, volume concentration, the amount of interfacial tension and the ratio of component viscosities. The resulting system of differential equations satisfactorily describes the real processes of deformation of dispersed phase droplets during the flow of melts of polymer mixtures in the entrance zone of the forming hole. An increase in the elasticity of a drop reduces its ability to deform, and a decrease in the interfacial tension increases this indicator, which makes it possible to obtain fibrils with nanosized diameters.

2.2.2. Software for checking the adequacy of the mathematical model of the deformation of polymer droplets of the dispersed phase. In situ formation of microfibrils of one polymer in the matrix of another has been implemented for many pairs of polymers by methods of blowing, extrusion, electro- and 3D forming (Section 1.3). Published monographs

and articles contain a significant number of experimental results regarding the influence of various factors on the formation of microfibrillar morphology during the flow of thermodynamically incompatible polymer mixtures. Theoretical studies on mathematical modeling of the behavior of polymer dispersions and quantitative characteristics of structure formation processes lag behind significantly. The development of models allows describing already existing regularities, as well as predicting the behavior of polymer mixtures when mixing ingredients that have not yet been studied. At the same time, the practical use of the mathematical model is possible only after checking its adequacy.

The adequacy of the created model was checked by comparing the values of drop deformation calculated using it with experimental results. A three-component system consisting of two polymers (dispersed phase – polypropylene and dispersion medium – co-polyamide) and a modifying additive – compatibilizer (polyethylsiloxane liquid of the PES-5 brand) was used for research. The content of the components of the mixture (in fractions of the unit) was marked: x_1 - PP; x_2 – SPA; x_3 – PES-5, at this $x_1 + x_3 + x_3 = 1$. The influence of the compatibilizer on the dimensional characteristics of the structural elements was monitored by the following parameters: y_1 – average diameter of PP microfibrils (μm); y_2, y_3 – the mass fraction of continuous and short microfibrils (wt. %), respectively.

The mathematical model of the problem in the form of dependencies of the output parameters on the input factors has the following form [186]:

$$y_1 = -4.116 \cdot x_1 - 17.514 \cdot x_2 + 282329.625 \cdot x_3 + 68.274 \cdot x_1 \cdot x_2 -$$
$$- 256070.625 \cdot x_1 \cdot x_3 - 259088.141 \cdot x_2 \cdot x_3 - 105018.922 \cdot x_1 \cdot x_2 \cdot x_3$$
$$y_2 = -304.896 \cdot x_1 - 24.166 \cdot x_2 - 1728495.000 \cdot x_3 + 915.084 \cdot x_1 \cdot x_2 +$$
$$+ 1774424.375 \cdot x_1 \cdot x_3 + 1722008.500 \cdot x_2 \cdot x_3 - 39065.992 \cdot x_1 \cdot x_2 \cdot x_3$$

$$(2.13)$$

$$y_3 = 159.977 \cdot x_1 + 75.998 \cdot x_2 + 223290.094 \cdot x_3 - 445.488 \cdot x_1 \cdot x_2 -$$
$$- 275577.375 \cdot x_1 \cdot x_3 - 249046.531 \cdot x_2 \cdot x_3 + 152957.391 \cdot x_1 \cdot x_2 \cdot x_3$$

The coefficients of this model were obtained by the method of least squares at the values of the independent variables, which are presented in Table 2.4.

Table 2.4. Simplex-lattice design of the experiment
to build a model

Point number	x_1	x_2	x_3
1	0.5000	0.4995	0.0005
2	0.5000	0.4950	0.0050
3	0.2000	0.7992	0.0008
4	0.5000	0.4975	0.0025
5	0.3500	0.6493	0.0007
6	0.3500	0.6475	0.0025
7	0.4000	0.5980	0.0020

From the existing methods of checking the adequacy of regression models, the one based on the possibility of repeating the experiment with the same values of the independent variables was chosen. An incomplete cubic polynomial was

chosen to build the model (2.13), since such functions describe the behavior of three-component mixed systems quite qualitatively [187,188]. In accordance with the methodology of planning the experiment with mixtures, a simplex-lattice plan was used. The latter ensures a uniform distribution of experimental points on the area, which is a simplex of the appropriate dimension (for a three-component mixture this is a regular triangle on the plane). Since certain restrictions are imposed on the content of the components of the mixture by the conditions of the problem (in our case, it is $0.2 \le x_1 \le 0.55$; $0.4 \le x_2 \le 0.8$; $0.0005 \le x_3 \le 0.005$; $x_1 + x_3 + x_3 = 1$), a subregion corresponding to these restrictions was selected programmatically on the complete simplex, and then an area "similar" to the original simplex was chosen within the selected subregion, i.e., a triangle (although not necessarily correct). The model (2.13) was built on a triangle given by the matrix A - the matrix of the coordinates of its vertices:

$$A = \begin{pmatrix} 0.5 & 0.5 & 0.2 \\ 0.4995 & 0.4950 & 0.7995 \\ 0.0005 & 0.005 & 0.0008 \end{pmatrix}$$

According to the simplex-lattice method, seven points of the experimental plan were obtained for the constructed transformed simplex (Table 2.4).

The specified plan is obtained using a linear transformation determined by the matrix A and applied to the column vectors of the "pseudo-coordinates" of the points of the standard plan for the incomplete cubic model in the complete simplex [187,188].

175

In order to ensure the possibility to use the methods of regression analysis of the model in the future, in particular, to check its adequacy, one more point was added to the plan (Table 2.5).

Table 2.5. An additional point to the experimental plan

Номер точки	x_1	x_2	x_3
8	0.5500	0.4475	0.0025

By definition, the task of mathematical modeling was to establish the relationship between one group of variables (independent variables, factors) and another group (dependent variables, response functions). At the same time, the parameters of the selected model were evaluated, its adequacy was checked and, in the case of a positive solution to the last question, a conclusion was drawn about the possibility of using the built model to study the influence of various factors on the degree of deformation of the polymer droplets of the dispersed phase in the matrix.

Taking into account the provisions regarding general linear regression models, it was assumed that the dependent variable y with accuracy to the random additive error $\square$ can be represented as a linear combination of factor variables (independent variables, regressors) $x_0, x_1,\ldots, x_{p-1}$:

$$y = \beta_0\, x_0 + \ldots + \beta_{p-1}\, x_{p-1} + \varepsilon, \qquad (2.14)$$

where: $\beta_0,\ldots, \beta_{p-1}$ – coefficients of the mathematical model

As a result of the assumption, a sample of volume n was made, which is a collection of experimentally obtained n sets of

176

numbers of the form: $(x_{i0},\ldots,x_{i,p-1}, y_i)$, $i = 1,2,\ldots,n$, where x_{ij} is the value of the j-th regressor (j-th independent variable) at the *i-th* observation, y_i is the corresponding value of the dependent variable y. The magnitude of the error ε at the ith observation was denoted by ε_i.

To check the adequacy of a linear data model, a fairly common method is to compare estimates of error variances obtained, on the one hand, using this model, and on the other hand, independently. This is equivalent to testing some linear hypothesis by computing and analyzing the corresponding Fisher F-ratio.

At the first stage, the ith observation point (vector-line) of the independent variable was marked with the letter x_i for the experimental data, i.e. $x_i = (x_{i0}, \ldots, x_{i,p-1})$, $i = 1, 2,\ldots, n$. It is known that this method requires the presence of several observations of y in at least one of the points x_i. It was assumed that this requirement is fulfilled, i.e., among the points x_i there are those that are repeated. In this case, $x_1, x_1,\ldots, x_m$ are different observation points, and the number of observations in at least one of them is greater than 1. The specified F-statistic looks like this:

$$F = \frac{S_1^2}{S_2^2}$$

(2.15)
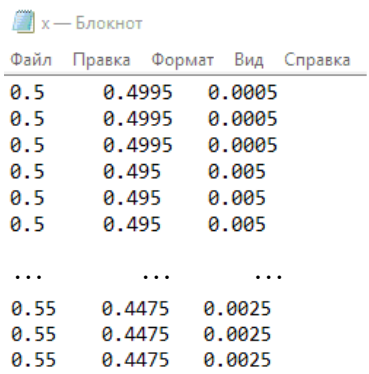
where
$$S_1^2 = \frac{1}{m-p}\sum_{i=1}^{m} n_i \left(\hat{y}_i - \bar{y}_i\right)^2,$$

$$S_2^2 = \frac{1}{n-m}\sum_{i=1}^{m}\sum_{j=1}^{n_i}(y_{ij} - \bar{y}_i)^2$$

$y_{i1}, \ldots y_{in_i}, \ i = 1, \ldots, m$ – value of the output variable observed at the point $\boldsymbol{x} = \boldsymbol{x}^i$; n_i – the number of experiments at the i-th point

Provided that m $m > p$, the aspect ratio $\dfrac{S_1^2}{S_2^2}$ (a variant from the set of F- ratios) has a Fisher distribution $F(m-p, \ n-m)$ [40,188]. According to the general provisions, the hypothesis about the adequacy of the model $\hat{y}$ is not accepted for the level of significance α, if the indicated ratio exceeds the quantile of the level $(1 - \alpha)$ of the Fisher distribution. Otherwise, the hypothesis is accepted. This check is implemented by the developed software.

According to the above, 8 different points were determined for the created model, each of which is repeated three times (that is, 24 observations in total). The input file, which contains the values of x_i, is shown in Fig. 2.5.

Fig. 2.5. File *x.txt* - coordinates of observation

To check the adequacy of the model (2.13), it was transformed into a generalized linear form by replacing the variables:

$$z_1 = x_1; \; z_2 = x_2; \; z_3 = x_3; \; z_{12} = x_1 x_2; \; z_{13} = x_1 x_3; \; z_{23} = x_2 x_3; \; z_{123} = x_1 x_2 x_3$$

The model (2.13) will have the following form:

$$\hat{y} = \beta_1 z_1 + \beta_2 z_2 + \beta_3 z_3 + \beta_{12} z_{12} + \beta_{13} z_{13} + \beta_{23} z_{23} + \beta_{123} z_{123} \quad (2.16)$$

After inputting the x_i data, the plan matrix for the developed model was programmatically formed:

$$X = \begin{array}{c|ccccccc} & x_1 & x_2 & x_3 & x_1 x_2 & x_1 x_3 & x_2 x_3 & x_1 x_2 x_3 \\ 1.1 & 0.500 & 0.4995 & 0.0005 & 0.24975 & 0.00025 & 0.00024975 & 0.000124875 \\ 1.2 & 0.500 & 0.4995 & 0.0005 & 0.24975 & 0.00025 & 0.00024975 & 0.000124875 \\ 1.3 & 0.500 & 0.4995 & 0.0005 & 0.24975 & 0.00025 & 0.00024975 & 0.000124875 \\ 2.1 & 0.500 & 0.4950 & 0.0050 & 0.24750 & 0.00250 & 0.00247500 & 0.001237500 \\ 2.2 & 0.500 & 0.4950 & 0.0050 & 0.24750 & 0.00250 & 0.00247500 & 0.001237500 \\ 2.3 & 0.500 & 0.4950 & 0.0050 & 0.24750 & 0.00250 & 0.00247500 & 0.001237500 \\ ... & ... & ... & ... & ... & ... & ... & ... \\ 8.1 & 0.5500 & 0.4475 & 0.0025 & 0.246125 & 0.001375 & 0.00111875 & 0.0006153125 \\ 8.2 & 0.5500 & 0.4475 & 0.0025 & 0.246125 & 0.001375 & 0.00111875 & 0.0006153125 \\ 8.3 & 0.5500 & 0.4475 & 0.0025 & 0.246125 & 0.001375 & 0.00111875 & 0.0006153125 \end{array}$$

In fig. 2.6 presents this matrix, which for the convenience of the user is displayed in the form window using software created in the C++ language using modern programming methods [189,190]:

Fig. 2.6. The matrix of the plan formed by software

For example, the following observational data were obtained for the variable y_1 (Fig. 2.7).

Fig. 2.7. File *y.txt* – experimental data of observations y_1

Average values calculated by the software for each observation point and the corresponding estimates of the regression function for the variable y_1 of the model (2.16) are shown in Fig. 2.8.

Fig. 2.8. Values of regression function estimates and mean values of y
obtained in the created software

Subsequently, Fisher's F-ratio was found for all output variables of the model (2.16) using the created software application. The values given in fig. 2.9.

a)   b)   c)

Fig. 2.9. F-ratios obtained in the software application
for y_1 (a), y_2 (b) та y_3 (c)

At the final stage, after performing all the listed operations, decisions were made regarding the hypothesis regarding the adequacy of the developed mathematical model.

As a result, we obtained: for α = 0.01 $F(m - p, \quad n - m)$ = F(8$\square$-7, 24$\square$-8) = = F(1, 16)=8.531, that is, for all y from the model (2.16), the calculated ratio $\dfrac{S_1^2}{S_2^2}$ is

less than the value $F(m-p, \ n-m)$. Therefore, the hypothesis about the adequacy of the model is confirmed.

Thus, with the help of specially created software (listing - see the appendix), the adequacy of the mathematical model of the deformation of the polymer droplets of the dispersed phase in the matrix during the flow of the polymer dispersion from the wide channel of the forming hole to the narrow channel was checked by checking the corresponding linear hypotheses. The model turned out to be adequate, which gives grounds for its use in further research, in particular, for forecasting the behavior of the system, as well as for optimizing its parameters. In addition, the created software can be applied to a wider range of multi-component systems.

2.2.3. Mathematical modeling of the deformation of a droplet of a dispersed phase component in melts of nanofilled polymer mixtures. It is known that a promising direction of modification of polymers and their mixtures is the creation of nanocomposites, in which a complex of desired properties is achieved due to the optimal combination of components (see sections 1.2 and 1.3). The use of fillers of different sizes, shapes and chemical nature allows to improve the mechanical properties of materials and give them new functional characteristics (non-flammability, bactericidal, electrical conductivity, sorption capacity, etc.). Thus, the introduction of silicon dioxide nanoparticles and composite additives based on it into the melt of the polypropylene/copolyamide mixture made it possible to regulate the PP structure formation processes in the SPA matrix and, thus, to improve the structure

of the filter material. Filters based on such materials combine high cleaning efficiency and productivity, and the presence of a nanofiller in the structure of the filter layer gives them bactericidal properties [28,36].

In order to create new nanomaterials and regulate their properties, it is necessary to conduct fundamental research and establish the relevant laws. However, due to the complexity and multifactorial nature of experiments, empirical approaches prevail over theoretical ones. Using the method of mathematical modeling when studying the influence of nano-additives on the processes of structure formation in melts of incompatible polymer mixtures allows to speed up this process and generalize the experimental results.

During the flow of polymer dispersions, the component of the dispersed phase forms various types of structures: liquid cylinders (jets), layers, drops, etc. To describe the rheological behavior of melts of polymer dispersions, the same laws of classical mechanics are used as for modeling low-molecular systems (suspensions and emulsions) [173]. At the same time, polymer mixtures are a special class of colloidal dispersions of the "polymer in polymer" type. Its important difference is the formation of an interphase transition layer between the two components, the properties of which differ sharply from the similar characteristics of the polymer melt in the volume. In nanofilled systems, an interfacial layer is also formed around the nanoparticle at the filler/polymer interface, the thickness of which varies between $(0.0004 \div 0.16)$ µm [94]. At the same time, depending on the degree of affinity between the polymer and the additive, nanoparticles can be localized in the volume

of the melt or at the boundary of the phase separation and affect the surface tension and rheological properties of the components.

The mathematical model of the deformation of the droplets of the dispersed phase component (system of differential equations 2.10) developed from the standpoint of the structural-continuum approach allows determining the influence of volume concentration, rheological properties of the ingredients, and changes in surface tension on the formation of the morphology of the polymer composite. The advantage of this model is that it takes into account all the basic provisions of continuum mechanics (the integrity of the medium, the inseparability of the functions characterizing its movement and state) and the peculiarities of the structure of the dispersed phase. The shape of the droplet was modeled as an ellipsoid of rotation, which changes its size in the process of interaction with the dispersion medium, but retains its volume. The deformation of the drop depending on the orientation in the flow was taken into account using the tensor of the strain rate of uniaxial tension.

The modifying effect of nano-additives in the melts of polymer mixtures is manifested, first of all, through their influence on the compatibility of components (reduction in the value of interfacial tension) and on the change in the ratio of visco-elastic characteristics of the starting polymers (see section 1.3). It is known that solid fillers cause a thickening thixotropic effect, which leads to an increase in the viscosity of polymer melts [62,68]. An increase in viscosity also occurs when specific bonds are formed between functional groups of

184

polymers and nanoparticles. The elasticity of melts, as a rule, decreases due to the limitation of the mobility of macromolecule chains in the presence of solid nanoparticles. When modifying melts of polymer mixtures, the additive is usually pre-introduced into one of the components. The influence of nanoparticles on the change in viscosity of melts of the dispersed phase or dispersion medium can be calculated using Einstein's formula for dilute suspensions (equation 2.1). To compare the data calculated using the model (system of equations 2.11) and experimental studies, the influence of additives of silica brand A-300 and methylsilica, which were introduced in the amount of (0.1÷5.0) by mass, was studied. %, on the viscosity of the polypropylene melt. It was established that with an increase in the content of nanofiller, the viscosity increases by 1.3 and 1.5 times, respectively. Within the margin of error, it coincides with the effective viscosity determined by formula (2.1). At the same time, the viscosity ratio increases, remaining less than unity (0.37÷0.49) [156]. Calculations made with the help of the model showed that such a change in rheological parameters does not significantly affect the amount of deformation of the dispersed phase droplets. However, experimental studies show that the introduction of (0.1÷5.0) wt. % of silicon dioxide in the melt of the PP/SPA and PP/PVA mixture improves the process of formation of PP fibrils in the matrix: their average diameter is almost halved and the homogeneity of the distribution increases [80,81]. This is due to the effect of nanoparticles on interfacial phenomena, namely, a decrease in the value of surface tension at the boundary of phase separation.

It follows from the fundamental classical relations that describe the thermodynamic equilibrium in low-molecular dispersed systems that the dispersive medium during the flow acts on the droplet dispersed in it with a force that is proportional to the gradient of the shear rate, the viscosity of the medium and is a function of the ratio of the viscosities of the components. A drop of dispersed phase polymer resists deformation with force [183]:

$$T_\gamma = 2\,\gamma_{\alpha\beta}/r \qquad\qquad (2.17)$$

where: $\gamma_{\alpha\beta}$ – interphase tension; r – drop radius

At the same time, the drop's ability to deform is largely determined by its elasticity. In the mathematical model (2.11), the counteraction of the deformation drop is taken into account through the value of the modulus of elasticity G, which is included in the equation for determining the rheological constant λ_I. To assess the influence of the interfacial tension on the ability to deform droplets of the dispersed phase, changes were made to the expression for determining the rheological constant λ_I, based on the fact that $G = T_\gamma$. Under the condition of equilibrium of the forces of internal elasticity (G) and resistance to deformation (T_γ), the equation for determining λ_I will have the form (2.12) [39].

Модифіковану The modified model was checked for adequacy, that is, the ability to predict the results of research in some area with the required accuracy, by comparing the values of drop deformation calculated with its help, with experimental data. For this purpose, the results of studies on the influence of compatibilizer additives (PES-5 organosilicon liquid and ethylene copolymer with vinyl acetate CEVA) on the

186

interfacial tension and the structure of polypropylene/copolyamide mixture extrudates were used. Calculations carried out with the help of the model show that the modified mathematical model describes the real process of deformation of a polymer droplet of the dispersed phase in the inlet zone, namely: q is a function of the interfacial tension and the volume concentration of polypropylene (Table 2.6).

Table 2.6. Dependence of the deformation of the dispersed phase droplet on the value of the interfacial tension in the original and compatibilized PP/SPA mixtures

Name and composition of the mixture, vol. %	$\gamma_{\alpha\beta}$, mN/m	$\bar{d}$, μm	q
PP/SPA 22,3/77,7	2,60	3,8	103
PP/SPA 33,0/67,0	2,60	5,7	230
PP/SPA 50,4/49,6	microfibrils are not formed		
PP/SPA /PES-5 22,3/77,6/0,1	1,90	1,8	160
PP/SPA /SEVA 50,4/47,5/2,5	1,85	4,0	517
PP/SPA /SEVA /PES-5 50,4/46,8/2,5/0,3	1,30	2,8	929
PP/SPA /SEVA /PES-5 50,4/47,6/1,7,0,3	0,53	1,8	3240

Table 2.7 compares the experimental data that reflect the nature of the structure formation processes in the extrudates of nano-filled methylsilica PP/SPA and PP/PVA mixtures when the interfacial tension changes, and the q values calculated using the polypropylene droplet value model. The data in the table show that the values of interfacial tension,

determined using the theory of liquid cylinder collapse, for nanofilled compositions are significantly lower, compared to the original mixture.

Table 2.7. Dependence of the deformation of the dispersed phase droplet on the value of the interfacial tension in nanofilled mixtures

The name of the mixture	$\gamma_{\alpha\beta}$, mN/m	$\overline{d}$, μm	q
PP/SPA	2,60	4,0	98
PP/SPA / methylsilica	0,75	2,6	343
PP/PVA	0,73	3,5	349
PP/PVA/methylsilica	0,47	1,7	542

This leads to a decrease in energy expenditure for the formation of new surfaces of the dispersed phase, that is, it contributes to the dispersion and deformation of PP droplets in the matrix polymer: the amount of deformation in nanofilled systems increases sharply, which contributes to a decrease in the average diameter of PP microfibrils by (1.5÷2.1) times. The results obtained using the model are in good agreement with the experimental data regarding the effect of the nanoadditive on the structure formation processes, namely: the introduction of the filler contributes to a decrease in the average diameter of polypropylene microfibrils due to a decrease in the surface tension at the phase separation boundary.

2.2.4. Mathematical modeling and computer visualization of the process of deformation of a polymer droplet of a dispersed phase in a matrix. Mixing polymers is not only a simple, affordable and effective method of their

modification, but also ensures the achievement of unique effects. An example of this is the phenomenon of *in situ* formation of micro- and nano-sized fibrils in the dispersion medium by the component of the dispersed phase [1,3,12,24-36]. This made it possible to develop a new method of obtaining self-reinforced polymer composites and thin fibrous materials with new functional properties. Today, the possibility of practical application of such products as soon as possible contributes to the conduct of experimental research and their superiority over theoretical research. However, only a scientifically based approach to the selection of components of the mixture, its composition, establishing the relationship between the macrorheological properties of the starting polymers and the morphology of the system will allow obtaining materials with predetermined indicators. When conducting experiments, researchers are always forced to consider many different options, relying on their own experience and intuition. At the same time, traditional methods are often long-term and require significant financial costs. Acceleration and improvement of research related to multifactorial experiments and finding optimal solutions is facilitated by the use of methods of mathematical and computer modeling of complex phenomena and processes taking place in polymer systems.

The study of dispersed polymer mixtures by the method of mathematical modeling showed that to describe the macro- and microrheological behavior of their melts, the approaches of classical mechanics and structural models, which are used in modeling systems such as suspensions, emulsions,

and colloidal solutions, can be used. The most suitable for the development of mathematical dispersion models is the structural-continuum approach, which combines phenomenological and structural methods and makes it possible to take into account all the basic provisions of continuum mechanics and the peculiarities of the behavior of the dispersed phase [172,173,175]. The mathematical model of the deformation of the droplets of the dispersed phase component during the melt flow of the polymer mixture, developed from the standpoint of the structural-continuum approach, is a system of differential equations (2.10, 2.11) and allows determining the orientation of the droplets in the flow, the amount of deformation depending on the rheological properties of the components of the mixture, the bulk the concentration of the dispersed phase and the value of the interfacial tension [37-39]. In order to further study the influence of various factors on the processes of structure formation during the flow of polymer dispersion and to visually demonstrate this phenomenon to students during training, software was developed for computer visualization of the formation of fibrils of one polymer in the matrix of another [191].

Theoretical studies in the mechanics of polymer systems show that during the flow of melts in the dispersion medium, stresses arise that are transmitted to the droplets of the dispersed phase and ensure their deformation and orientation in the flow. With small velocity gradients, the drop takes the shape of an ellipsoid of rotation, and with large ones, it turns into a liquid cylinder. For the processing of polymers and their

mixtures, extrusion equipment is used, in which there is always a zone where the melt flows from a wide tank to a narrow one. With such a flow geometry, longitudinal and shear deformation are superimposed on each other, the flow lines converge, forming a cone. At the same time, the local velocity vectors have two components: in the direction of the flow – the stretching velocity and in the transverse direction – the shear velocity. Only tensile stresses act on the flow axis, which originate far from the entrance to the hole, increase in magnitude, and reach a maximum at the entrance to the forming nozzle [182]. Under the action of these stresses, the microstructure of their extrudates is formed during the flow of melts of the mixtures.

In the model created by us, a cylindrical coordinate system was used to analyze the velocity field in the entrance zone, since the streamlines at the entrance to the channel have a radial velocity component. The shape of the drop was assumed to be an ellipsoid, and its deformation was taken into account using the tensor of the strain rate of uniaxial tension. The mathematical model (2.11) was solved numerically by the Runge-Kutta method with the help of a specially written program (listing - see the appendix) [190,192]. As a result, we obtained parameter values that are a function of the duration of the melt flow of the polymer mixture in the entrance zone of the forming channel.

The computer model makes it possible to simulate the melt flow of a mixture of polymers and the deformation of a droplet of a component of the dispersed phase, changing the main factors affecting the process, in particular - the viscosity

of the incoming polymers and the amount of surface tension at the boundary of the phase separation, as well as the hydrodynamic parameter - the deflection angle the symmetry axis of the drop from the flow axis.

The main task of the computer modeling and visualization stage was the modification and expansion of the existing software. The created software can be conventionally divided into two parts: computational (mathematical) and graphic (visualization part). With the help of previously developed software [40], the system of differential equations (2.11) was solved in the form of time-dependent functions (these functions were tabulated by software). At the stage of visualization, based on the obtained results, a drop model of the component of the dispersed phase was built. According to the created model, the drop is an ellipsoid, and its projection on the plane is an ellipse. A special algorithm was developed for constructing an ellipse, since standard graphical procedures of programming languages do not allow constructing an "oblique" ellipse. In order to display the process of deformation of the drop in time, the transfer of data from the calculation part of the software to the graphic part, which took place at discrete moments of time, was implemented. The animation effect was achieved by redrawing the output window at these moments. The main form of the program with a graphic demonstration panel is presented in fig. 2.10, on which the drop is shown at the initial moment of time (that is, it is not yet deformed). At the same time, the angle between the flow direction and the axis of rotation of the ellipsoid (θ) was 0.4 radians.
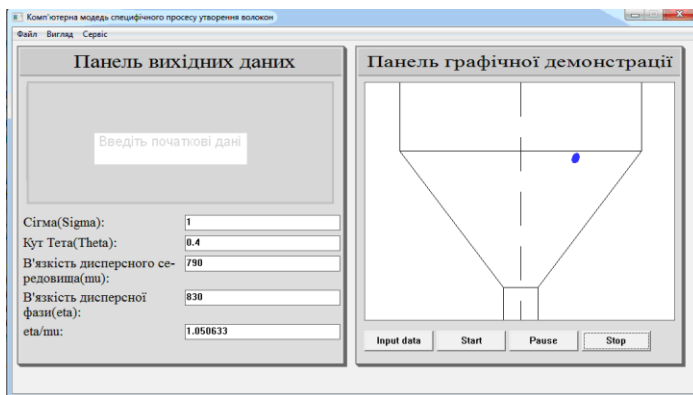
Fig. 2.10. Computer model of polymer droplet deformation
of the dispersed phase in the matrix

It is known that the ability of a drop to deform and transition into a jet (microfibril) is affected by many factors, the main ones of which are the ratio of viscosities and elasticities of the melts of the mixed components and the degree of their interaction in the interfacial layer. From the point of view of hydrodynamics, the process of dispersing polymer droplets in polymer-polymer systems occurs most effectively when the values of viscosities and elasticities of the dispersed phase and the dispersion medium are close [182,198,199], i.e., the amount of droplet deformation (q) is a function of the viscosity ratio (K) polymers of the dispersed phase (η) and matrix (μ). The results of studies performed on many polymer mixtures (see section 1.3, 1.4.) show that the deviation of the value of K from unity leads to a deterioration of the conditions for the formation of a microfibrillar structure: the average diameter of microfibrils increases, other types of structures (particles, films) are formed. Modeling of the effect of the ratio of viscosities of the components on the value of q

was carried out under other identical conditions: the content of the fiber-forming polymer was 30.0 vol. %, $\theta = 0.4$, the value of the interfacial tension $\gamma_{\alpha\beta} = 0.5$. Shown in fig. 2.11, the image of the process of stretching a drop in a flow clearly demonstrates the indicated dependence - with an increase in the ratio of viscosities of the components, the ability to deform the droplets of the dispersed phase decreases.
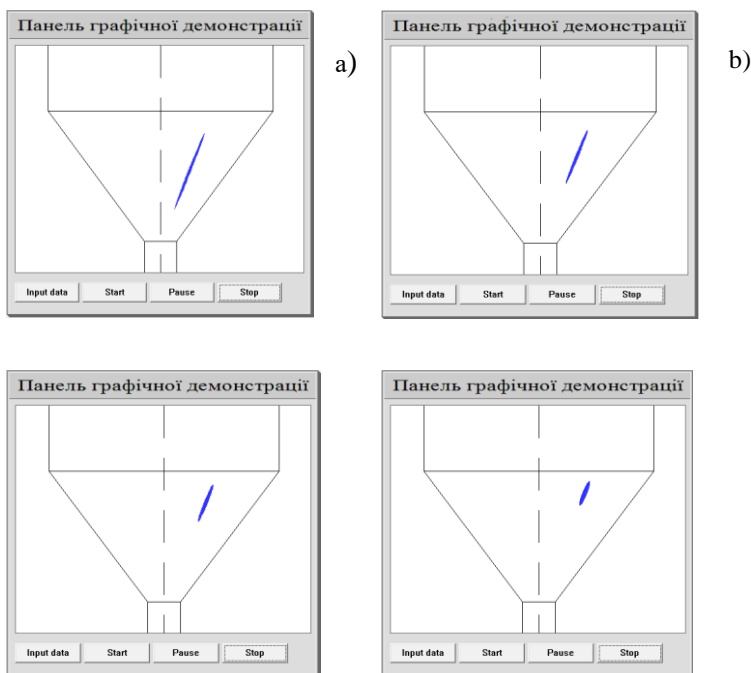

Fig. 2.11. A computer model of the effect of the ratio of viscosities of the polymer of dispersed phase and matrix on the deformation of the drop: K = 1.0 (a); K = 2.5 (c); K = 6.7 (c); K = 10.0 (d)

It is known that the dispersion medium during the flow acts on a drop dispersed in it with a force that can deform it, if there is sufficient interaction between the two polymers of the mixture

in the transition layer. It follows from the fundamental relations regarding equilibrium in dispersed systems that the most effective factor that allows regulating the parameters of the phase structure is the value of the interphase tension. From the point of view of thermodynamics, surface tension is the work of forming a unit area of a new surface by stretching the old one. The specific work of dispersion is proportional to the value of the interfacial tension, that is, its reduction increases the degree of deformation, which makes it possible to obtain microfibrils with smaller diameters. This is clearly confirmed by the animation presented in fig. 2.12.
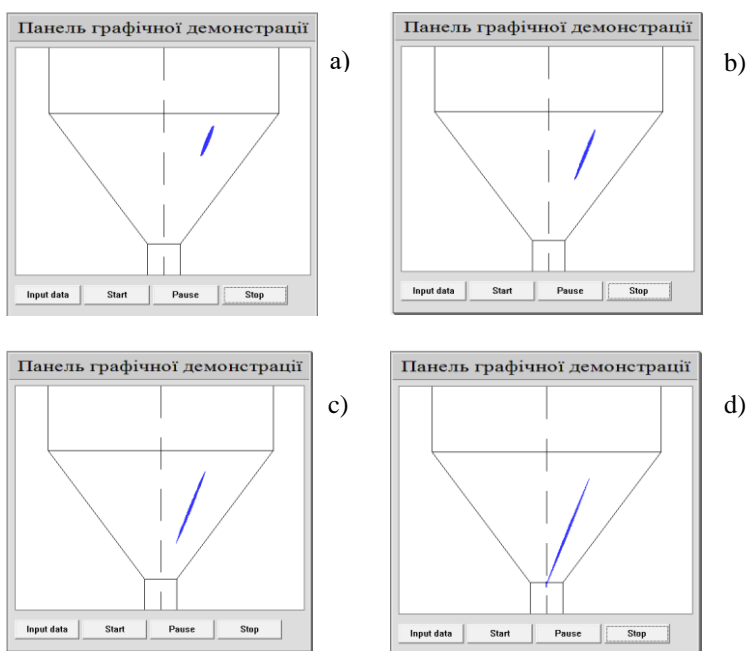

Fig. 2.12. Computer model of the dependence of drop deformation on surface tension: $\gamma_{\alpha\beta} = 3,0$ (a); $\gamma_{\alpha\beta} = 2,0$ (b); $\gamma_{\alpha\beta} = 1,0$ (c); $\gamma_{\alpha\beta} = 0,1$ (d)

Researches carried out by the method of mathematical modeling showed that the formation of fibrils of one polymer in the matrix of another is most effectively implemented under the condition that the ratio of the viscosities of the components is equal to 1.0, the value of the interfacial tension is minimal, and the drop is located closest to the central axis of the flow. The simultaneous use of the optimal values of all the listed parameters causes the maximum deformation of the drop.

Thus, the created computer animation model adequately reflects the real processes of deformation of drops of one polymer in the mass of another polymer during the flow of melts of mixtures in the entrance zone of the forming hole. Modification and expansion of the existing software made it possible to clearly demonstrate the process of transforming an ellipsoid into a cylinder, that is, the formation of a microfibrillar morphology. The created software is a contribution to theoretical and practical research on droplet deformation in polymer-polymer systems. It makes it possible to visualize the process with the simultaneous change of several parameters without conducting long-term experiments, as well as to predict the behavior of the system if a third substance is added to it (a compatibilizer, a nanofiller), which is one of the methods of imparting new unique properties to polymer composites by adjusting the structure.

2.2.5. Software for calculating the parameters of the kinetics of the disintegration of liquid jets of one polymer in the matrix of another and the value of interfacial tension. As shown in sections 1.2-1.4, the properties of polymer composites are determined by the phase structure of the component of the dispersed phase in the matrix, which depends on the degree of their thermodynamic compatibility (absolutely compatible homogeneous systems, partially compatible and completely incompatible). In incompatible systems, a microfibrillar morphology often occurs, in which one component forms in the mass of another many liquid jets (microfibrils) with diameters from tens of fractions to several micrometers. Considerable interest in such structures is due to the fact that the self-reinforcement effect is achieved during the formation of composite materials, the degree of which can be adjusted by changing the value of the ratio of the length and diameter of the fibrils of the dispersed phase component [24,27,153,154]. Microfibers with a unique structure and properties and new thin-fiber materials based on them (cotton-like synthetic fibers and threads, precision filter materials, sorbents, etc.) are obtained by processing melts of polymer mixtures [27,28,34-36]. The formation of microfibrils (microfibers) is a special type of structure formation, during which there is deformation and merging of droplets of the dispersed phase in the jet, which must maintain their stability in the channel of the forming hole and upon exiting it. The final morphology is the result of a balance between the processes of deformation and decay, on the one hand, and coalescence, on the other. Deformation, capillary instability

and coalescence are effective factors in creating the desired structure of the polymer dispersion. Establishing the patterns of jet disintegration of one polymer in the matrix of another is important for controlling the processes of polymer mixing and fiber formation. Thus, the life time of the liquid jet determines the possibility of realizing the formation of microfibers of one polymer in the matrix of another, and the temperature of their disintegration determines the operating conditions.

Based on the above, one of the important microrheological processes affecting the morphology of the polymer mixture is the disintegration of deformed droplets or liquid cylinders. Breakdown will occur when the spherical droplet is elongated enough to form an ellipsoid or filamentous liquid cylinder. The variables that control the degree of deformation will also determine the critical conditions of disintegration. Such parameters are the ratio of the viscosities of the polymer of the dispersed phase and the matrix and the Weber number. A liquid polymer jet is thermodynamically unstable due to an unfavorable surface-to-volume ratio. By its nature, the destruction of a liquid cylinder is a transient phenomenon. Before disintegration, thickening and thinning are formed on the surface of the cylinder, which leads to an increase in its surface energy, and destruction is the result of the system's desire to decrease it (Fig. 2.13). To study the regularities of the disintegration of liquid jets of one polymer in the matrix of another, a technique was developed [139,140], based on the measurement of the growth rate of capillary waves, in accordance with the classical Tomotika theory.
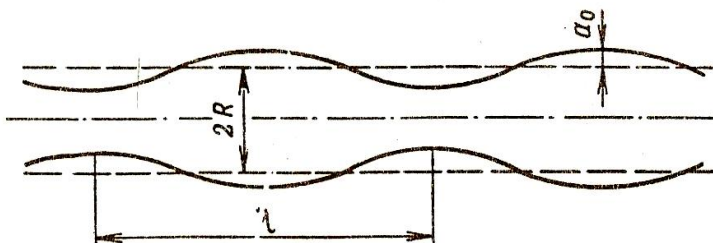
Fig. 2.13. Schematic representation of a liquid cylinder in action
of destructive wave

For the experiments, we used the original mixture of polypropylene/copolyamide with a composition of 30/70 by weight. % and a nanofilled composition containing 3.0 wt. % titanium oxide/silica nanoadditives. In order to evaluate the kinetics of jet decay and determine the value of the surface tension of polymer mixtures ($\gamma_{\alpha\beta}$), extrudates were previously formed from them, longitudinal sections with a thickness of (10÷20) μm were made, they were placed on a glass slide in an immersion medium and heated on the stage of an MP-6 microscope according to constant rate of temperature rise (0.6 degrees/s). After certain time intervals, different stages of jet disintegration (microfibrils) were photographed. At the appropriate temperature, the jet began to collapse in places of reduced cross-section under the action of interphase tension forces and disintegrated into a chain of droplets (see Fig. 1.15). The initial jet diameter (d_0), thickness diameters (d_e), and droplet diameters (d_k), formed under the influence of temperature, and the distance between their centers (λ_m) were measured from microphotographs. For each pair of polymers, up to 100 photographs were analyzed, and since up to

10 microfibrils fell into one frame, the total number of r_k and λ_m values exceeded 1000. The time of decay was taken as the time during which the majority of them in the cross-section was destroyed. The lowest temperature at which microfibrils disintegrated was recorded. This temperature determines the scope of their operation. Calculations were performed according to the well-known algorithm [193] using specially developed software [190,192].

The input data for the program were the results of processing microphotographs taken at appropriate time intervals (t), on which the diameters of "varicose" thickenings ($d_в$) were measured and entered into the text files "*Волокна.txt*". An example of an input file is shown in Fig. 2.14.
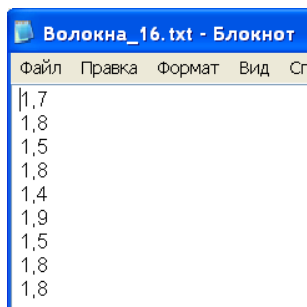

Fig. 2.14. Data input file for "varicose" cylinders

After the disintegration of the jets, the diameters of the drops (d_k) and the distance between their centers, which corresponds to the wavelength of the destructive excitation (λ_m), were determined. The data were entered into the text files "*Частки.txt*" and "*Лямбда.txt*", their appearance is similar to the file for fibers. The number of suitable input files depends

on the number of photomicrographs, as well as on the presence of corresponding types of structures. In addition, the time points at which each frame was photographed were entered from a separate file ("Time.txt" file). Using the program, the average diameter of the initial microfibrils (d_0) and the average value of $d_в$ for each t were calculated.

The cause of the destruction of the liquid jet is the occurrence of wave-like disturbances on its surface, the amplitude (a) of which increases exponentially with time [138]. Jets break up under the condition that the magnitude of the perturbation amplitude becomes equal to their radius. In logarithmic coordinates, the dependence of a on t is expressed by a straight line.

$$\ln a = \ln a_0 + qt \qquad (2.30)$$

The tangent of the angle of inclination of this straight line to the abscissa axis is the coefficient of instability q.
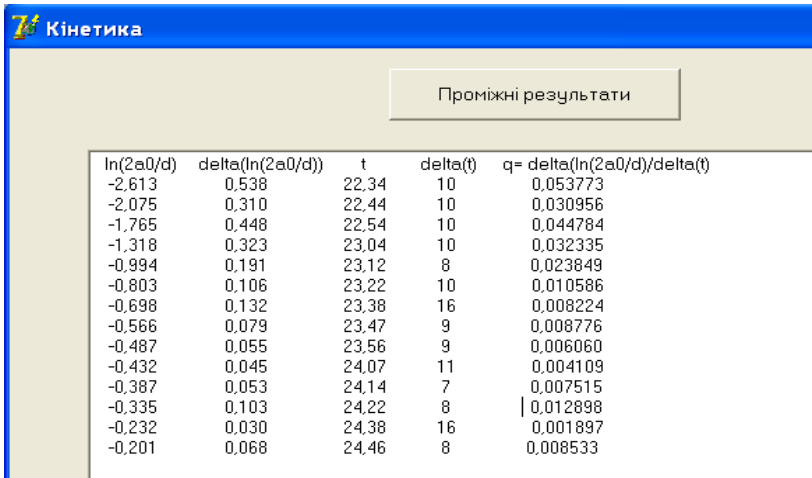
At the same time, the value q is a complex function of the wave number and the ratio of the viscosities of the mixture components:

$$q = \frac{\gamma_{\alpha\beta}}{2\eta R} \cdot F(\chi, K) \qquad (2.31)$$

To determine the value of the instability coefficient, first calculated $\ln\left(\dfrac{d_в - d_0}{d_0}\right)$ and then determined q by the formula:

$$q = \frac{\Delta \ln\left(\dfrac{2(d_в - d_0)}{d_0}\right)}{\Delta t} \qquad (2.32)$$

201

The calculated values were tabulated. The intermediate results of the program are shown in Fig. 2.15.

ln(2a0/d)	delta(ln(2a0/d))	t	delta(t)	q= delta(ln(2a0/d)/delta(t)
-2,613	0,538	22,34	10	0,053773
-2,075	0,310	22,44	10	0,030956
-1,765	0,448	22,54	10	0,044784
-1,318	0,323	23,04	10	0,032335
-0,994	0,191	23,12	8	0,023849
-0,803	0,106	23,22	10	0,010586
-0,698	0,132	23,38	16	0,008224
-0,566	0,079	23,47	9	0,008776
-0,487	0,055	23,56	9	0,006060
-0,432	0,045	24,07	11	0,004109
-0,387	0,053	24,14	7	0,007515
-0,335	0,103	24,22	8	0,012898
-0,232	0,030	24,38	16	0,001897
-0,201	0,068	24,46	8	0,008533

Fig. 2.15. Intermediate results of the program

To estimate the value of the surface tension at the separation boundary of the components of the mixture, the dependence was used [138]:

$$\gamma_{\alpha\beta} = \frac{q \cdot \mu \cdot d_0}{\Omega(\chi, K)} \qquad (2.33)$$

where μ – matrix polymer melt viscosity;

χ – the wave number of the destructive disturbance;

Ω – a tabulated function determined from the curve of the dependence of χ on K.

The wave number of the destructive disturbance was calculated according to the formula:

$$\chi = \frac{2\pi R}{\lambda_m} \qquad (2.34)$$

where R – jet radius before breakup.

The value of R was found from the equation:

$$r_k = \left(3R\lambda_m / 4\right)^{\frac{1}{3}} \qquad (2.35)$$

In logarithmic form it has the form:

$$\lg R = \frac{3}{2}\lg r_k - \frac{1}{2}\lg \lambda_m + 0.0625 \qquad (2.36)$$

In order to determine R, the average values of the diameter (d_k), the radius of the drops (r_k), the wave magnitude of the destructive disturbance (λ_m), as well as the ratio of the viscosities of the dispersed phase component (PP) and the matrix (SPA) were calculated $K = \dfrac{\eta}{\mu}$.

Based on the found parameters of the wave number and the ratio of component viscosities, the value of the tabulated function Ω was found from the dependence graph $\chi = f(K)$. The program prompts the user to enter its value (Fig. 2.16).

eta/mu	0,291139240506329
xi	0,969881310638298

Ввести Омега (з графіка)

Omega=	0,044

Ввести дані

Fig. 2.16. Entering the value of the tabulated function Ω

After that, final calculations of the surface tension at the phase separation boundary were performed with the help of the program (Fig. 2.17).
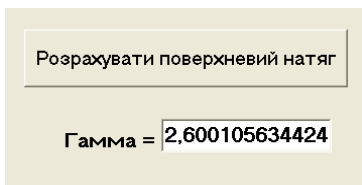
Fig. 2.17. Calculation of surface tension

To assess the stability of liquid jets of one polymer in the matrix of another, the reduced values of the droplet radius (r_k/R) and life time ($t_{ж}/R$) were also determined.

For example, in the table 2.8 and 2.9 show data on the influence of titanium oxide/silica nanoadditive on the patterns of disintegration of polypropylene microfibrils in the co-polyamide matrix and on the value of the interfacial tension, calculated using the developed program.

Table 2.8. The effect of nanoadditive on the parameters of PP microfibril disintegration in the SPA matrix

The name of additive	R, μm	$r_{к}$, μm	λ_m, μm	$r_к/R$	$2\pi R/\lambda_m$	$t_{ж}$, с	$t_{ж}/R$, s/ μm
without additive	2,1	3,1	13,8	1,8	0,69	56	37
titanium oxide/silica	1,5	2,7	9,2	1,6	1,42	130	62

Table 2.9. The results of determining the values of the interfacial tension and the coefficient of instability according to the kinetics of the disintegration of PP microfibrils in the SPA matrix

The name of additive	Ω	q	$\gamma_{\alpha\beta}$, mN/m
without additive	0,18	0,0618	2,60
titanium oxide/silica	0,04	0,0247	1,52

Thus, software was developed in the Delphi environment in the Object Pascal language, which allows processing the experimental results of the kinetics of disintegration of liquid jets of the dispersed phase polymer in the matrix component. Calculations in the program were carried out using the dependences obtained from measuring the growth rate of capillary waves in liquid jets according to the classical theory of Tomotika. The created software makes it possible to determine the main parameters of the process for binary and multicomponent mixtures of polymers, namely: the value of interfacial tension, life time and the coefficient of instability of liquid jets, and also allows to significantly simplify the process of processing experimental results, shorten its term and increase efficiency.

ПЕРЕЛІК ДЖЕРЕЛ ПОСИЛАННЯ

1. Thomas S., Shanks R., Chandrasekharakurup S. Design and Applications of Nanostructured Polymer Blends and Nanocomposite Systems. – New York: William Andrew. – 2015. – 442 p.

2. Fu S., Sun Z., Huang P., Li Yu., Hu N. Some basic aspects of polymer nanocomposites: a critical review // Nano Materials Science. – 2019. – № 1. – p. 2-32.

3. Utracki L., Wilkie C. A. Polymer blends handbook. – Heidelberg: Springer Heidelberg Dordrecht, 2014. – 2378 p.

4. Muralisrinivasan N.S. Polymer Blends and Composites. Chemistry and technology. - New York: John Wiley & Sons. – 2017. – 352 p.

5. Isayev A.I. Encyclopedia of Polymer Blends. New York,: John Wiley & Sons. – 2016. – V. 4. – 450 p.

6. Mittal V. Functional Polymer Blends. Synthesis, properties, and Performance. – Boca Raton: CRC Press. – 2016. - 354 p.

7. Utracki L.A. Commercial Polymer Blends.- Heidelberg: Springer Science & Business Media. – 1998.–675 p.

8. Bianko S. Carbon nanotubes – from Research to Applications. – Rijeka, Croatia: InTech. – 2011. – 358 p.

9. Mechanical Properties of polemer Based on Nanostructure and Morphology / edited by Michler G.H., Balta-Calleja F.J. – Boca Raton: Taylor & Francis Group, 2005. – 450 p.

10. Shen J.F., Huang W.S., Wu L.P., Hu Y.Z., Ye M.X. The reinforcement role of different amino-functionalized multi-walled carbon nanotubes in epoxy nanocomposites // Composited Sci. and Technol. – 2007. – V.67, № 16. – p. 3041-3050

11. Zukas T., Jankauskauite V., Baltusnikas A. The Influence of Nanofillers on the Mechanical Properties of Carbon Fibre Reinforced Methyl Methacrylate Composite // Mater. Sci. – 2012. – V. 18, № 3. – p. 1320-1392.

12. Rezanova N.M., Meĺnik I.A., Tsebrenko M.V., Korshun A.V. Preparation of Nano-Filled Polypropylene Microfibers // Fibre Chem. – 2014. – V.46. – P. 21-27.

13. Andricic B., Kovacic T., Klaric I. Properties of Recycled Material Containing Poly(vinyl Chloride), Polypropylene, and Calcium Carbonate Nanofiller // Polym. Eng. Sci. – 2008. – V.48, № 3. – P. 572-577.

14. Shi G., He L. J., Chen C. Z., Liu J. F., Liu Q. Z., Chen H. Y. A Novel Nanocomposite Based on Recycled Poly(Ethylene Terephthalate)/ABS Blends and Nano-SiO$_2$ // Adv. Mater. Res. – 2010. – V. 150. – P. 857-860.

15. Fang C., Nie L., Liu S., Yu R., An N., Li S. Characterization of Polypropylene-Polyethylene Blends Made of Waste Materials with Compatibilizer and Nano-Filler // Compos. Part B Eng. – 2013. – V. 55 – P. 498-505.

16. Chen R. S., Ahmad S., Gan S., Ab Ghani M. H., Salleh M. N. Effects of Compatibilizer, Compounding Method, Extrusion Parameters, and Nanofiller Loading in Clay-Reinforced Recycled HDPE/PET Nanocomposites. // J. Appl. Polym. Sci. – 2015. – V. 132, №29. – P. 319-325.

17. Yang H., Li B., Zhang Q., Du R., Fu Q. Simultaneous Enhancement of Electrical Conductivity and Impact Strength via Formation of Carbon Black-Filler Network in PP/EPDM Blends. // Polym. Adv. Technol. – 2011. – V. 22, № 6. – P. 857-862.

18. Dai K., Xu X.D., Li Z.M. Electricflly condactive cardon dlak (CB) filled in situ microfibrillar poly(ethylene tereftalate) (PET)/poly(ethylene) (PE) composite with a seolective CB distribution // Polymer – 2007. – V. 48. –   P. 849-859.

19. Harrats C., Thomas S., Groeninckx G. Micro- and nanostructured multiphase polymer blend systems phase morphology

and interfaces: monograph. Boca Raton, London New York: Taylor & Francis Group Inc., 2006. 473 p.

20. Sfiligoj Smole M., Stana Kleinschek K.   Nanofilled polypropylene fibres: in book Nanofibers and nanotechnology in textiles / by edit. P.J. Brown, K.S. Stevens. monograph, North America: Wootheat Publishing, 2007. 530 p.

21. Fakoori E., Karami, H. Preparation and Characterization of ZnO-PP Nanocomposite Fibers and Non-Woven Fabrics // J. Text. Inst. 2018. – V. 109,   № 9. – P. 1152–1158.

22. Biomedical Applications of Polymeric Nanofibers // by editors R. Jayakumar, Shantikumar V.Nair. – New York: Springer. – 2012. – 283 p.

23. Ravikumar S., Gokulakrishnan R., Boomi P. In vitro antibacterial activity of the metal oxide nanoparticle against urinary tract infectious bacterial pathogens // Asian Pacific J. of Tropical Disease . – 2012. – №4. – P. 85-89.

24. Thomas S., Mishra R., Kalarikka N. Micro and nano fibrillar composites (mfcs and nfcs) from polymer blends. – Woodhead Publishing. – 2017. – 372 p.

25. Doan V.A., Yamaguchi M. Interphase transfer of nanofillers and functional liquid between immiscible polymer pairs // Recent Res. Devel. Mat. Sci. – 2013. – №.10. – P. 59-88.

26. Tran N. H. A., Brünig H., Boldt R., Heinrich G. Morphology Development from Rod-like to Nanofibrillar Structures of Dispersed Poly (Lactic Acid) Phase in a Binary Blend with Poly (Vinyl Alcohol) Matrix along the Spinline // Polymer. – 2014. – V. 55, № 24. – P. 6354-6363.

27. Резанова Н.М., Будаш Ю.О., Плаван В.П. Інноваційні технології хімічних волокон. – Київ: КНУТД. – 2017. – 240 с.

28. Tsebrenko M. V., Rezanova V. G., Tsebrenko I. O. Features of obtaining of polypropylene microfibers with nanosize fillers // J. of Mater. Sci. and Eng. – 2010. – V. 4, № 6. – P. 36-44.

29. Li W., Karger-Koksis J., Schlarb A.K. Dispersion of TiO_2 Particles in $PET/PP/TiO_2$ and $PET/PP/PP$-g-MA/TiO_2 Composites Prepared with Different Blending Procedure // Macromol. Mater. Eng. – 2009. – № 294. – P. 582-589.

30. V.G.Rezanova, V.I. Shchotkina Mathematical modeling of dispersed phase drop deformation in nano-filled polymer mixture melts // K.: Вісник КНУТД. – 2015. – № 3 (86). – C. 209-214

31. Rezanova V., Tsebrenko M. Influence of binary additives of compatibilizers on the micro- and macrorheological properties of melts of polypropylene-copolyamide mixtures //J. of Eng. Phys. and Thermophys. – 2009. – V. 81, № 4, P.766-773.

32. Резанова Н.М., Плаван В.П., Дзюбенко Л.С., Сап'яненко О.О., Горбик П.П., Коршун А.В. Структуроутворення у компатибілізованих нанонаповнених розтопах поліпропілен/пластифікований полівініловий спирт // Наносистеми, наноматеріали, нанотехнології. – 2018. – Т. 16, № 1, – С. 55 – 70.

33. Резанова Н.М., Савченко Б.М., Плаван В.П., Булах В.Ю., Сова Н.В. Закономірності одержання нанонаповнених полімерних матеріалів з матрично-фібрилярною структурою // Наносистеми, наноматеріали, нанотехнології. – 2017.– Т.15, №3. – С.559-571.

34. Rezanova N.M., Plavan V.P., Rezanova V.G., Bohatyryov V.M. Regularities of producing of nano-filled polypropylene microfibers // Vlakna a Textil. – 2016. – №2. – P.3-8.

35. Rezanova N.M., Rezanova V.G., Plavan V.P., Viltsaniuk O.O. The influence of nano-additives on the formation of matrix-

fibrillar structure in the polymer mixture melts and on the properties of complex threads // Vlakna a Textil. – 2017. – №2 – P. 37-42.

36. Rezanova N.M, Rezanova V.G., Plavan V.P., Viltsaniuk O. O. Polypropylene fine-fiber filter materials modified with nano-additives // Functional Mat. − 2019**.** − V.26, №2. − P. 389-396.

37. Rezanova V.G., Prydatchenko Yu.V., Tsebrenko M.V. Mathematical model of strain of a dispersed-phase in flow of molten polymer blends // J. of Eng. Phis. and Thermophis. − 2006**.** − V.78, №5. − P. 975-982.

38. Rezanova V.G.,   Shchotkina V.I.,   Tsebrenko M.V. Planning the experiment and optimization of the content of nanoadition in polypropylene monothreads // К.: Вісник КНУТД. – 2014. –   № 2. – С. 42-47

39. Резанова   В.Г.,   Цебренко   М.В.   Математичне моделювання   процесу   деформування   дисперсної   фази   в розплавах сумішей полімерів // Вісник КНУТД. – 2008. –   № 2. – С.30 - 33.

40. Щербань В.Ю.,   Краснитський С.М., Резанова В.Г. Математичні моделі в САПР. Обрані розділи та приклади застосування. – К.: КНУТД, 2011. – 219с.

41. Резанова В.Г., Резанова Н.М., Коршун А.В. Дослідження морфології сумішей полімерів з використанням розробленого програмного забезпечення // Вісник КНУТД. – 2017. – №2. – С.120–127.

42. Резанова В.Г., Цебренко М.В., Цебренко І.О., Мельник І.А. Оптимізація процесу волокноутворення в нанонаповнених сумішах поліпропілен/співполіамід // Вісник КНУТД. – 2009. – №2. – С.79 - 83.

43.   Anthony L.A. Science and thechnology of polymer nanomer nanofibers. – Hoboken, New Jersey. USA.: John Wiley & Sons, Inc., 2008. – 424 p.

44. Hassan T., Salam A., Khan A. Functional nanocomposites and their potential applications: a review. *J. of Polym. Research*. 2021. Vol. 28, № 2.

45. Нові функціональні речовини і матеріали хімічного виробництва: зб. матеріалів цільової програми наукових досліджень НАН України / НАН України. Київ: Академперіодика, 2021. 332 с.

46. Резанова В.Г. Резанова Н.М. Програмне забезпечення для дослідження полімерних систем : монографія. Київ: АртЕк, 2020. 358 с.

47. Guo Z., Li T. Fundamentals and Application of Nanomaterials. – Boston/London: Artechhouse, 2009. – 249 p.

48. Rezanova N., Plavan V., Viltsaniuk O. Precision filtering materials from nanofilled polypropylene microfibers. *Membrane and sorption processes and technologies*: Book of abstracts III Ukrainian-Polish scientific conference, Kyiv, 12-14 December. 2017. P. 72-74.

49. Kratshmer W. Solid C_{60}: a new form of carbon // Nature. – 1990. – V. 347. – P. 354–388.

50. Marulanda J.V. Carbon Nanotubes. – Vucovar.: In-teh, India. – 2010. – 630 p.

51. Nurazzi N.M., Asyraf M.R.M., Khalina A., Abdullah N., Sabaruddin F.A., Kamarudin S.H., Ahmad S., Mahat A.M., Lee Ch.L., Aisyah H.A., Norrrahim M.N.F., Ilyas R. A., Harussani M. M., Ishak M. R., Sapuan S. M. Fabrication, Functionalization, and Application of Carbon Nanotube-Reinforced Polymer Composite: An Overview. *Polymer*. 2021. №13. P.1047- 1091.

52. Liu S., Keong A, Xu R., Wei J., Tan Ch.M., Yang Y., Chen Y. Antibacterial action of dispersed single-walled carbon nanotubes on Escherichia coli and Bacillus subtilis investigated by

atomic force microscopy // The Royal Soc. of Chem. – 2010. – № 2. – P. 2744-2750.

53. Obraztsova E.A., Lukashev E.P., Zarubina A.P., Parkhomenko I.M., Yaminsky I.V. Bactericidal Action of Single-Walled Carbon Nanotubes // Moscow Univer. Phys. Bulletin. – 2009. – V. 64, № 3. – P.320-323.

54. Jin K., Eyer S., Dean W., Kitto D., Bates F.S., Ellison C.J. Bimodal nano- and micro-fiber nonwovens by melt blowing immiscible ternary polymer blends. *Industrial and Eng. Chem. Res.* 2020. Vol. 59, № 12, № P. 5238–5246.

55. Nichols W.T., Keto J.W., Henneke D.E., Brock J.R., Malyavanatham G., Becker M.F., Glicksman H.D. Large-scale production of nanocrystals by laser ablation of microparticles in a flowing aerosol // Appl. Phys. Lett. – 2001. – V.78. – P. 1128-1134.

56. Pezer D.P. Silver nanoparticles. – Vukovar, Croatia: Intex. – 2010. – 421 p.

57. Huang M., Schlarb A.K. Polypropylene/poly(ethylene terephthalate) microfibrillar reinforced composites manufactured by fused filament fabricatio. *J. Appl. Polym. Sci.* 2021. Vol. 138, № 23. P. e50557..

58. Чекман I.С., Дорошенко А.М. Клініко-фармакологічні властивості наночастинок заліза // Український медичний часопис (електронний ресурс). – 2010. – №3. – Режим доступу: https://www.umj.com.ua/article/2911/kliniko-farmakologichni-vlastivosti-nanochastinok-zaliza

59. Naik R.R., Stringer S.J., Agarwal G., Jones S.E., Stone M.O. Biomimetic synthesis and patterning of silver nanoparticles // Nature Mater. – 2002. – V.1. – P. 169-172.

60. Morones J.R., Elechigurra J.L., Camacho A., Holt K., Kouri J.B., Ramirez J.T., Yacaman M.J. The bactericidal effect of

silver nanoparticles // Nanotetechnilogy. – 2005. – V.16. – P. 2346-2353.

61. Pal S., Tak Y.K., Song J.M. Does the Antibacterial Activity of Silver Nanoparticles Depend on the Shape of the Nanoparticle. A Study of the Gram-Negative Bacterium Escherichia coli // Appl. Environ. Micribiol. – 2007. – V.73. – P. 1712 -1720.

62. Manson J.A., Sperling L.H. Polymer blends and composites. – New York: Plenum Press. – 1976, 440 p.

63. Egger S., Lehman R.P., Height M.J., Loessner M.J., Schuppler M. Antimicrobial Properties of a Navel Silver-Silica Nanocomposite Material // Appl. and Environment. Microbiol. – 2009. – V. 75, № 9. – P. 2973-2976.

64. Chang Q., He H., Ma Z. Efficient disinfection of Escherichia coli in water by silver loaded alumina // J. of Inorganic Biochem. – 2008. – № 102. – P. 1736-1742.

65. Chen M., Yan L., He H., Chang Q., Yu Y., Qu J. Catalytic sterilization of Escherichia coli K 12 on Ag/Al_2O_3 surface // J. of Inorganic Biochem. – 2007. – № 101. – P. 817-823.

66. Kanjwal M.A., Barakat N.M., Shceikh F.A., Balk W., Khil M.S., Kim H.Y. Efect of silver Content and Morphology on the catalic Activity of Silver-grafted Titanium Oxide Nanostructure // Fibers and Polym. – 2010. – V. 11, № 5. – P. 700-709.

67. Rezanova, N.M., Budash, Yu.O., Plavan, V.P., Bessarabov, V.I. Formation of microfibrillar structure of polypropylene/copolyamide blends in the presence of nanoparticles of metal oxides. *Voprosy khimii i khimicheskoi tekhnologii*. 2021. № 1. P.71-78.

68. Polymer Blends / Ed. by Paul D.R., Bucknall C.B. – New York: John Wiley & Sons, Inc. – 2000, V.1. – 618 p.

69. Shi D., Ke Z., Gao Y., Wu J., Rheology and morphology of reactively compatidilized PP/PA6 blends // Macromol. – 2002. – № 35. – P. 8005-8012.

70. Papadopulou C.P., Kalfoglou N.K., Comparison of compatibilizer effektiveness for PET/PP blends; their mechanical, thermal and morphology characterization // Polymer. – 2000. – №41. – P. 2543-2555.

71. Gersappe D., Irvine D., Balazs A.C., Liu Y., Sokolov J., Rafailovich M., Schwarz S., Peiffer D.G. The Use of Graft Copolymers to Bind Immiscible Blends // Science. – 1994. – V. 265. – P.1072-1074.

72. Xiu H., Bai H. W., Huang C. M., Jiang F., Chem F., Deng H., Wang K., Zang Q., Fu Q. Improving impact toughness of polylactide/poly(ether)urethane blends via designing the phase morphology assistend by hydrophilic silica nanoparticles // Polym. – 2014. –V.6, № 55. – P. 1593-1600.

73. Luna M.S., Filippone G. Effects of Nanoparticles on the Morphology of Immiscible Polymer Blends – Challenges and Opportunities. // Eur. Polym. J. – 2016. – №79. – P. 198-218.

74. Nuzzo A., Bilotti E., Peijs T., Acierno D., Filippone G. Nanoparticle-Induced Co-Continuity in Immiscible Polymer Blends. A Comparative Study on Bio-Based PLA-PA11 Blends Filled with Organoclay, Sepiolite, and Carbon Nanotubes // Polym. – 2014. – № 55, №19. – P. 4908-4919.

75. Taguet A., Cassagnau P., Lopez-Cuesta J.-M. Structuration, Selective Dispersion and Compatibilizing Effect of (Nano)fillers in Polymer Blends // Prog. Polym. Sci. – 2014. – V.8, № 39. – P. 1526-1563.

76. Huang S., Bai L., Trifkovic M., Cheng X., Macosko C. W. Controlling the Morphology of Immiscible Cocontinuous Polymer Blends via Silica Nanoparticles Jammed at the Interface //

Macromol. – 2016. – V. 10, №49. – P. 3911-3918.

77. Bai L., He S., Fruehwirth J. W., Stein A., Macosko C. W., Cheng X. Localizing Graphene at the Interface of Cocontinuous Polymer Blends: Morphology, Rheology, and Conductivity of Cocontinuous Conductive Polymer Composites // J. Rheol. (N. Y. N. Y). – 2017. – V. 4, № 61. – P. 575-587.

78. Sangroniz L., Palacios J. K., Fernandez M., Eguiazabal J.I., Santamaria A., Muller A.J. Linear on non-linear rheological behavior of polypropylene/polyamide blends modified with a compatibilizer agent and nanosolica and its relationship with the morphology // Europ. Polym. J. – 2016. – №.83. – P. 10-21.

79. Резанова Н.М., Цебренко М.В., Мельник І.А., Коршун А.В., Данилова Г.П. Закономірності течії та структуроутворення в розплавах сумішей поліпропілен/полівініловий спирт/ кремнезем // Полімер. журнал. – 2014. – №. 3. – С.183-189.

80. Резанова Н.М., Цебренко М.В., Мельник І.А., Коршун А.В. Вплив добавок метилкремнезему на мікро- та макрореологічні властивості розплавів сумішей поліпропілен/полівініловий спирт // Вісник КНУТД. – 2014. – №1. – С. 17-25.

81. Резанова Н.М., Цебренко М.В., Мельник І.А., Цебренко І.О., Дзюбенко Л.С., Сап'яненко О.О., Горбик П.П. Вплив хімічної природи матричного компоненту на структуроутворення в розплавах сумішей полімерів // Хімія, фізика та технологія поверхні. – 2015. – Т.6., № 3. – С. 354-363.

82. Reza S., Hyeong Y., Migeun K., Woo J., Kyu H. Morphological Evaluation of PP/PS Blends Filled with Different Types of Clays by Nonlinear Reological Analysis // Macromol. – 2016. – №49. – P.3148-3160.

83. Qi D., Cao Z., Ziener U. Recent Advances in the

Preparation of Hybrid Nanoparticles in Miniemulsions // Adv. Colloid Interface Sci. – 2014. – № 211. – P. 47-62.

84. Luo S., Yu S., Sun R., Wong C. P. Nano Ag-Deposited BaTiO$_3$ Hybrid Particles as Fillers for Polymeric Dielectric Composites: Toward High Dielectric Constant and Suppressed Loss // ACS Appl. Mater. Interfaces. – 2014. – V. 1, № 6. – P. 176-182.

85. Ba Linh N. T., Min Y. K., Lee B.-T. Hybrid Hydroxyapatite Nanoparticles-Loaded PCL/GE Blend Fibers for Bone Tissue Engineering // J. Biomater. Sci. Polym. Ed. – 2013. – V.5, № 24. – P. 520-538.

86. Chen G., Li P., Huang Y., Kong M., Yang Q., Li G. Hybrid Nanoparticles with Different Surface Chemistries Show Higher Efficiency in Compatibilizing Immiscible Polymer Blends // Compos. Sci. Technol. – 2014. – №105. – P. 37-43.

87. Ebrahim J. D., Basil D. F. Localization of micro and nano- silica particles in high interfacial tension poly(lactic acid)/low density polyethylene system // Polym. – 2015. – №77. – P.156-166.

88. Mallick S., Kar P., Khatua B. B. Morphology and Properties of Nylon 6 and High Density Polyethylene Blends in Presence of Nanoclay and PE-g-MA // J. Appl. Polym. Sci. – 2012. – V.3, № 123. – P. 1801-1811.

89. Xiu H., Bai H. W., Huang C. M., Xu C. L., Li X. Y., Fu Q. Selective localization of titanium dioxide nanoparticles at the interface and its effect on the impact toughness of poly(L-lactide)/poly(ether)urethane blends // XPRESS Polymer Letters. – 2013. – V. 7, № 3. – P. 261-271.

90. Chow W.S., Mohd Ishak Z.A. Polyamide blend-based nanocomposites: A review // eXPRESS Polymer Letters. – 2015. – V. 9, № 3. – P. 21-232.

91. Zhang W., Lin M., Winesett A., Dhez O., Kilcoyne A. L., Ade H., Rubinstein M., Shafi K. V. P. M., Ulman A., Gersappe

D., Tenne R., Rafailovich M., Sokolov J., Frisch H. L. The Use of Functionalized Nanoparticles as Non-Specific Compatibilizers for Polymer Blends // Polym. Adv. Technol . – 2011. – V.1, №22. – P. 65-71.

92. Baudouin A.-C., Auhl D., Tao F., Devaux J., Bailly C. Polymer Blend Emulsion Stabilization Using Carbon Nanotubes Interfacial Confinement // Polym. – 2011. – V. 1, №52. – P. 149-156.

93. Hong J. S., Namkung H., Ahn K. H., Lee S. J., Kim C. The Role of Organically Modified Layered Silicate in the Breakup and Coalescence of Droplets in PBT/PE Blends // Polym. – 2006. – V. 11, № 47. – P. 3967-3975.

94. Pukanszky B. Interfaces and interphases in multicomponent materials: past, present, future // Europ. Polym. J. – 2005. – V.41, №4. – P. 645 - 662.

95. Suresh G. Advani. Processing and Properties of Nanocomposites. – Toh Tuck Link Singapure: World Scientific Publishing Co. – 2007. – 548 p.

96. Резанова Н.М., Будаш Ю.О., Плаван В.П., Коршун А.В., Пристинський С. В. Регулювання стійкості рідких мікроструменів поліпропілену в матриці співполіаміду за рахунок нанодобавок. *Технології та інжиніринг.* 2021. №2. С.60-69.

. 97. Chen G.-X., Li Y. J., Shimizu H. Ultrahigh-shear processing for the preparation of polymer/carbon nanotube composites // Carbon. – 2007. – V.45, №12. – P. 2334-2340.

98. Wang G., Qu Z., Liu L., Shi Q., Guo J. Study of SMA graft modified MWNT/PVC composite materials // Mater. Sci. and Eng. – 2008. – V. 472A. – P. 136-139.

99. Левченко В.В., Мамуня Є.П., Буато Ж., Давиденко В.В., Лебедєв Є.В. Електричні властивості та морфологія

нанокомпозитів на основі суміші полімерів та вуглецевих нанотрубок // Тези доповідей XII Української конференції з високомолекулярних сполук. – Київ, 18-21 жовтня 2010. –   С. 138.

100. Hong K.H., Pack J.L., Sul I.H., Your J.H., Kong T.J. Preparation of Antimicrobial Polyvinyl alcohol nanofibers containing silver Nanoparticles // J. of Polym. Sci.: part B. Polym. Physics. – 2006. – V.44. – P. 2468-2474.

101. Beloshenko V., Chishko V., Plavan V., Rezanova N., Savchenko B., Sova N., Vozniak I. Production of Filter Material from Polypropylene/Copolyamide Blend by Material Extrusion-Based Additive Manufacturing: Role of Production Conditions and ZrO_2 Nanoparticles. *3D Printing and Additive Manufacturing*. 2021.Vol.8, №4. P.253-262..

102. Budash Y., Rezanova N., Plavan V., Rezanova V. Thermally and organomodified montmorillonite as effective regulators of the structure formation process in polypropylene/polystyrene blends. *Polym. and Polym. Composites.* 2022. Vol. 30. P. 1–8

103. Azubuike L., Sundararaj U. Interface Strengthening of PS/aPA Polymer Blend Nanocomposites via In Situ Compatibilization: Enhancement of Electrical and Rheological Properties. *Materials*. 2021. Vol. 14, №17. P. 4813.

104. Tskhe Y., Buzgo M., Simaite A. Electorospun nanofibers with photocatalytic particles fo carbon sorption. *Nanotech / Biotech France 2021 and joint virtual conferences*: Book of abstracts International Conference, 23-25 June. 2021 P.77..

105. Резанова В.Г. Композиційна суперпозиція в'язкості по швидкості зсуву у розплавах компатибілізованих сумішей поліпропілен / співполіамід // Вісник КНУТД. – 2011. - №1. – с. 74-77.

106. Krissanasaeranee M., Vongsetskul Th., Rangkupan R., Supaphol P., Wongkasemjit S. Preparation of Ultra-Fine Silica Fibers using Electrospun Poly(Vinyl Alcohol) / Silatrane Composite Fibers as Precursor // J. Am. Ceram. Soc. – 2008. – V. 91, № 9. – P. 2835-2835.

107. Nanofibers and nanotechnology in textiles / ed by P.J. Brown, K.S. Stevens. – North America.: Wootheat Publishing, 2007. – 530 p.

108. Yan X., Cayla A., Devaux E., Salaun F. Microstructure Evolution of Immiscible PP-PVA Blends Tuned by Polymer Ratio and Silica Nanoparticles // Polym. – 2018. – № 10. – P. 1031-1039.

109. Cresnar K.P., Aulova A., Bikiaris D.N., Lambropoulou D., Kuzmic K., Zemljic L.F. [1,*]Incorporation of Metal-Based Nanoadditives into the PLA Matrix: Effect of Surface Properties on Antibacterial Activity and Mechanical Performance of PLA Nanoadditive Films. *Molecules.* 2021. Vol.26, №14. P.4161..

110. Kojima Y., Usuki A., Kawasumi M., Okada A., Kurauchi T., Kamigaito O. Synthesis of nylon 6-clay hybrid by montmorillonite intercalated with e-caprolactan // J. Polym. Sci. – 1993. – Part A., V. 31. – P. 983-986.

111. Utracki L.A. Clay-Containing nanocomposites. – UK.: Rapza Technology limited. – 2004. – V.2. – 325 p.

112. Belyaev P., Rezanova N., Viltsaniuk O. Comparative assessment of biocompatibility of a new surgical suture material made of polypropylene modified with carbon nanotubes and silver nanoparticles. *Scientific heritage*. 2020. Vol.2, №49. P.17-22.

113. Вільцанюк О.А., Бєляєв П.В., Резанова Н.М. Нанокомпозитний хірургічний шовний матеріал / *Запалення: Морфологічні, патофізічні, терапевтичні та хірургічні*

аспекти: Тези доповідей IV Науково-практичної конференції, Вінниця, 4 грудня 2015. С. 12-14.

114. Mehta S., Mirabella F.M., Rufener K., Bafna A. Thermoplastic olefin/clay nanocomposites: Morphology and mechanical properties // J. Appl. Polym. Sci. – 2004. – V. 92. – P. 928-936.

115. Hasegava N., Usuki A. Silicate layer exfoliation polyolefin/clay nanocomposites based on maleic anhydride modified polyolefins and organophiliic clay // J. of Appl. Polym. Sci. – 2004. – V. 93. – P 946-957.

116. Дзюбенко Л.С., Сап'яненко О.О., Горбик П.П., Плаван В.П., Резанова Н.М., Лутковський Р.А., Вільцанюк О.А. Властивості шовного матеріалу з поліпропілену модифікованого частинками нанорозмірного срібла та кремнезему // Наносистеми, наноматеріали, нанотехнології. – 2018. – Т. 16, № 2, – С. 347-362.

117. Вільцанюк О.А., Бєляєв П.В., Резанова Н.М., Плаван В.П. Властивості нанокомпозитного шовного матеріалу. Пластична, реконструктивна і естетична хірургія / *Клініко-технологічні виклики в етапній та реконструктивній хірургії.*: Матеріали XVII міжнародної конференції, Київ, 30 листопада – 2 грудня 2017. С. 10-11.

118. Wang R., Chi N., Zheng S., Clutter E., Rathnayake C. Electro-Spun Silk-CNT Fibers to Stimulate Fibroblasts for Connective Tissue Repair. *Nanotech / Biotech France 2021 and joint virtual conferences*: Book of abstracts InternationalConference, 23-25 June. 2021 P.74

119. Zhang B., Wong J. S.-P., Shi D., Yam R. C.-M., Li R. K.-Y. Investigation on the Mechanical Performances of Ternary Nylon 6/SEBS Elastomer/nano-SiO_2 Hybrid Composites with Controlled Morphology // J. Appl. Polym. Sci. – 2010. – V. 1, № 115. – P.

469–479.

120. A. Dattat, H. H. Chen, D. G. Baird The effect of compatibilization on blends of polypropylene with a liquid-crystalline polymer. Polymer, 1993, Vol.34, N. 4. – p. 759-766

121. Guo J., Briggs N., Crossley S., Grady B.P. Morphology of Polystyrene/poly(methyl Methacrylate) Blends: Effects of Carbon Nanotubes Aspect Ratio and Surface Modification // AIChE J. – 2015. – V. 61, № 10. – P. 3500–3510.

122. Abbasi Moud A., Javadi A., Nazockdast H., Fathi A., Altstaedt V. Effect of Dispersion and Selective Localization of Carbon Nanotubes on Rheology and Electrical Conductivity of Polyamide 6 (PA6), Polypropylene (PP), and PA6/PP Nanocomposites // J. Polym. Sci. Part B Polym. Phys. – 2015. – V. 53, №5, P. 368–378.

123. Chen J., Shi Y., Yang J., Zhang N., Huang T., Chen C., Wang Y., Zhou Z. A Simple Strategy to Achieve Very Low Percolation Threshold via the Selective Distribution of Carbon Nanotubes at the Interface of Polymer Blends // J. Mater. Chem. – 2012. – V. 22, № 42. – P. 2398-2404.

124. Trifkovic M., Hedegaard A. T., Sheikhzadeh M., Huang S., Macosko C. W. Stabilization of PE/PEO Cocontinuous Blends by Interfacial Nanoclays // Macromolecules. – 2015. – V. 48, № 13. – P. 4631-4644.

125. Kerboua N., Cinausero N., Sadoun T., Lopez-Cuesta J. M. Effect of Organoclay in an Immiscible Poly(ethylene Terephtalate) Waste/poly(methyl Methacrylate) Blend // J. Appl. Polym. Sci. – 2010. – V.1, № 117. P. 129-137.

126. Magalhaes N. F., Dahmouche K., Lopes G. K., Andrade C. T. Using an Organically-Modified Montmorillonite to Compatibilize a Biodegradable Blend // Appl. Clay Sci. – 2013. – № 72. – P. 1-8.

127. Ferreira W. H., Carmo M. M., Silva A. L., Andrade C. T.

Effect of Structure and Viscosity of the Components on Some Properties of Starch-Rich Hybrid Blends // Carbohydr. Polym. – 2015. – № 117. – P. 988-995.

128. Nuzzo A., Coiai S., Carroccio S. C., Dintcheva N. T., Gambarotti C. Filippone G. Heat-Resistant Fully Bio-Based Nanocomposite Blends Based on Poly(lactic Acid) // Macromol. Mater. Eng. – 2014 – V. 299, № 1. – P. 31-40.

129. Vrsaljko D., Macut D., Kovačević V. Potential Role of Nanofillers as Compatibilizers in Immiscible PLA/LDPE Blends // J. Appl. Polym. Sci. – 2015. – V. 132, № 6. – P. 119-127.

130. Yu F., Huang H.-X. Simultaneously Toughening and Reinforcing Poly(lactic Acid)/thermoplastic Polyurethane Blend via Enhancing Interfacial Adhesion by Hydrophobic Silica Nanoparticles // Polym. Test. – 2015. – № 45. – P. 107-113.

131. Baklavaridis A., Zuburtikudis I., Panayiotou C. Porous Composite Structures Derived from Multiphase Polymer Blends // Polym. Eng. Sci. – 2015. – V.55, №8. – P. 1856-1863.

132. Mural P. K., Banerjee A., Rana M. S., Shukla A., Padmanabhan B., Bhadra S., Madras G., Bose S. Polyolefin Based Antibacterial Membranes Derived from PE/PEO Blends Compatibilized with Amine Terminated Graphene Oxide and Maleated PE // J. Mater. Chem. – 2014. – V. 2, № 41. P. 17635-17648.

133. Kumar, S.; Mural, P.; Sharma, M.; Shukla, A.; Bhadra, S.; Padmanabhan, B.; Madras, G.; Bose, S.; Parak, W. J.; Mahmoudi, M. Porous membranes designed from bi-phasic polymeric blends containing silver decorated reduced graphene oxide synthesized via a facile one-pot approach // RSC Adv. – 2015. – V.5, № 41. – P. 3441–3451.

134. Tsebrenko M.V., Yudin A.V., Ablasova T.I., Vinogradov G.V. Mechanism of fibrillation in the flow of molten polymer mixtures // Polymer. – 1976. – V. 17. – P. 831-834.

135. Krause S. Polymer – polymer miscibility // Pure and Applied Chem. – 1986. – V.58, №12. – P.1553-1560.

136. Резанова Н.М., Мельник І.А., Цебренко М.В., Петренко О.О., Овдійчук Г.В. Явище специфічного волокноутворення в сумішах поліпропілен/полівініловий спирт // Хімічна промисловість України. – 2013. – №2. – С. 62-67.

137. Starita J.M. Microstructure of melt blended polymer systems // Trans. Soc. Rheol. – 1972. – V.16, № 2. – P. 339–367.

138. Tomotika S. On the stability of a cylindrical thread of a viscous liquid surrounded by another viscous fluid // Proc. Roy. Soc. – 1935. – V. A150. – P. 322-337.

139. Han C. D., Funatsu K. An experimental study of droplet deformation and breakup in pressure-driven flows through converging and uniform channels // J. Rheol. – 1978. – V.22, № 2. – P.113-133.

140. Tsebrenko M.V., Danilova G.P., Malkin A. Ya. Ultrafine Fibers in Flow of Mixtures of non-Newtonian Polymer melts // J. Non-Newtonian Fluid Mech. – 1989. – V. 31. – P.1 – 26.

141. La Mantia F. P., Valenza A., Paci M., Magagnini P. L. Rheology-Morphology Relationships in Nylon 6/liquid-Crystalline Polymer Blends // Polym. Eng. Sci. – 1990. – V.1, № 30. – P.7-12.

142. Tran N. H. A, Brünig, H., Landwehr M.A., Vogel R., Heinrich G. Controlling micro- and nanofibrillar morphology of polymer blends in low-speed melt spinning process. Part II: Influences of extrusion rate on morphological changes of PLA/PVA through a capillary die // J. Appl. Polym. Sci. – 2016. – № 133. – P.442-573.

143. Beloshenko V.A., Plavan V.P., Rezanova N.M., Savchenko

B.M., Vozniak I. Production of high-performance multi-layer fine-fibrous filter materials by application of material extrusion-based additive manufacturing // The Int. J. of Adv. Manufac. Techn. – 2019. – №.101. – P. 2681-2688.

144. Pan Z., Chen Y., Zhu M., Jiang C., Xu Z., Lu W., Pionteck J. The Non-uniform Phase Structure in Blend Fiber. II. The Migration Phonomenon in Melt Spinnig // Fibers and Polymers. – 2010. – V. 11, №4. – P.625-631.

145. Pan Z., Zhu M., Chen Y., Chen L., Wu W., Yu C., Xu Z., Cheng L. The Variation of Fibrils Namber in the Sea-island Fiber – Low Density Polyethylene/Polyamide-6 // Fibers and Polymers. – 2010. – V. 11, №3. – P.494-499.

146. Veenstra H., Van Dam J., Posthuma B. A. On the Coarsening of Co-Continuous Morphologies in Polymer Blends: Effect of Interfacial Tension, Viscosity and Physical Cross-Links. // Polymer. – 2000. – V. 8, № 41. – P. 3037-3045.

147. Kong M., Huang Y., L.Y., Wang S., Yang Q., Li G. Flow-Induced Morphological Instability in Nanosilica-Filled Polyamide 6/polystyrene Blends // Polymer. – 2014. – V. 16, №55. – P. 4348-4357.

148. Liu X.-Q., Sun Z.-Y., Bao R.-Y., Yang W., Xie B.-H., Yang M.-B., Teyssibé P., Zaitsev V. Nanoparticle Retarded Shape Relaxation of Dispersed Droplets in Polymer Blends: An Understanding from the Viewpoint of Molecular Movement. // RSC Adv. – 2014. – V. 77, №4. – P. 1059-1068.

149. Xiu H., Zhou Y., Dai J., Huang C., Bai H., Zhang Q., Fu Q. Formation of New Electric Double Percolation via Carbon Black Induced Co-Continuous like Morphology. // RSC Adv. – 2014. – V.70, № 4. – P. 3773-3796.

150. Vermant J., Cioccolo G., Golapan K., Moldenaers P. Coalescence Suppression in Model Immiscible Polymer Blends by

Nano-Sized Colloidal Particles // Rheol. Acta. – 2004. – V. 5, №43. – P. 529-538.

151. Filippone G., Acierno D. Clustering of Coated Droplets in Clay-Filled Polymer Blends. // Macromol. Mater. Eng. – 2012. – V. 9, № 297. – P. 923-928.

152. Chen Y., Yang Q., Huang Y., Liao X., Niu Y. Influence of Phase Coarsening and Filler Agglomeration on Electrical and Rheological Properties of MWNTs-Filled PP/PMMA Composites under Annealing. // Polymer. – 2015. – №79. – P. 159-170.

153. Li W., Schlarb A.K., Evstatiev M. Study of PET/PP/TiO$_2$ microfibrillar-structured composites: Part 2. Morphology and mechanical properties // J. Appl. Polym. Sci. – 2009. – V. 113. – P. 3300-3306.

154. Li W., Schlarb A.K., Evstatiev M. Study of PET/PP/TiO$_2$ microfibrillar-structured composites: Part 1. Preparation, morphology and dynamic mechanical analysis of fibrillized blends // J. Appl. Polym. Sci. – 2009. – V. 113. – P. 1471-1479.

155. Цебренко М.В., Резанова В.Г., Картель М.Т., Мельник І.А., Приходько Г.П. Закономірності одержання нанонаповнених поліпропіленових мікроволокон // Збірник наукових праць «Хімія, фізика та технологія поверхні». – 2013. – Т.4, №3 . – С. 305-313.

156. Tsebrenko M.V., Rezanova V.G., Tsebrenko I.A. Polypropylene microfibers with filler in nano state // Chem. & Chem. Technol. – 2010. – V.4, №3. – P. 253-260.

157. Плаван В.П., Барсуков В.З., Резанова Н.М., Баула О.П. Перспективні полімерні матеріали та технології. – К: КНУТД, 2015. – 452 с.

158. Filters and Filtration Handbook / Ed. by Ch. Dickenson. – Oxford: Elsevier Advanced Technology, 1992. – 780 p.

159. Astarita G., Marrucci G. Principles of non-Newtonian fluid mechanics // McGraw-Hill, 1974. - 296 p.

160. Debayan Maity, Jorge San Martin, Takéo Takahashi, Marius Tucsnak. Analysis of a simplified model of rigid structure floating in a viscous fluid. Journal of Nonlinear Science, 2019, 29 (5), pp.1975-2020.

161. Карвацький А. Я. Механіка суцільних середовищ. – К.: КПІ ім. Ігоря Сікорського, 2016. – 290 с.:

162. Einstein A. Uber die von molekularkinetischen Theorie der Warme deforderte Beweggung von in ruhenden Flussigkeiten suspendierten Teilhen // Annalen der Physik. – 1906. – V.19 – S.298-306.

163. Jeffery G.B. The motion of ellipsoidal particles immersed in a viscous fluid // Proc. Roy. Soc. – 1922. – V. A102, №715. – P. 161-179.

164. Prager S. Stress-strain relations on a suspension of dumbels // Trans. Soc. Rheol. – 1957. – V.1. – P.53-62.

165. An Introduction to Continuum Mechanics // Edited by Morton E. Gurtin, Carnegie-Mellon University, Pittsburgh, Pennsylvania, Vol. 158, 1981. - 265 p.

166. Hinch E.J. An averaged-equation approach to particle interactions in a fluid suspensions // J. Fluid Mech. – 1977. – V.83, №4. – P.695-720.

167. Goddart J.D. An elastohydrodynamic theory for the rheology concentrated particles // J. Non-Newton, Fluid Mech. – 1977. – V.37, №1-2. – P.85-97.

168. Kevin G.N., Joseph B.K. Effective viscosity of a periodic suspension //   J. Fluid Mech. – 1984. – V.142, №2. – P.269-287.

169. Marianna Kontopoulou Applied Polymer Rheology: Polymeric Fluids with Industrial Applications // Wiley, - 2011. - 368 p.

170. Yu. V. Pridatchenko, Yu. I. Shmakov Rheological equations of state of weakly concentrated suspensions of rigid ellipsoidal particles // Journal of Applied Mechanics and Technical Physics, Vol. 14, No. 1. – 1973. – p. 118-119

171. Yu. V. Pridatchenko, Yu. I. Shmakov Effect of internal viscosity and elasticity of ellipsoidal macromolecules on the rheological behavior of dilute polymer solutions. rheological equations of state // Journal of Applied Mechanics and Technical Physics, Vol. 17, No. 3, 1976. – p. 373-376.

. 172. E. Yu. Taran, Yu. V. Pridatchenko Rheological behavior of dilute suspensions of rigid axisymmetric particles // Journal of Engineering Physics and Thermophysics, Vol. 62, No. 1, 1992. – p. 44-51.

173. E. Yu. Taran Rheological equation of state of dilute suspensions of rigid dumbbells having spheres at the ends // Applied Mechanics, Vol. 13, No. 4, 1977. – p. 399-403.

174. E. Yu. Taran, Yu. V. Pridatchenko, V. A. Gryaznova Features of the Formation of Composite Materials in Anisotropic Liquid Systems with Elongated Suspended Particles // Mechanics of Composite Materials, Vol. 37, No. 3, 2001. – p. 251-256.

175. Затонацька Т.Г., Придатченко Ю.В., Таран Є.Ю. Реологічна поведінка розбавлених суспезій деформівних частинок // Доповіді НАН України. – 1998. – №10. – С.88-93.

176. Ericksen J.L. Theory of anisotropic fluids // Trans. Soc. Rheol. – 1960. – V. 4, №1. – P.29-39.

177. Hobbs S.Y., Dekkers M.J., Watkins V.H. Effect of interfacial forces on polymer blend morphologies // Polymer. – 1988. –V.29, №9. – P.1598-1603.

178. Guo H.F., Packirisamy S., Gvozdic N.V., Meir D.J. Prediction and manipulation of the phase morphologies of multiphase polymer blends. 1.Ternary systems // Polymer. – 1997 – V.4. – P. 785-794.

179. Guo H.-F., Gvozdic N. V., Meier D. Z. Prediction and manipulation of the phase morphologies of multiphase polymer blends: 2. Quaternary systems // Polymer. – 1997. Vol. 38, №19. –P. 4915-4923.

180. Резанова В.Г., Цебренко М.В., Придатченко Ю.В. Дослідження закономірностей деформування полімеру дисперсної фази при течії розплаву суміші полімерів з використанням математичного моделювання // Вісник КНУТД. – 2003. – №2. – С.183-184.

181. Tsebrenko M.V., Rezanova N.M., Vinogradov G.V. Rheology of molten blends of polyoxymethylene and ethylene-vinyl acetate copolymer and the microstructure of extrudates as a function of their melt viscosities // Polym. Eng. and Sci. – 1980. – V.20, № 15. – P.1023-1028.

182. Chan C.D. Rheology and processing of polymeric materials // Volume 1: Polymer Rheology. – 2007. – 736 p.

183. Taylor G.I. The formation of emulsions in definable fluids of flow // Proc. Roy. Soc. – London, 1934. – V.A 146. – P. 501-526.

184. Van Oene H. Modes of dispersion of viscoelastic fluids in flow // J.Colloid Interface Sci. – 1972. – V.40, №3. – P.448-467.

185. Van Oene H. Rheology of Polymer Blends and Dispersion // Polymer. – 1978. – V.1, ch.7. – P. 295-352.

186. Резанова В.Г. Програмне забезпечення для математичного моделювання специфічного волокноутворення // Інформаційні технології в науці, виробництві та підприємництві. – К.: Освіта України, 2017. – С. 20-24.

187. Резанова В.Г., Резанова Н.М. Програмне забезпечення

для оптимізації складу багатокомпонентних сумішей. - К.:АртЕк. - 2022. 315 с.

188. N. R. Draper, H. Smith Applied Regression Analysis. - John Wiley & Sons, 1998. - 736 p.

189. 4. Stanley B. Lippman, Josée Lajoie, Barbara E. My C++ Primer, Addison-Wesley: 2012. – 976 p.

.   190. Stroustrup B. Programming: Principles and Practice Using C++ (2nd Edition). Addison-Wesley Professional, 2014. – 1312 p.

191. Резанова В.Г. Математичне моделювання та компютерна візуалізація процесу специфічного волокно утворення // К.: Вісник КНУТД. - № 4, 2017. -   с. 19-26

192. Stroustrup B. The C++ Programming Language Fourth Edition. Addison-Wesley, 2013. – 1366 p.

193. Резанова В.Г., Резанова Н.М., Коршун А.В. Дослідження морфології сумішей полімерів з використанням розробленого програмного забезпечення // Вісник КНУТД – 2017. – №2. – С.120–127.

ЛІСТИНГ ПРОГРАМ

1. Основні процедури та функції для розрахунків за математичною моделлю деформації полімерної краплі в потоці

```
Unit1
procedure FuncTeta(CurrT,CurrTeta,CurrQ:real;Var FTeta:real);
var l3:real;
begin
 if CurrQ>0 then begin
 lambda3(CurrQ, l3);
 FTeta:=(-3/4)*d{CurrQ}*l3*sin(2*CurrTeta);
 end
else   Form1.Memo3.Lines.Add('Chastitsa vyvernulas
naiznanku!!!!!');
end;


procedure FuncQ(CurrT,CurrTeta,CurrQ:real;Var FQ:real);
var l1,l2,l3:real;
begin
if CurrQ>0 then begin
lambda1(CurrQ, l1);
lambda2(CurrQ, l2);
lambda3(CurrQ, l3);
FQ:=(3/2)*CurrQ*(l1+(d{CurrQ}/2)*(l2*R0*R0*power(CurrQ,4/3)
+l3)
   *(2-3*sin(CurrTeta)*sin(CurrTeta)));
   end;
end;


procedure lambda1(CurrQ:real;Var Fl1:real);
var a,b,M,
   alfa0,beta0,alfa0_,beta0_,alfa0__,beta0__:real;
begin
if CurrQ>0 then begin
```

```
b:=R0*power(CurrQ,(-1/3));
a:=R0*power(CurrQ,2/3);
FIalfa0(CurrQ,alfa0);
 FIbeta0(CurrQ,beta0);
 FIbeta0_(CurrQ,beta0_);
 FIalfa0_(CurrQ,alfa0_);
 FIbeta0__(CurrQ,beta0__);
 FIalfa0__(CurrQ,alfa0__);
M:=4/(a*Sqr(b)*(2+3*a*Sqr(b)*(eta/mu)*beta0__))*
  (
   5/(6*(alfa0+2*beta0-2*beta0_*(Sqr(a)+Sqr(b))))-
(   (100*beta0_*Sqr(a)*(2*beta0_*Sqr(a)-alfa0-2*beta0))/
   ((alfa0+2*beta0)*(alfa0+2*beta0-2*beta0_*(Sqr(a)+Sqr(b)))) )*
   (
    1/(24*a*beta0)-1/(2*Sqr(beta0_)*Sqr(a)-(alfa0+2*beta0))
   )
   );
  Fl1:=(
      ( -2*a*Sqr(b)*beta0__*G*(a/A0*(1-q0/CurrQ)) )
      /
      ( mu*(2+3*a*Sqr(b)*beta0__*(eta/mu)) )
        )*(1-M*Fr);
  end
else   Form1.Memo3.Lines.Add('Chastitsa vyvernulas
naiznanku!!!!!');
end;

procedure lambda2(CurrQ:real;Var Fl2:real);
var a,b,pr1,pr2,M,N,
   alfa0,beta0,alfa0_,beta0_,alfa0__,beta0__ :real;
begin
if CurrQ>0 then begin
b:=R0*power(CurrQ,(-1/3));
 a:=R0*power(CurrQ,2/3);
 FIalfa0(CurrQ,alfa0);
FIbeta0(CurrQ,beta0);
 FIbeta0_(CurrQ,beta0_);
 FIalfa0_(CurrQ,alfa0_);
```

231

```
FIbeta0__(CurrQ,beta0__);
FIalfa0__(CurrQ,alfa0__);
M:=4/(a*Sqr(b)*(2+3*a*Sqr(b)*(eta/mu)*beta0__))*
  (
   5/(6*(alfa0+2*beta0-2*beta0_*(Sqr(a)+Sqr(b))))-
(   (100*beta0_*Sqr(a)*(2*beta0_*Sqr(a)-alfa0-2*beta0))/
   ((alfa0+2*beta0)*(alfa0+2*beta0-2*beta0_*(Sqr(a)+Sqr(b)))) )*
   (
    1/(24*a*beta0)-1/(2*Sqr(beta0_)*Sqr(a)-(alfa0+2*beta0))
   )
  );
N:=(4/(a*Sqr(b)))* (
   10/(18*beta0__)+5*beta0__/(8*Sqr(Sqr(b))*Sqr(alfa0_))-
   (10*(beta0__-alfa0__)*(2*Sqr(b)*alfa0_+3*beta0__))/
   (72*Sqr(Sqr(b))*Sqr(alfa0_))
        );
Bb:=Sqr(a)*alfa0+sqr(b)*beta0;
pr1:=Sqr(a)+Sqr(b);
pr2:=Sqr(a)-Sqr(b);
  Fl2:=(2+(N-2*M)*Fr)/(Sqr(a)*(2+3*a*Sqr(b)*beta0__*(eta/mu)))
  -
  (pr2+((15*pr2*(alfa0+beta0)+4*pr1*(beta0-
alfa0))/(6*a*Sqr(b)*beta0_*Bb))*Fr)
  /
  (pr1+((15*Sqr(pr2)+4*Sqr(pr1))/(6*a*Sqr(b)*Bb))*Fr);
  end
else  Form1.Memo3.Lines.Add('Chastitsa vyvernulas
naiznanku!!!!!');
end;

procedure lambda3(CurrQ:real;Var Fl3:real);
var a,b,pr1,pr2,alfa0,beta0,alfa0_,beta0_,alfa0__,beta0__:real;
begin
if CurrQ>0 then begin
b:=R0*power(CurrQ,(-1/3));
 a:=R0*power(CurrQ,2/3);
FIalfa0(CurrQ,alfa0);
 FIbeta0(CurrQ,beta0);
```

```
 FIbeta0_(CurrQ,beta0_);
Bb:=Sqr(a)*alfa0+sqr(b)*beta0;
pr1:=Sqr(a)+Sqr(b);
pr2:=Sqr(a)-Sqr(b);
Fl3:=(pr2+((15*pr2*(alfa0+beta0)+4*pr1*(beta0-
alfa0))/(6*a*Sqr(b)*beta0_*Bb))*Fr)
  /
  (pr1+((15*Sqr(pr2)+4*Sqr(pr1))/(6*a*Sqr(b)*Bb))*Fr);
  end
else  Form1.Memo3.Lines.Add('Chastitsa vyvernulas
naiznanku!!!!!');
end;

procedure M_Runge_Kutta(CurrT,CurrTeta,CurrQ,h:real;Var
Yk1,Zk1:real);
var k1,k2,k3,k4,
   m1,m2,m3,m4,
   FQ,FTeta:real;
begin
if CurrQ>0 then begin
FuncQ(CurrT,CurrTeta,CurrQ,FQ);
 FuncTeta(CurrT,CurrTeta,CurrQ,FTeta);
 k1:=FTeta*h;
 m1:=FQ*h;
 FuncQ(CurrT+h/2,CurrTeta+k1/2,CurrQ+m1/2,FQ);
 FuncTeta(CurrT+h/2,CurrTeta+k1/2,CurrQ+m1/2,FTeta);
 k2:=FTeta*h;
 m2:=FQ*h;
 FuncQ(CurrT+h/2,CurrTeta+k2/2,CurrQ+m2/2,FQ);
 FuncTeta(CurrT+h/2,CurrTeta+k2/2,CurrQ+m2/2,FTeta);
 k3:=FTeta*h;
 m3:=FQ*h;
 FuncQ(CurrT+h,CurrTeta+k3,CurrQ+m3,FQ);
 FuncTeta(CurrT+h,CurrTeta+k3,CurrQ+m3,FTeta);
 k4:=FTeta*h;
 m4:=FQ*h;
 Yk1:=CurrTeta+(1/6)*(k1+2*k2+2*k3+k4);
 Zk1:=CurrQ+(1/6)*(m1+2*m2+2*m3+m4);
```
233

```pascal
 End;
end;
//              alfa and beta calculation
procedure FPalfa0(CurrQ:real;Var Falfa0:real);
var b,Ab,a:real;
 begin
 if CurrQ>0 then begin
b:=R0*power(CurrQ,(-1/3));
 a:=R0*power(CurrQ,2/3);
 if CurrQ>1.01 then
        begin
        Ab:=CurrQ*CurrQ/(CurrQ*CurrQ-1)-
(CurrQ*ln(CurrQ+sqrt(CurrQ*CurrQ-1)))
          /(power(CurrQ*CurrQ-1,3/2));
        Falfa0:=(2-2*Ab)/(a*b*b);
         end
        else
 if CurrQ<0.99 then
         begin
        Ab:=CurrQ*CurrQ/(CurrQ*CurrQ-1)+(CurrQ/power(1-
CurrQ*CurrQ,3/2))*
         (3.1415/2-ArcTan(CurrQ/sqrt(1-CurrQ*CurrQ)));
        Falfa0:=(2-2*Ab)/(a*b*b);
          end
 else
        Falfa0:=2/(3*a*a*a);
    end
else  Form1.Memo3.Lines.Add('Chastitsa vyvernulas
naiznanku!!!!!');
 end;

 procedure FPalfa0_(CurrQ:real;Var Falfa0_:real);
var b,a,Ab:real;
 begin
 if CurrQ>0 then begin
b:=R0*power(CurrQ,(-1/3));
 a:=R0*power(CurrQ,2/3);
 if CurrQ>1.01 then
```

234

```
        begin
        Ab:=CurrQ*CurrQ/(CurrQ*CurrQ-1)-
(CurrQ*ln(CurrQ+sqrt(CurrQ*CurrQ-1)))
          /(power(CurrQ*CurrQ-1,3/2));
        Falfa0_:=(2*CurrQ*CurrQ-3*Ab)/(4*(CurrQ*CurrQ-
1)*(a*b*b*b*b));
         end
        else
 if CurrQ<0.99 then
         begin
        Ab:=CurrQ*CurrQ/(CurrQ*CurrQ-1)+(CurrQ/power(1-
CurrQ*CurrQ,3/2))*
          (3.1415/2-ArcTan(CurrQ/sqrt(1-CurrQ*CurrQ)));
        Falfa0_:=(2*CurrQ*CurrQ-3*Ab)/(4*(CurrQ*CurrQ-
1)*(a*b*b*b*b));
          end
 else
        Falfa0_:=2/(5*a*a*a*a*a);
        end
  else   Form1.Memo3.Lines.Add('Chastitsa vyvernulas
naiznanku!!!!!');
 end;

 procedure FPalfa0__(CurrQ:real;Var Falfa0__:real);
var b,a,Ab:real;
 begin
  if CurrQ>0 then begin
  b:=R0*power(CurrQ,(-1/3));
 a:=R0*power(CurrQ,2/3);
 if CurrQ>1.01 then
         begin
        Ab:=CurrQ*CurrQ/(CurrQ*CurrQ-1)-
(CurrQ*ln(CurrQ+sqrt(CurrQ*CurrQ-1)))
          /(power(CurrQ*CurrQ-1,3/2));
        Falfa0__:=((4*CurrQ*CurrQ-1)*Ab-2*CurrQ*CurrQ)
             /(4*(CurrQ*CurrQ-1)*(a*b*b));
          end
        else
```

235

```pascal
 if CurrQ<0.99 then
        begin
      Ab:=CurrQ*CurrQ/(CurrQ*CurrQ-1)+(CurrQ/power(1-
CurrQ*CurrQ,3/2))*
        (3.1415/2-ArcTan(CurrQ/sqrt(1-CurrQ*CurrQ)));
      Falfa0__:=((4*CurrQ*CurrQ-1)*Ab-
2*CurrQ*CurrQ)/(4*(CurrQ*CurrQ-1)*(a*b*b));
        end
 else
      Falfa0__:=4/(15*a*a*a);
      end
else   Form1.Memo3.Lines.Add('Chastitsa vyvernulas
naiznanku!!!!!');
 end;

 procedure FPbeta0(CurrQ:real;Var Fbeta0:real);
 var b,a,Ab:real;
 begin
 if CurrQ>0 then begin
b:=R0*power(CurrQ,(-1/3));
 a:=R0*power(CurrQ,2/3);
 if CurrQ>1.01 then
        begin
      Ab:=CurrQ*CurrQ/(CurrQ*CurrQ-1)-
(CurrQ*ln(CurrQ+sqrt(CurrQ*CurrQ-1)))
        /(power(CurrQ*CurrQ-1,3/2));
      Fbeta0:=Ab/(a*b*b);
       end
      else
 if CurrQ<0.99 then
        begin
      Ab:=CurrQ*CurrQ/(CurrQ*CurrQ-1)+(CurrQ/power(1-
CurrQ*CurrQ,3/2))*
        (3.1415/2-ArcTan(CurrQ/sqrt(1-CurrQ*CurrQ)));
      Fbeta0:=Ab/(a*b*b);
        end
 else
      Fbeta0:=2/(3*a*a*a);
```

```
    end
else   Form1.Memo3.Lines.Add();
 end;

 procedure FPbeta0_(CurrQ:real;Var Fbeta0_:real);
var b,a,Ab:real;
 begin
if CurrQ>0 then begin
 b:=R0*power(CurrQ,(-1/3));
 a:=R0*power(CurrQ,2/3);
 if CurrQ>1.01 then
         begin
        Ab:=CurrQ*CurrQ/(CurrQ*CurrQ-1)-
(CurrQ*ln(CurrQ+sqrt(CurrQ*CurrQ-1)))
          /(power(CurrQ*CurrQ-1,3/2));
        Fbeta0_:=(3*Ab-2)/((CurrQ*CurrQ-1)*(a*b*b*b*b));
         end
        else
 if CurrQ<0.99 then
         begin
        Ab:=CurrQ*CurrQ/(CurrQ*CurrQ-1)+(CurrQ/power(1-
CurrQ*CurrQ,3/2))*
         (3.1415/2-ArcTan(CurrQ/sqrt(1-CurrQ*CurrQ)));
        Fbeta0_:=(3*Ab-2)/((CurrQ*CurrQ-1)*(a*b*b*b*b));
         end
 else
        Fbeta0_:=2/(5*a*a*a*a*a);
       end
   else   Form1.Memo3.Lines.Add(!!');
 end;

 procedure FPbeta0__(CurrQ:real;Var Fbeta0__:real);
var b,a,Ab:real;
 begin
if CurrQ>0 then begin
 b:=R0*power(CurrQ,(-1/3));
 a:=R0*power(CurrQ,2/3);
 if CurrQ>1.01 then
```

237

```pascal
       begin
       Ab:=CurrQ*CurrQ/(CurrQ*CurrQ-1)-
(CurrQ*ln(CurrQ+sqrt(CurrQ*CurrQ-1)))
          /(power(CurrQ*CurrQ-1,3/2));
       Fbeta0__:=(2*CurrQ*CurrQ-(2*CurrQ*CurrQ+1)*Ab)/
            ((CurrQ*CurrQ-1)*(a*b*b));
        end
       else
 if CurrQ<0.99 then
        begin
       Ab:=CurrQ*CurrQ/(CurrQ*CurrQ-1)+(CurrQ/power(1-
CurrQ*CurrQ,3/2))*
          (3.1415/2-ArcTan(CurrQ/sqrt(1-CurrQ*CurrQ)));
       Fbeta0__:=(2*CurrQ*CurrQ-(2*CurrQ*CurrQ+1)*Ab)/
            ((CurrQ*CurrQ-1)*(a*b*b));
         end
 else
       Fbeta0__:=4/(15*a*a*a);
   end
   else   Form1.Memo3.Lines.Add('Chastitsa vyvernulas
naiznanku!!!!!');
 end;

//           alfa and beta calculation by integrals
procedure FIalfa0(CurrQ:real;Var FIalfa0:real);
var ni,mi,i:integer;
   hi,delta,c,b,a,
   nizgr,verhgr,
   f0,fni,fk1,fk2,
   lambda,Sum:real;
 begin
if CurrQ>0 then begin

 b:=R0*power(CurrQ,(-1/3));
 a:=R0*power(CurrQ,2/3);
 c:=b;
 nizgr:=0;
 Sum:=0;
```
238

```
 verhgr:=10;
 mi:=100;
 ni:=2*mi;
 hi:=(verhgr-nizgr)/ni;
 lambda:=nizgr;
delta:=Sqrt((a*a+lambda)*(b*b+lambda)*(c*c+lambda));
f0:=1/((a*a+lambda)*delta);
// f0:=1/(1+lambda);
Sum:=Sum+f0;
for i:=1 to mi do
 begin
   lambda:=lambda+hi;
   delta:=Sqrt((a*a+lambda)*(b*b+lambda)*(c*c+lambda));
  fk1:=1/((a*a+lambda)*delta);
   fk1:=1/(1+lambda);
   Sum:=Sum+4*fk1;
   lambda:=lambda+hi;
   delta:=Sqrt((a*a+lambda)*(b*b+lambda)*(c*c+lambda));
   fk2:=1/((a*a+lambda)*delta);
   //fk2:=1/(1+lambda);
   if lambda=verhgr then Sum:=Sum+fk2
               else Sum:=Sum+2*fk2;
 end;
 FIalfa0:=Sum*hi/3;
    end
   else   Form1.Memo3.Lines.Add(!');
 end;

 procedure FIalfa0_(CurrQ:real;Var FIalfa0_:real);
var ni,mi,i:integer;
   hi,delta,c,b,a,
   nizgr,verhgr,
   f0,fni,fk1,fk2,
   lambda,Sum:real;
 begin
 if CurrQ>0 then begin
 b:=R0*power(CurrQ,(-1/3));
 a:=R0*power(CurrQ,2/3);
```

```
 c:=b;
 nizgr:=0;
 Sum:=0;
 verhgr:=10;
 mi:=100;
 ni:=2*mi;
 hi:=(verhgr-nizgr)/ni;
 lambda:=nizgr;
 delta:=Sqrt((a*a+lambda)*(b*b+lambda)*(c*c+lambda));
 f0:=1/((b*b+lambda)*(c*c+lambda)*delta);
Sum:=Sum+f0;
for i:=1 to mi do
  begin
   lambda:=lambda+hi;
  delta:=Sqrt((a*a+lambda)*(b*b+lambda)*(c*c+lambda));
   fk1:=1/((b*b+lambda)*(c*c+lambda)*delta);
   Sum:=Sum+4*fk1;
   lambda:=lambda+hi;
    delta:=Sqrt((a*a+lambda)*(b*b+lambda)*(c*c+lambda));
   fk2:=1/((b*b+lambda)*(c*c+lambda)*delta);
   if lambda=verhgr then Sum:=Sum+fk2
               else Sum:=Sum+2*fk2;
  end;
 FIalfa0_:=Sum*hi/3;
   end
   else   Form1.Memo3.Lines.Add('Chastitsa vyvernulas
naiznanku!!!!!');
 end;

 procedure FIalfa0__(CurrQ:real;Var FIalfa0__:real);
var ni,mi,i:integer;
   hi,delta,c,b,a,
   nizgr,verhgr,
   f0,fni,fk1,fk2,
   lambda,Sum:real;
 begin
 if CurrQ>0 then begin
  b:=R0*power(CurrQ,(-1/3));
```
240

```
 a:=R0*power(CurrQ,2/3);
 c:=b;
nizgr:=0;
 Sum:=0;
 verhgr:=10;
 mi:=100;
 ni:=2*mi;
 hi:=(verhgr-nizgr)/ni;
 lambda:=nizgr;
 delta:=Sqrt((a*a+lambda)*(b*b+lambda)*(c*c+lambda));
 f0:=lambda/((b*b+lambda)*(c*c+lambda)*delta);
Sum:=Sum+f0;
for i:=1 to mi do
  begin
    lambda:=lambda+hi;
delta:=Sqrt((a*a+lambda)*(b*b+lambda)*(c*c+lambda));
    fk1:=lambda/((b*b+lambda)*(c*c+lambda)*delta);
    Sum:=Sum+4*fk1;
    lambda:=lambda+hi;
delta:=Sqrt((a*a+lambda)*(b*b+lambda)*(c*c+lambda));
    fk2:=lambda/((b*b+lambda)*(c*c+lambda)*delta);
    if lambda=verhgr then Sum:=Sum+fk2
                else Sum:=Sum+2*fk2;
  end;
  FIalfa0__:=Sum*hi/3;
    end
    else   Form1.Memo3.Lines.Add('Chastitsa vyvernulas
naiznanku!!!!!');
 end;

 procedure FIbeta0(CurrQ:real;Var FIbeta0:real);
var ni,mi,i:integer;
   hi,delta,c,b,a,
   nizgr,verhgr,
   f0,fni,fk1,fk2,
   lambda,Sum:real;
 begin
 if CurrQ>0 then begin
```

241

```pascal
   b:=R0*power(CurrQ,(-1/3));
  a:=R0*power(CurrQ,2/3);
  c:=b;
  nizgr:=0;
  Sum:=0;
  verhgr:=10;
  mi:=100;
  ni:=2*mi;
  hi:=(verhgr-nizgr)/ni;
  lambda:=nizgr;
delta:=Sqrt((a*a+lambda)*(b*b+lambda)*(c*c+lambda));
 f0:=1/((b*b+lambda)*delta);
Sum:=Sum+f0;
for i:=1 to mi do
  begin
    lambda:=lambda+hi;
delta:=Sqrt((a*a+lambda)*(b*b+lambda)*(c*c+lambda));
    fk1:=1/((b*b+lambda)*delta);
    Sum:=Sum+4*fk1;
    lambda:=lambda+hi;
delta:=Sqrt((a*a+lambda)*(b*b+lambda)*(c*c+lambda));
    fk2:=1/((b*b+lambda)*delta);
    if lambda=verhgr then Sum:=Sum+fk2
              else Sum:=Sum+2*fk2;
  end;
  FIbeta0:=Sum*hi/3;
    end
    else   Form1.Memo3.Lines.Add('Chastitsa vyvernulas
naiznanku!!!!!');
 end;

 procedure FIbeta0_(CurrQ:real;Var FIbeta0_:real);
var ni,mi,i:integer;
   hi,delta,c,b,a,
   nizgr,verhgr,
   f0,fni,fk1,fk2,
   lambda,Sum:real;
 begin
```

```pascal
 if CurrQ>0 then begin
   b:=R0*power(CurrQ,(-1/3));
  a:=R0*power(CurrQ,2/3);
  c:=b;
  nizgr:=0;
  Sum:=0;
  verhgr:=10;
  mi:=100;
  ni:=2*mi;
  hi:=(verhgr-nizgr)/ni;
  lambda:=nizgr;
 delta:=Sqrt((a*a+lambda)*(b*b+lambda)*(c*c+lambda));
  f0:=1/((a*a+lambda)*(c*c+lambda)*delta);
 Sum:=Sum+f0;
 for i:=1 to mi do
  begin
    lambda:=lambda+hi;
 delta:=Sqrt((a*a+lambda)*(b*b+lambda)*(c*c+lambda));
    fk1:=1/((a*a+lambda)*(c*c+lambda)*delta);
    Sum:=Sum+4*fk1;
    lambda:=lambda+hi;
 delta:=Sqrt((a*a+lambda)*(b*b+lambda)*(c*c+lambda));
    fk2:=1/((a*a+lambda)*(c*c+lambda)*delta);
    if lambda=verhgr then Sum:=Sum+fk2
              else Sum:=Sum+2*fk2;
  end;
  FIbeta0_:=Sum*hi/3;
   end
   else   Form1.Memo3.Lines.Add('Chastitsa vyvernulas
naiznanku!!!!!');
 end;

 procedure FIbeta0__(CurrQ:real;Var FIbeta0__:real);
var ni,mi,i:integer;
   hi,delta,c,b,a,
   nizgr,verhgr,
   f0,fni,fk1,fk2,
   lambda,Sum:real;
```

243

```
 begin
 if CurrQ>0 then begin
  b:=R0*power(CurrQ,(-1/3));
 a:=R0*power(CurrQ,2/3);
 c:=b;
 nizgr:=0;
 Sum:=0;
 {verhgr:=100;
 mi:=10000;}
 verhgr:=10;
 mi:=1000;
 ni:=2*mi;
 hi:=(verhgr-nizgr)/ni;
 lambda:=nizgr;
delta:=Sqrt((a*a+lambda)*(b*b+lambda)*(c*c+lambda));

 f0:=lambda/((a*a+lambda)*(c*c+lambda)*delta);
Sum:=Sum+f0;
for i:=1 to mi do
  begin
   lambda:=lambda+hi;
delta:=Sqrt((a*a+lambda)*(b*b+lambda)*(c*c+lambda));
   fk1:=lambda/((a*a+lambda)*(c*c+lambda)*delta);
   Sum:=Sum+4*fk1;
   lambda:=lambda+hi;
delta:=Sqrt((a*a+lambda)*(b*b+lambda)*(c*c+lambda));
   fk2:=lambda/((a*a+lambda)*(c*c+lambda)*delta);
   if lambda=verhgr then Sum:=Sum+fk2
             else Sum:=Sum+2*fk2;
  end;
  FIbeta0__:=Sum*hi/3;
   end
   else   Form1.Memo3.Lines.Add('Chastitsa vyvernulas
naiznanku!!!!!');
 end;

procedure TForm1.FormCreate(Sender: TObject);
 var i:integer;
```

```
   k:real;
begin
Form1.Button2.Visible:=False;
eta:=830;
Form1.Edit3.Text:=FloatToStr(eta);
mu:=790;
Form1.Edit2.Text:=FloatToStr(mu);
 Form1.Edit9 .Text:=FloatToStr(eta/mu);
d_:=0.0000069;
Form1.Edit11.Text:=FloatToStr(d_);
Fr:=0.306;
Form1.Edit4.Text:=FloatToStr(Fr);
R0:=0.000055;
R0_3:=R0*R0*R0;
V:=(4/3)*3.1415*R0*R0*R0;
Form1.Edit1.Text:=FloatToStr(V);
Form1.Edit12.Text:=FloatToStr(R0);
T0:=0;
CurrT:=T0;
Teta0:=0.7 ;
CurrTeta:=Teta0;
Form1.Edit6.Text:=FloatToStr(Teta0);
Q0:=1.000001;
CurrQ:=Q0;
Form1.Edit5.Text:=FloatToStr(Q0);
  Sigma:=2.6;
K:=0.1482000e8;
G:=(Sigma*K/R0)*(power(CurrQ,2/3)/(1-Q0/(CurrQ+0.0000001)));
Form1.Edit7.Text:=FloatToStr(G);
 b0:=R0*power(CurrQ,(-1/3));
 A0:=R0*power(CurrQ,2/3);
h:=0.0000000004;
Form1.Edit8.Text:=FloatToStr(h);
d:=1.08;
Form1.Edit10.Text:=FloatToStr(d);
Height1:=0.01;
for i:=0 to 100 do
   begin
```

```
     k:=i*3*10e-3;
   L:=((40*10e-5/5.5)/d)*(exp(d*k)+1);
      Form1.Memo5.Lines.Add(FloatToStr(L));
   end;
end;

procedure TForm1.Button5Click(Sender: TObject);
var i:integer;
begin
for i:=1 to 5 do
 begin
 M_Runge_Kutta(CurrT,CurrTeta,CurrQ,h, Yk1,Zk1);
CurrTeta:=Yk1;
CurrQ:=Zk1;
 Form1.Memo1.Lines.Add(FloatToStr(CurrT));
Form1.Memo2.Lines.Add(FloatToStr(CurrTeta));
Form1.Memo3.Lines.Add(FloatToStr(CurrQ));
 CurrT:=CurrT+h;
  end;
Aex:=Sqrt(R0_3/d_);
Qex:=Aex/d_;
Form1.Memo4.Lines.Add(FloatToStr(Qex));
end;

procedure TForm1.Button7Click(Sender: TObject);
begin
  Fr:=StrToFloat(Edit4.Text);
 eta:=StrToFloat(Edit3.Text);
 mu:=StrToFloat(Edit2.Text);
   Form1.Edit9 .Text:=FloatToStr(eta/mu);
R0:=StrToFloat(Edit12.Text);
 R0_3:=R0*R0*R0;
V:=(4/3)*3.1415*R0_3;
Form1.Edit1.Text:=FloatToStr(V);
 d:=StrToFloat(Edit10.Text);
 d_:=StrToFloat(Edit11.Text);
  G:=StrToFloat(Edit7.Text);
  Teta0:=StrToFloat(Edit6.Text);
```

246

```
   CurrTeta:=Teta0;
   h:=StrToFloat(Edit8.Text);
    Q0:=StrToFloat(Edit5.Text);
 CurrQ:=Q0;
b0:=R0*power(CurrQ,(-1/3));
a0:=R0*power(CurrQ,2/3);
end;
end.
```

2. Основні процедури та функції для перевірки адекватності математичної моделі формування мікрофібриллярної структури

```
int n,m,p,nm,*ni;
float **X, *K;
float *OFR(float **X, float *K, int n)
  {
   float *ofr;
   ofr = new float [n];
   for(int i = 0; i < n; i++)
   {
        ofr[i] =
K[0]*X[i][0]+K[1]*X[i][1]+K[2]*X[i][2]+K[3]*X[i][0]*X[i][1]

+K[4]*X[i][0]*X[i][2]+K[5]*X[i][1]*X[i][2]+K[6]*X[i][0]*X[i][1]
*X[i][2];
   }
   return ofr;
  };

float **Y;

float  **read_y(char *file_y)
{
 FILE  *input=fopen(file_y,"rt");
 float **Y;
 Y=new float *[n];
 for (int i=0;i<n;i++)
  {
   Y[i]=new float[ni[i]];
  }
 for (int i=0;i<n;i++)
  {
   for (int j=0;j<ni[i];j++)
   {
    fscanf(input,"%f",&Y[i][j]);
```

```cpp
   }
  }
 fclose(input);
 return Y;
}

float *SR(float **Y, int *ny, int n)
 {
  float *ysr;
  ysr = new float [n];
  for(int i = 0; i < n; i++)
  {
   for(int j = 0; j < ny[i]; j++)
   {
    ysr[i] +=Y[i][j]/ny[i];
   }
  }
  return ysr;
 };

float S12(float *Ofr, float *Ysr, float **Y,
       int *ny, int n, int m, int p)
 {
  float S1 = 0;

  for(int i = 0; i < n; i++)
  {
  S1 += (ny[i]*pow((Ofr[i] - Ysr[i]), 2)) / (m - p);
  }
  float S2 = 0;

  for(int i = 0; i < n; i++)
  {
   for(int j = 0; j < ni[i]; j++)
   {
  S2 += (pow((Y[i][j] - Ysr[i]), 2)) / (n - m);
   }
  }
```

249

```
  float S = S1 / S2;
      return S;
  };

void __fastcall TForm1::Button1Click(TObject *Sender)
{
FILE *input=fopen("vvod_file_o_x.txt","rt");
fscanf(input,"%d", &m);
 fscanf(input,"%d", &n);
 fscanf(input,"%d", &p);
if (m>n) nm=m; else nm=n;
ni=new int[nm];
  for (int i=0;i<nm;i++)
  {
  fscanf(input,"%d",&ni[i]);
  }
  X=new float *[n];
  for (int i=0;i<n;i++)
  {
   X[i]=new float[3];
  }
  for (int i=0;i<n;i++)
  {
  for (int j=0;j<3;j++)
  {
  fscanf(input,"%f",&X[i][j]);
  Memo1->Text=Memo1->Text+FloatToStrF(X[i][j], ffFixed, 6, 5)
+"   ";
  }
  Memo1->Lines->Add("");
  }
  fclose(input);

  float **MatrPlan;
  MatrPlan = new float *[n];
  for (int i = 0; i < n; i++){
   MatrPlan[i] = new float [p];
   }
```

250

```
   for (int i = 0; i < n; i++)
    {
    for (int j = 0; j < p; j++)
     {
     MatrPlan[i][0] = X[i][0];
     MatrPlan[i][1] = X[i][1];
     MatrPlan[i][2] = X[i][2];
     MatrPlan[i][3] = X[i][0] * X[i][1];
     MatrPlan[i][4] = X[i][0] * X[i][2];
     MatrPlan[i][5] = X[i][1] * X[i][2];
     MatrPlan[i][6] = X[i][0] * X[i][1] * X[i][2];
     Memo3->Text=Memo3->Text+FloatToStrF(MatrPlan[i][j],
ffFixed, 6, 5) + "   ";
     }
    Memo3->Lines->Add("");
    }
   FILE  *input1=fopen("vvod_file_koef.txt","rt");
   K=new float [p];
   for (int i=0;i<p;i++)
    {
    fscanf(input1,"%f",&K[i]);
    }
   fclose(input1);
   float *Ofr;
   Ofr = new float [n];
   for (int i = 0; i < n; i++)
    {
    Ofr = OFR(X, K, n);
    Memo5->Text=Memo5->Text+FloatToStrF((Ofr[i]), ffFixed, 6, 5);
    Memo5->Lines->Add("");
    };
     Y=new float *[n];
   for (int i=0;i<n;i++)
    {
    Y[i]=new float[ni[i]];
    }
   Y=read_y("vvod_file_y.txt") ;
   for (int i=0;i<n;i++)
```

251

```
 {
 for (int j=0;j<ni[i];j++)
 {
 Memo2->Text=Memo2->Text+FloatToStrF(Y[i][j], ffFixed, 6, 5)
+ "   ";
 }
 Memo2->Lines->Add("");
 }

 float *Ysr;
 Ysr = new float [n];
 Ysr = SR(Y, ni, n);
 for (int i = 0; i < n; i++)
 {
 Memo6->Text=Memo6->Text+FloatToStrF(Ysr[i], ffFixed, 6, 5);
 Memo6->Lines->Add("");
 };
 float S;
 S = S12(Ofr, Ysr, Y, ni, n, m, p);
 Memo7->Text=Memo7->Text+FloatToStrF(S, ffFixed, 6, 5);
}
```

3. Основні процедури та функції для візуалізації деформації полімерної краплі в потоці

```
MatModelOfFormatingFiber::MatModelOfFormatingFiber()
{
        eta = 830; mu = 790;
        d_ = 0.0000069;        Fr = 0.306;
        R0 = 0.000055; R0_3 = R0 * R0 * R0;
        V = (4.0 / 3.0) * 3.1415 * R0 * R0 * R0;
        T0 = 0; CurrT = T0;
        Teta0 = 0.7; CurrTeta = Teta0;
        q0 = 1.000001; CurrQ = q0;
        Sigma = 2.6; K = 0.1482000e8;
        G = (Sigma*K / R0)*(pow(CurrQ, 2 / 3) / (1 - q0 / (CurrQ +
0.0000001)));
        B0 = R0 * pow(CurrQ, (-1 / 3));
        A0 = R0 * pow(CurrQ, 2 / 3);
        h = 0.0000000004; d = 1.08;
        double k; Height1 = 0.01;
        for (int i = 0; i < 100; i++)
        {
                k = double(i) * 3.0 * 10e-03;
                L = ((40.0 * 10e-05 / 5.5) / d) * (exp(d * k) + 1.0);
                sourceDate.L[i] = L;
        }
        funckOfModel = FunckOfModel(R0, d, eta, mu, G, A0, q0,
Fr);
}

SourceDate MatModelOfFormatingFiber::GetSourceDate()
{
        sourceDate.q0 = q0;
        sourceDate.Teta0 = Teta0;
        sourceDate.Fr = Fr;
        sourceDate.R0 = R0;
        sourceDate.d_ = d_;
        sourceDate.h = h;
```

```cpp
        sourceDate.mu = mu;
        sourceDate.G = G;
        sourceDate.d = d;
        sourceDate.eta = eta;
        sourceDate.V = V;
        return sourceDate;
}

void MatModelOfFormatingFiber::RungeKutty()
{
        double k1, k2, k3, k4,
                m1, m2, m3, m4,
                FQ, FTeta;
        for (int i = 0; i < 5; i++)
        {
                if (CurrQ > 0)
                {

                        FQ = funckOfModel.FunckQ(CurrT,
CurrTeta, CurrQ);
                        FTeta = funckOfModel.FunckTeta(CurrT,
CurrTeta, CurrQ);
                        k1 = FTeta * h;
                        m1 = FQ * h;
                        FQ = funckOfModel.FunckQ(CurrT + h /
2.0, CurrTeta + k1 / 2.0, CurrQ + m1 / 2.0);
                        FTeta = funckOfModel.FunckTeta(CurrT +
h / 2.0, CurrTeta + k1 / 2.0, CurrQ + m1 / 2.0);
                        k2 = FTeta * h;
                        m2 = FQ * h;
                        FQ = funckOfModel.FunckQ(CurrT + h /
2.0, CurrTeta + k2 / 2.0, CurrQ + m2 / 2.0);
                        FTeta = funckOfModel.FunckTeta(CurrT +
h / 2.0, CurrTeta + k2 / 2.0, CurrQ + m2 / 2.0);
                        k3 = FTeta * h;
                        m3 = FQ * h;
```

```cpp
                                FQ = funckOfModel.FunckQ(CurrT + h,
CurrTeta + k3, CurrQ + m3);
                                FTeta = funckOfModel.FunckTeta(CurrT +
h, CurrTeta + k3, CurrQ + m3);
                                k4 = FTeta * h;
                                m4 = FQ * h;

                                CurrTeta = CurrTeta + (1.0 / 6.0) * (k1 + 2.0
* k2 + 2.0 * k3 + k4);
                                CurrQ = CurrQ + (1.0 / 6.0) * (m1 + 2.0 *
m2 + 2.0 * m3 + m4);
                                calcResult.t[i] = CurrT;
                                calcResult.Teta[i] = CurrTeta;
                                calcResult.Q[i] = CurrQ;
                                CurrT = CurrT + h;
                }
                else
                {
                                MessageBox(NULL, L"The particle have
turned inside out!!!", L"Warning", NULL);
                }
        }
}

void MatModelOfFormatingFiber::SetNewDate(SourceDate
NewDate)
{
        q0 = sourceDate.q0;
        Teta0 = sourceDate.Teta0;
        Fr = sourceDate.Fr;
        R0 = sourceDate.R0;
        d_ = sourceDate.d_;
        h = sourceDate.h;
        mu = sourceDate.mu;
        G = sourceDate.G;
        d = sourceDate.d;
        eta = sourceDate.eta;
        V = sourceDate.V;
```

255

```cpp
}

CalcResult MatModelOfFormatingFiber::GetResultOfProccesing()
{
        RungeKutty();
        return calcResult;
}

MatModelOfFormatingFiber matModel;
LRESULT CALLBACK WndProc(HWND, UINT, WPARAM,
LPARAM);
int WINAPI WinMain(HINSTANCE hInstance, HINSTANCE
hPrevInstance, LPSTR lpCmdLine, int nCmdShow)
{
        WNDCLASSEX wcex;
        wcex.cbSize = sizeof(WNDCLASSEX);
        wcex.style = CS_HREDRAW | CS_VREDRAW;
        wcex.lpfnWndProc = WndProc;
        wcex.cbClsExtra = 0;
        wcex.cbWndExtra = 0;
        wcex.hInstance = hInstance;
        wcex.hIcon = LoadIcon(hInstance,
MAKEINTRESOURCE(IDI_APPLICATION));
        wcex.hCursor = LoadCursor(NULL, IDC_ARROW);
        wcex.hbrBackground = (HBRUSH)(COLOR_WINDOW);
        wcex.lpszMenuName = NULL;
        wcex.lpszClassName = szWindowClass;
        wcex.hIconSm = LoadIcon(wcex.hInstance,
MAKEINTRESOURCE(IDI_APPLICATION));
        if (!RegisterClassEx(&wcex))
        {
                MessageBox(NULL, _T("Call to RegisterClassEx
failed!"),
                        _T("Win32 guided tour"), NULL);
                return 1;
        }
        hInst = hInstance;
```

256

```cpp
        HWND hWnd = CreateWindow(szWindowClass, szTitle,
WS_SYSMENU | WS_MINIMIZEBOX | WS_MAXIMIZE,
                CW_USEDEFAULT, CW_USEDEFAULT,
                1000, 545, NULL, NULL, hInstance, NULL);
        if (!hWnd)
        {
                MessageBox(NULL, _T("Call to CreateWindow
failed!"), _T("Win32 guided tour"),
                        NULL);
                return 1;
        }

        label1 = CreateWindow(L"static", L"Source data",
WS_VISIBLE | WS_CHILD, 220, 10, 100, 25, hWnd, NULL,
                hInstance, NULL);
        label2 = CreateWindow(L"static", L"Result data",
WS_VISIBLE | WS_CHILD, 700, 10, 100, 25, hWnd, NULL,
                hInstance, NULL);
        //label3 = CreateWindow(L"static", L"Information data",
WS_VISIBLE | WS_CHILD, 590, 10, 150, 25,
        //      hWnd, NULL, hInstance, NULL);
        label4 = CreateWindow(L"static", L"Amound of
deformation(Q0):", WS_VISIBLE | WS_CHILD,
                10, 55, 230, 25, hWnd, NULL, hInstance, NULL);
        label5 = CreateWindow(L"static", L"The angle of
Theta(Teta):", WS_VISIBLE | WS_CHILD,
                10, 110, 200, 25, hWnd, NULL, hInstance, NULL);
        label6 = CreateWindow(L"static", L"The concept of volume
for disperse phase(Fr):", WS_VISIBLE | WS_CHILD,
                10, 165, 200, 45, hWnd, NULL, hInstance, NULL);
        label7 = CreateWindow(L"static", L"R0:", WS_VISIBLE |
WS_CHILD, 10, 240, 200, 25, hWnd, NULL,
                hInstance, NULL);
        label8 = CreateWindow(L"static", L"d_(b):", WS_VISIBLE |
WS_CHILD, 10, 295, 200, 25, hWnd, NULL,
                hInstance, NULL);
        label9 = CreateWindow(L"static", L"Step size(h):",
WS_VISIBLE | WS_CHILD, 10, 350, 200, 25, hWnd, NULL,
```

```
                    hInstance, NULL);
        label10 = CreateWindow(L"static", L"The volume of
polymer(V):", WS_VISIBLE | WS_CHILD, 266, 240, 200, 45,
                    hWnd, NULL, hInstance, NULL);
        label11 = CreateWindow(L"static", L"The module of
polymer(G):", WS_VISIBLE | WS_CHILD, 266, 55, 250, 25,
                    hWnd, NULL, hInstance, NULL);
        label12 = CreateWindow(L"static", L"The intensity of
current(d):", WS_VISIBLE | WS_CHILD, 266, 110, 250, 25,
                    hWnd, NULL, hInstance, NULL);
        label13 = CreateWindow(L"static", L"The viscosity of
disperse phase(eta):", WS_VISIBLE | WS_CHILD, 266,
                    165, 200, 45, hWnd, NULL, hInstance, NULL);
        label14 = CreateWindow(L"static", L"The viscosity of
disperse environment(mu):", WS_VISIBLE | WS_CHILD, 10,
                    405, 200, 45, hWnd, NULL, hInstance, NULL);
        label15 = CreateWindow(L"static", L"eta/mu:",
WS_VISIBLE | WS_CHILD, 266,
                    315, 240, 25, hWnd, NULL, hInstance, NULL);


        label16 = CreateWindow(L"static", L"t(independent
varieble):", WS_VISIBLE | WS_CHILD,
                    521, 55, 145, 45, hWnd, NULL, hInstance, NULL);
        label17 = CreateWindow(L"static", L"Teta(Calculated
value):", WS_VISIBLE | WS_CHILD,
                    671, 55, 145, 45, hWnd, NULL, hInstance, NULL);
        label18 = CreateWindow(L"static", L"Q(Calculated value):",
WS_VISIBLE | WS_CHILD,
                    821, 55, 145, 45, hWnd, NULL, hInstance, NULL);
        label19 = CreateWindow(L"static", L"L(t):", WS_VISIBLE |
WS_CHILD,
                    621, 240, 250, 25, hWnd, NULL, hInstance, NULL);
        label20 = CreateWindow(L"static", L"Q(experiment
value):", WS_VISIBLE | WS_CHILD,
                    771, 240, 250, 25, hWnd, NULL, hInstance, NULL);
        edit13 = CreateWindow(L"edit", NULL, WS_VISIBLE |
WS_CHILD | ES_MULTILINE | WS_BORDER,
```

```
                521, 100, 145, 105, hWnd, (HMENU)1, hInst,
NULL);
        edit14 = CreateWindow(L"edit", NULL, WS_VISIBLE |
WS_CHILD | ES_MULTILINE | WS_BORDER,
                671, 100, 145, 105, hWnd, (HMENU)2, hInst,
NULL);
        edit15 = CreateWindow(L"edit", NULL, WS_VISIBLE |
WS_CHILD | ES_MULTILINE | WS_BORDER,
                821, 100, 145, 105, hWnd, (HMENU)3, hInst,
NULL);

        button1 = CreateWindow(L"BUTTON", L"Real calc",
WS_VISIBLE | WS_CHILD | BS_PUSHBUTTON,
                526, 410, 100, 50, hWnd, (HMENU)1000, hInstance,
NULL);
        ShowWindow(hWnd, nCmdShow);
        UpdateWindow(hWnd);
        MSG msg;
        while (GetMessage(&msg, NULL, 0, 0))
        {
                TranslateMessage(&msg);
                DispatchMessage(&msg);
        }

        return (int)msg.lParam;
}

LRESULT CALLBACK WndProc(HWND hWnd, UINT message,
WPARAM wParam, LPARAM lParam)
{
        PAINTSTRUCT ps;
        HDC hdc;
        switch (message)
        {
        case WM_PAINT:
                POINT pt;
                hdc = BeginPaint(hWnd, &ps);
                HPEN hPen;
```

```
                hPen = CreatePen(PS_SOLID, 1, RGB(179, 179,
179));
                HPEN hOldPen;
                hOldPen = (HPEN)SelectObject(hdc, hPen);
                MoveToEx(hdc, 260, 40, &pt);
                LineTo(hdc, 260, 545);
                MoveToEx(hdc, 516, 0, &pt);
                LineTo(hdc, 516, 545);
                MoveToEx(hdc, 0, 40, &pt);
                LineTo(hdc, 1000, 40);
                MoveToEx(hdc, 260, 380, &pt);
                LineTo(hdc, 1000, 380);
                SelectObject(hdc, hOldPen);
                DeleteObject(hPen);

                for (int i = 0; i < 361; i++)
                {
                        Ang = atan(tan(i * dAng) * A / B);
                        double X = A * cos(Ang);
                        double Y = B * sin(Ang);
                        ArL[i] = sqrt(X * X + Y * Y);
                }

                for (int i = 0; i < 361; i++)
                {
                        Ang = (i - Slope) * dAng;
                        ArPx[i] = (X0 + ArL[i] * cos(Ang));
                        ArPy[i] = Y0 - ArL[i] * sin(Ang);
                }
                for (int i = 0; i < 361; i++)
                {
                        SetPixel(hdc, ArPx[i], ArPy[i], RGB(0, 0,
0));
                }
                EndPaint(hWnd, &ps);
                break;
        case WM_DESTROY:
                PostQuitMessage(0);
```

```
            break;
    case WM_CREATE:
    {
            char buff[100];

            matModel = MatModelOfFormatingFiber();
            result = matModel.GetSourceDate();
            res = matModel.GetResultOfProccesing();
            edit1 = CreateWindow(L"edit", NULL,
WS_VISIBLE | WS_CHILD | ES_MULTILINE | WS_BORDER,
                    10, 80, 245, 25, hWnd, NULL, hInst,
NULL);
            edit2 = CreateWindow(L"edit", NULL,
WS_VISIBLE | WS_CHILD | ES_MULTILINE | WS_BORDER,
                    10, 135, 245, 25, hWnd, NULL, hInst,
NULL);
            edit3 = CreateWindow(L"edit", NULL,
WS_VISIBLE | WS_CHILD | ES_MULTILINE | WS_BORDER,
                    10, 210, 245, 25, hWnd, NULL, hInst,
NULL);
            edit4 = CreateWindow(L"edit", NULL,
WS_VISIBLE | WS_CHILD | ES_MULTILINE | WS_BORDER,
                    10, 265, 245, 25, hWnd, NULL, hInst,
NULL);
            edit5 = CreateWindow(L"edit", NULL,
WS_VISIBLE | WS_CHILD | ES_MULTILINE | WS_BORDER,
                    10, 320, 245, 25, hWnd, NULL, hInst,
NULL);
            edit6 = CreateWindow(L"edit", NULL,
WS_VISIBLE | WS_CHILD | ES_MULTILINE | WS_BORDER,
                    10, 375, 245, 25, hWnd, NULL, hInst,
NULL);
            edit7 = CreateWindow(L"edit", NULL,
WS_VISIBLE | WS_CHILD | ES_MULTILINE | WS_BORDER,
                    10, 450, 245, 25, hWnd, NULL, hInst,
NULL);
            edit8 = CreateWindow(L"edit", NULL,
WS_VISIBLE | WS_CHILD | ES_MULTILINE | WS_BORDER,
```

```
                        266, 80, 245, 25, hWnd, NULL, hInst,
NULL);
                edit9 = CreateWindow(L"edit", NULL,
WS_VISIBLE | WS_CHILD | ES_MULTILINE | WS_BORDER,
                        266, 135, 245, 25, hWnd, NULL, hInst,
NULL);
                edit10 = CreateWindow(L"edit", NULL,
WS_VISIBLE | WS_CHILD | ES_MULTILINE | WS_BORDER,
                        266, 210, 245, 25, hWnd, NULL, hInst,
NULL);
                edit11 = CreateWindow(L"edit", NULL,
WS_VISIBLE | WS_CHILD | ES_MULTILINE | WS_BORDER,
                        266, 285, 245, 25, hWnd, NULL, hInst,
NULL);
                edit12 = CreateWindow(L"edit", NULL,
WS_VISIBLE | WS_CHILD | ES_MULTILINE | WS_BORDER,
                        266, 340, 245, 25, hWnd, NULL, hInst,
NULL);
                edit16 = CreateWindow(L"edit", NULL,
WS_VISIBLE | WS_CHILD | ES_MULTILINE | WS_BORDER |
                        ES_AUTOVSCROLL | WS_VSCROLL,
                        521, 265, 220, 100, hWnd, NULL, hInst,
NULL);
                edit17 = CreateWindow(L"edit", NULL,
WS_VISIBLE | WS_CHILD | ES_MULTILINE | WS_BORDER |
                        EM_SETSEL | EM_REPLACESEL, 746,
265, 220, 100, hWnd, NULL, hInst, NULL);
                sprintf(buff, "%f", result.q0);
                SetWindowTextA(edit1, buff);
                sprintf(buff, "%f", result.Teta0);
                SetWindowTextA(edit2, buff);
                sprintf(buff, "%f", result.Fr);
                SetWindowTextA(edit3, buff);
                sprintf(buff, "%f", result.R0);
                SetWindowTextA(edit4, buff);
                sprintf(buff, "%.1e", result.d_);
                SetWindowTextA(edit5, buff);
                sprintf(buff, "%e", result.h);
```

```
                SetWindowTextA(edit6, buff);
                sprintf(buff, "%f", result.mu);
                SetWindowTextA(edit7, buff);
                sprintf(buff, "%e", result.G);
                SetWindowTextA(edit8, buff);
                sprintf(buff, "%f", result.d);
                SetWindowTextA(edit9, buff);
                sprintf(buff, "%f", result.eta);
                SetWindowTextA(edit10, buff);
                sprintf(buff, "%e", result.V);
                SetWindowTextA(edit11, buff);
                sprintf(buff, "%f", result.eta / result.mu);
                SetWindowTextA(edit12, buff);
                                int ndx =
GetWindowTextLength(edit16);
                SetFocus(edit16);
                for (int i = 99; i >= 0; i--)
                {
                        SendMessage(edit16, EM_SETSEL,
(WPARAM)ndx, (LPARAM)ndx);
                        sprintf(buff, "%f\n", result.L[i]);
                        SendMessageA(edit16, EM_REPLACESEL,
0, (LPARAM)buff);
                }
                break;
        }
                case WM_COMMAND:
        {
                if (wParam == 1000)
                {
                        char buff[264];
                        double Aex = sqrt(pow(result.R0, 3.0) /
result.d_) / result.d_;
                        sprintf(buff, "%f", Aex);
                        SetWindowTextA(edit17, buff);
                        int ndx1 = GetWindowTextLength(edit13);
                        int ndx2 = GetWindowTextLength(edit14);
                        SetFocus(edit13);
```

```cpp
                    for (int i = 4; i >= 0; i--)
                    {
                            SendMessage(edit13, EM_SETSEL,
(WPARAM)ndx1, (LPARAM)ndx1);
                            if (i != 4)
                            {
                                    sprintf(buff, "%.1e\r\n",
res.t[i]);
                            }
                            else
                            {
                                    sprintf(buff, "%.1e", res.t[i]);
                            }
                            SendMessageA(edit13,
EM_REPLACESEL, 0, (LPARAM)buff);
                    }
                    SetFocus(edit14);
                    for (int i = 4; i >= 0; i--)
                    {
                            SendMessage(edit14, EM_SETSEL,
(WPARAM)ndx1, (LPARAM)ndx1);
                            if (i != 4)
                            {
                                    sprintf(buff, "%.9e\r\n",
res.Teta[i]);
                            }
                            else
                            {
                                    sprintf(buff, "%.9e",
res.Teta[i]);
                            }
                            SendMessageA(edit14,
EM_REPLACESEL, 0, (LPARAM)buff);
                    }

                    SetFocus(edit15);
                    for (int i = 4; i >= 0; i--)
                    {
```

264

```c
                              SendMessage(edit15, EM_SETSEL,
(WPARAM)ndx1, (LPARAM)ndx1);
                              if (i != 4)
                              {
                                      sprintf(buff, "%.9e\r\n",
res.Q[i]);
                              }
                              else
                              {
                                      sprintf(buff, "%.9e",
res.Q[i]);
                              }
                              SendMessageA(edit15,
EM_REPLACESEL, 0, (LPARAM)buff);
                      }
              }
              break;
      }
              default:
              return DefWindowProc(hWnd, message, wParam,
lParam);
              break;
      }
      return 0;
}
```

CONTENTS

Резанова Вікторія Георгіївна,
Резанова Наталія Михайлівна

ПРОГРАМНЕ ЗАБЕЗПЕЧЕННЯ ДЛЯ ДОСЛІДЖЕННЯ МІКРОФІБРИЛЯРНИХ КОМПОЗИТІВ
(англійською мовою)

Редактор Резанова В.Г.
Дизайн та верстка авторські